Hepatitis B virus production is modulated through microRNA-99 family induced-autophagy

Inaugural-Dissertation

zur

Erlangung des Doktorgrades

Dr. rer. nat.

der Fakultät für

Biologie

an der

Universität Duisburg-Essen

Vorgelegt von

Yong Lin

Aus Wuhan, P.R.China

März 2017

Die der vorliegenden Arbeit zugrunde liegenden Experimente wurden am Institut für Virologie der Universität Duisburg-Essen durchgeführt.

1. Gutachter: Prof. Bernd Giebel

2. Gutachter: Prof. Mengji Lu

3. Gutachter: Prof. Matthias Gunzer

Vorsitzender des Prüfungsausschusses: Prof. Bernd Giebel

Tag der mündlichen Prüfung: 22.09.2017

Table of contents

1. Introduction

1.1 MicroRNA

1.1.1 MicroRNA biogenesis and functions

MicroRNAs (miRNAs) are a class of highly conserved small noncoding RNA with about 22 nucleotides.[1] Until now, more than 1700 mature miRNAs have been identified in human. The family of miRNA constitutes about 1-3% of the human genome. Most miRNA genes are situated within the intergenic regions and have their own transcription units. About a quarter are located within exons or introns of other coding genes where their transcription is controlled by the host genes. MiRNAs can be transcribed as monocistronic transcripts or in polycistronic clusters, the latter involve several miRNAs situated on a single transcript being controlled by the same promoter.[2]

The bulk of miRNAs are generated through the canonical pathway of miRNA biogenesis (Figure 1.1).[1, 3] In the nucleus, miRNA genes are transcribed as primary miRNAs (pri-miRNAs) by RNA polymerase II or III (RNA pol II or RNA pol III). For most mammalian miRNAs, pri-miRNAs folds into a hairpin structure characteristic of miRNA genes. The hairpin is recognized and cleaved to precursor miRNAs (pre-miRNAs) of about 50-150 nucleotides by by Drosha (an RNase III enzyme) and Dgcr8 (a crucial cofactor of Drosha) in the nucleus. The pre-miRNAs are then exported to the cytoplasm by a nuclear RNA-export factor exportin 5. In the cytoplasm, this is further excised to a short double-stranded RNA duplex by an RNAse III enzyme, Dicer. The miRNA duplex later separates into single-stranded mature miRNA, and incorporates into the RNA-induced silencing complex (RISC), which is composed of Argonaute proteins. Partial complementarity results in translational repression, while complete complementarity triggers mRNA degradation.

The interaction between miRNA and mRNA mainly depends on the seed sequence of miRNA (2-8 nt of 5' terminal).[4] Beside this region, the 3' terminal region are not essential but may compensate for weaker seed interaction. MiRNAs are post-transcriptional regulators, as they negatively regulate protein translation by a mechanism that depends on the complementarity between the miRNA and target messenger RNA. Moreover, there is also evidence that miRNAs regulate mRNA expression in alternative. As previous work revealed, some miRNAs can target the coding regions or the 5′-UTR to regulate gene expression whereas others can positively activate the translation of mRNA.[5, 6]

As the function of miRNA mainly depends on its seed sequence, target prediction databases (including TargetScan, miRanda and Pictar) are predicted that a single miRNA may

simultaneously target more than 100 mRNAs.[1, 7, 8] In contrast, a single mRNA could also be regulated by many miRNAs. Human miRNAs are potential to control the activity of 30-60% of all protein-coding genes. Thus, miRNAs are integrated into vast regulatory networks and participate in the regulation of diverse biological processes, such as proliferation, differentiation, apoptosis, immune response, and viral replication.[1, 9, 10]

Moreover, miRNAs could be considered as a possible form of intercellular communication in many diseases, including atherosclerosis, Parkinson's disease, fatty liver, and cancer.[11-17] As miRNAs are stable in plasma, plasma miRNAs are potential as novel biomarkers.[18, 19]

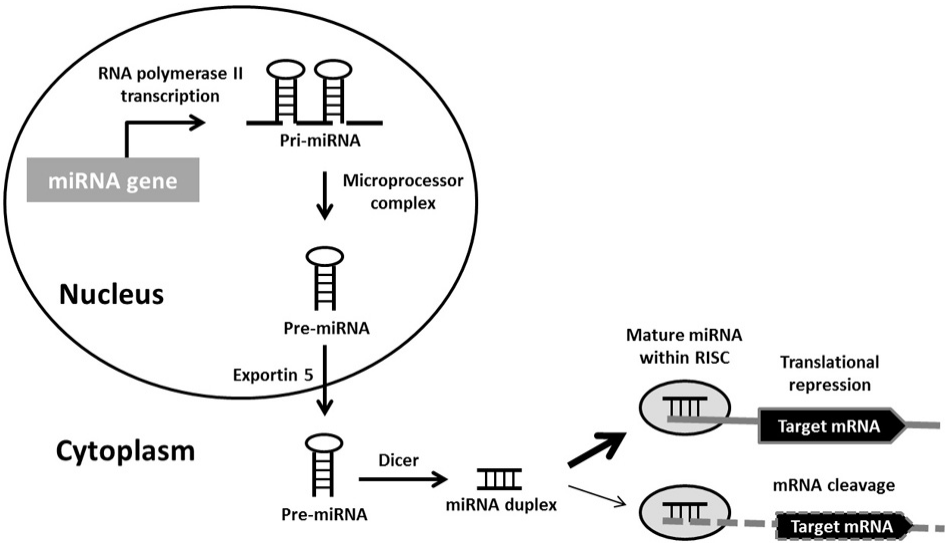

Figure 1.1 MicroRNA biogenesis

In the nucleus, miRNAs are transcribed as either monocistronic or polycistronic pri-miRNAs by Pol II. Pri-miRNAs cleaved by Drosha and Pasha to pre-miRNAs are exported to the cytoplasm by exportin 5. In the cytoplasm, pre-miRNAs are excised to double-stranded miRNA: miRNA* duplex of 20-23 nucleotides by Dicer. The miRNA duplex unwinds to single-stranded mature miRNA, and incorporates into RNA-induced silencing complex (RISC), which is composed of Argonaute proteins. The miRNA/RISC complex binds to the 3′-untranslated region (3′-UTR) of target cellular gene and negatively regulates gene expression with a mechanism depending on the complementarity between miRNA and its target mRNA. Perfect complementarity triggers mRNA degradation, while partial complementarity results in translational repression.[3]

1.1.2 MiRNA and HBV

miRNAs can modulate hepatitis B virus (HBV) replication through directly and indirectly affecting its transcription.[20-24] To date, some cellular miRNAs have been shown to modulate HBV transcription through regulating cellular factors, such as transcription factors and nuclear receptors, at the transcription level (Figure 1.2).[25-27] Our previous work showed that miR-1 and -449a overexpression by an epigenetic mechanism resulted in a marked increase in nuclear receptor farnesoid X receptor alpha (FXRα) expression, leading to enhanced activity of the HBV core promoter and subsequently HBV replication.[23, 28] MiR-372 and -373 are able

to promote HBV gene expression via a pathway involving nuclear factor I/B.[29] MiR-122 may indirectly act on HBV replication via downregulation of its target cyclin G1, thereby blocking the interaction between cyclin G1 and p53 and abrogating p53-mediated inhibition of HBV replication.[22] In contrast, miR-141 suppresses HBV expression and replication by targeting peroxisome proliferator-activated receptor (PPAR)-α.[30] Similarly, miRNA-130a targets the metabolic regulators PPAR-γ and its co-activator PGC1-α and thereby inhibits HBV replication.[27]

Alterations in miRNA expression profiles have emerged as important indicator of changes in gene expression that either favor or restrict virus replication.[31, 32] A set of circulating miRNAs are aberrantly expressed in the peripheral blood of chronically HBV-infected children and patients.[33-35] Among them, miR-125b had increased serum levels in the correlation with high HBV loads and was found to enhance HBV replication in a dose-dependent manner *in vitro*.[36] Interestingly, another miRNA, miR-99a, was consistently found to have elevated serum levels in CHB patients along with miR-122 and -125b, partly associated with hepatitis B e antigen (HBeAg) positivity.[33-35]

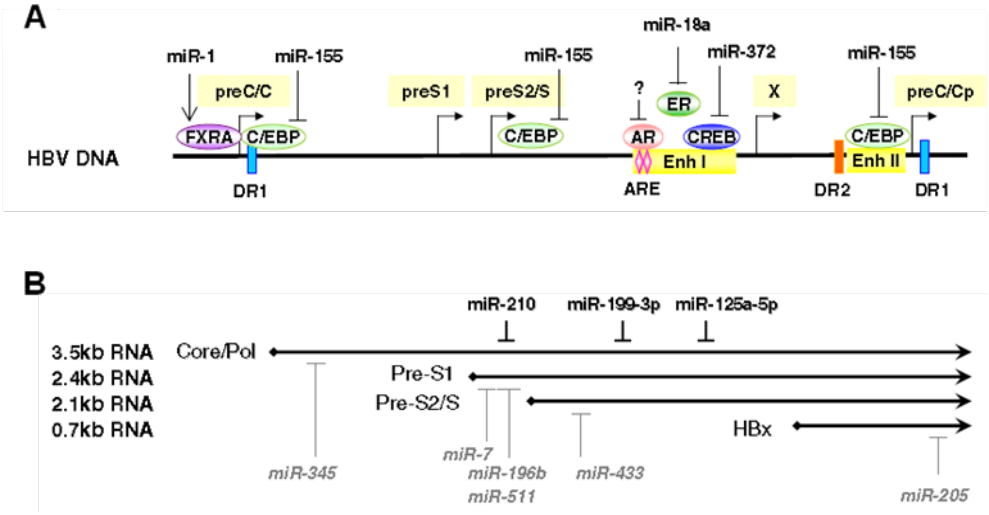

Figure 1.2 Cellular miRNAs effect on HBV transcription

(A) The HBV RNA start site for the major viral transcripts (Pre/core, PreS1, PreS, and X), and viral enhancer I and II are schematically depicted as boxes. DR I and DR II are two short repeats essential for viral replication. Two androgen response elements which are located at enhancer I region are represented as ARE. The miRNAs targeting cellular factors edentified for modulating HBV transcription and host cellular transcription factors binding to HBV genome are shown. (B) Positions of binding sequences in HBV transcripts proposed to be targeted by miRNAs are shown. MiRNAs which were predicted to probably bind HBV transcripts by four well established target-prediction software are represented as italic gray color.[20]

Besides host cellular miRNAs involving in regulating viral replication, a few viruses could also encode miRNAs to benefit its survival. For example, miRNAs encoded by herpes simplex virus appear to promote viral latency by inhibiting viral lytic replication. Further data

indicate that the consequences may be mediated by direct targeting of key viral replication genes or by modulating host relative factors.[31, 37]

Furthermore, virus infection can also change the miRNA expression profile.[25, 26, 33] Winther et al. found there were differential plasma miRNA profiles in HBeAg positive and HBeAg negative children with chronic hepatitis B.[33] Moreover, it was described that HBx significantly up-regulated the levels of 7 miRNA expression, but down-regulates the levels of 11 miRNA expression, respectively. However, an inverse correlation was noted between the expression of HBx and that of the highly-expressed members of the *let-7* family, including *let-7a*, *let-7b* and *let-7c*, in HCC patients.[38] Addtionally, HBV may explored some strategies to prevent infected cells from undergoing apoptosis and to escape from the immune responses in host cells through affecting the miRNA expression profile.[39]

1.2 Hepatitis B virus

1.2.1 Molecular structure

HBV is an enveloped double stranded DNA virus and belongs to the hepadnavirus family.[40] HBV consists of three kinds of particle forms, Dane particle, filaments and spheres (Figure 1.3). The mature virons (named Dane particle) are with a virion diameter of 42 nm. The viral particle consists of an outer lipid envelope and an icosahedral nucleocapsid core composed of protein. The nucleocapsid encloses the viral DNA and a DNA polymerase that has reverse transcriptase activity similar to retroviruses.[41] The outer envelope contains embedded proteins which are involved in viral binding and entry into susceptible cells. Besides the Dane particle, the subviral particles, including filaments and spheres, are pleomorphic and exised in patient serum, including filamentous and spherical bodies These two particles are not infectious and are composed of the lipid and protein that forms part of the surface of the virion, which is called the surface antigen (HBsAg), and is produced in excess during the life cycle of the virus.[42]

With about 3.2 kb genome, HBV is known as one of the smallest DNA virus.[43] HBV genome consists of four overlapping open reading frames encoding the multifunctional polymerase/reverse transcriptase (RT), the capsid-forming core protein, the three closely related envelope proteins, and the regulatory X protein. The HBV genome is partially double stranded, relaxed circular DNA represented by the bold inner circles. The rcDNA is converted to cccDNA, which serves as the template for transcription of the HBV RNA (3.5, 2.4, 2.1 and 0.7 kb). Pregenomic RNA (pgRNA) is selectively packaged inside core particles, followed by P protein-mediated (-) strand DNA synthesis, pgRNA degradation, and (+) strand DNA

synthesis to generate rcDNA. These RNAs are exported to cytoplasm for protein translation. Multiple transcripts are employed to express the seven viral proteins.

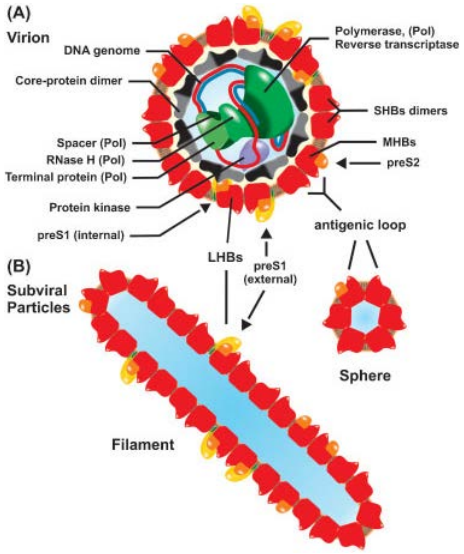

Figure 1.3 Schematic model of hepatitis B virus

(A) Virions and (B) subviral particles. The virion contains a partially double-stranded DNA genome, still associated with the viral polymerase (Pol) and encapsidated by 120 core-protein dimers. The core is enveloped by three viral surface proteins-the large (LHBs), middle (MHBs), and small (SHBs) proteins (shown as dimers) that are cocarboxyterminal and differ by protein length and glycosylation. The subviral particles (filaments and 22-nm spheres) do not contain a nucleocapsid and differ by their amount of LHBs.[40]

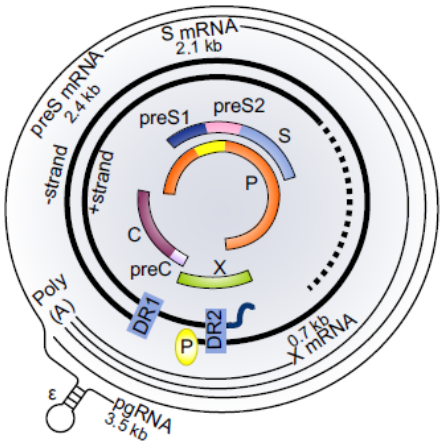

Figure 1.4 Genome organization of HBV

Genetic organization of the HBV genome and mechanisms of viral protein translation. Shown innermost is the P (polymerase) open reading frame (ORF) overlapping completely with the preS1/preS2/S ORF, and partially with preC/C ORF and X ORF. Next are partially double stranded DNA genome found inside virions, with the (-) strand DNA having the P protein attached to its 50 end and the (+) strand DNA having incomplete 30 end (dashed line). The two direct repeat (DR) sequences, DR1 and DR2, are critical for HBV DNA replication and genome circularization. The outmost are four classes of HBV RNAs transcribed from the cccDNA template: 0.7 kb X mRNA (for HBx protein), 2.1 kb S mRNA (for M and S proteins), 2.4 kb preS mRNA (for L protein), and

3.5 kb pgRNA (for core and P proteins). In addition, the 3.5 kb precore RNA (not shown) is used for HBeAg expression.[43]

1.2.2 Life cycle

HBV is one of a few known non-retroviral viruses which use reverse transcription as a part of its replication process.[40, 43] Thus, the viral life cycle is special and complicated (Figure 1.5).

Attachment: HBV can target the cells by binding to a receptor on the surface of the cell and enters it by endocytosis. Na^+-taurocholate cotransporting polypeptide (NTCP) has been found and recognized as a specific receptor of HBV.[44, 45] The early steps of HBV virion infecting hepatocytes are specific and probably irreversible binding to hepatocyte-specific preS1-receptor. This step presumably requires activation of the virus resulting in exposure of the myristoylated N-terminus of the L-protein.[46] The step of HBV entry are though two different entry pathways: one is endocytosis followed by release of nucleocapsids from endocytic vesicles; the other is fusion of the viral envelope at the plasma membrane.[47]

Penetration: The virus membrane then fuses with the host cell membrane releasing the DNA and core proteins into the cytoplasm.[47]

Uncoating: The nucleocapsid in cytoplasm could be transported along microtubules into nuclear.[48] Then, the partially double stranded viral DNA is dissociated from the core proteins and released into the nucleoplasm. The DNA is repaired to fully double stranded and transformed into covalently closed circular DNA (cccDNA) that serves as a template for transcription of four viral mRNAs.[49, 50]

Replication: The largest transcript pgRNA is used to make the new copies of the genome and to make the capsid core protein and the viral DNA polymerase. In the nucleus, rcDNA could be repaired and form cccDNA by viral polymerase, combined with host cellular enzymes.[51] The cccDNA serves as a transcriptional template in the nucleus and utilizes the cellular transcriptional machinery to produce all viral RNAs.[49] The RNA transcripts are then transported to the cytoplasm and translate into associated proteins, while pgRNA is assembled with core protein and polymerase proteins to form the RNA-containing nucleocapsid in cytoplasm. Maturation of RNA-containing nucleocapsid, including synthesis of the (-) DNA strand, pgRNA degradation and synthesis of the (+) DNA strand by the different enzyme activities of viral polymerase.[52]

Assembly: Four viral transcripts, including 3.5 kb preC RNA and pgRNA, 2.4 and 2.1 kb preS/S mRNAs, and 0.7 kb HBx, undergo additional processing and go on to form progeny virions. The long mRNA is then transported back to the cytoplasm where the virion P protein synthesizes DNA via its reverse transcriptase activity.[53, 54]

Release: Nucleocapsids can be directly bud into the endoplasmic reticulum (ER) or proximal Golgi membranes to acquire their glycoprotein envelope to trigger new virions secretion, or they are re-imported to nucleus to amplify the cccDNA pool.[55] This pathway is important for virus persistence in hepatocytes and also contributes to the relapse of viremia after stopping antiviral treatment in chronic HBV infected patients.[49]

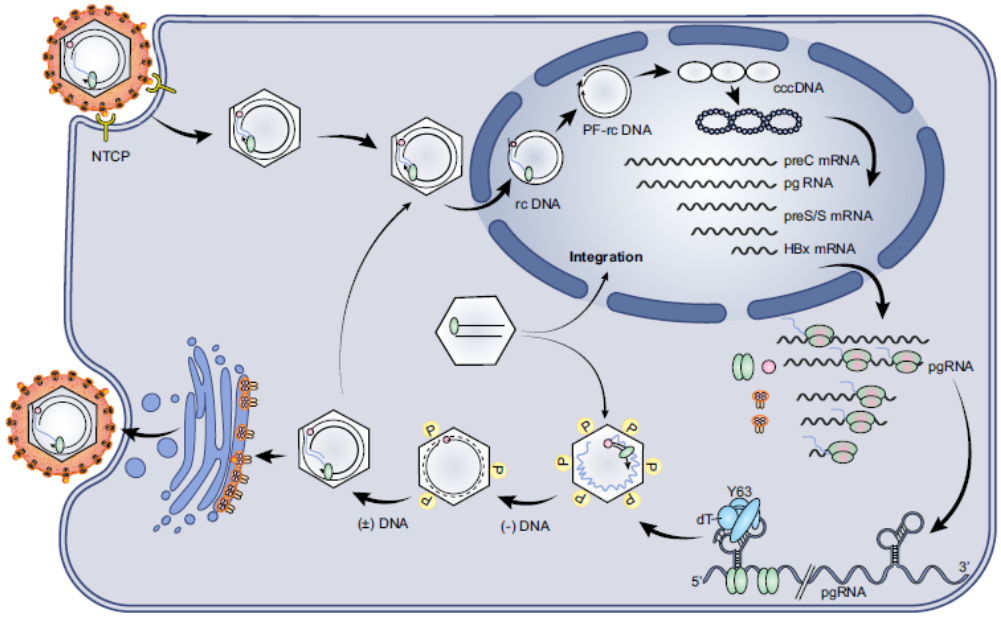

Figure 1.5 HBV life cycle

HBV enters hepatocytes through the specific receptor Na^+-taurocholate cotransporting polypeptide (NTCP), followed by uncoating, and nuclear transport of the rcDNA. The rcDNA is converted to cccDNA, which serves as the template for transcription of HBV mRNA. These RNAs are exported to cytoplasm for protein translation. pgRNA is selectively packaged inside core particles, followed by P protein-mediated (-) strand DNA synthesis (reverse transcription), pgRNA degradation, and (+) strand DNA synthesis to generate rcDNA. Mature core particles are enveloped for release as virions, or transported to the nucleus to generate more cccDNA.[43]

1.2.3 HBV-associated liver diseases

Until now, HBV infection is still one of the most common chronic viral infection in the world. Over 248 million individuals are carriers with HBsAg worldwide.[56] Normal people can be got HBV infection through contact with infected blood and semen, then led to acute or chronic infection. Acute HBV infection is self-limiting and may be self-cleaned in several months. However, chronic HBV infection is associated with an elevated risk of developing hepatitis, liver cirrhosis, and hepatocellular carcinoma (HCC).[47] Overall, as much as 40% of men and 15% of women with perinatally acquired HBV infection will die of liver cirrhosis or HCC.[57]

Currently, HCC is ranks the third leading cause of cancer-related deaths worldwide.[58] The liver tumor, which arises from hepatocytes, is often associated with liver cirrhosis resulting from chronic liver diseases. Among the environmental risk factors, the prevalence of chronic

hepatitis B and C virus infections is linked directly to the incidence of HCC. It is well known that the HBV DNA genome is able to integrate into the cellular chromosomal DNA, causing host genome rearrangements and enhancing the instability of the host chromosome, leading to large inverted duplications, deletions and chromosomal translocations.[59] So far, chronic and persistent infection with HBV is a major risk factor for the development of HCC. Approximately 25% of chronically HBV-infected individuals will develop HCC.[60] Chronic carriers of HBV have up to a 30-fold increased risk of HCC.[61] In areas of high HBV endemicity, persons with cirrhosis have an approximately 16-fold higher risk of HCC than the inactive carriers, and a 3-fold higher risk for HCC than those with chronic hepatitis but without cirrhosis.[62] Although the mechanisms of oncogenesis of HBV remain obscure, several factors have been identified to be associated with a high risk of developing HCC among chronic hepatitis B (CHB) patients. Such as HBx, which is not binding directly to DNA, but rather acts on cellular promoters by protein-protein interactions and by modulating cytoplasmic signaling pathways, appears to play a critical role in the development of HCC.[63-66] HBV exerts its oncogenic potential through a multi-factorial process, which includes both indirect and direct mechanisms that likely act synergistically.[67] Moreover, the association between HCC and HBV recurrence after liver transplantation, and the detection of cccDNA in HCC cells points toward the possibility of HBV replication in tumor cells. The latter could act as potential reservoirs for HBV recurrence, especially in patients who present with a recurrence of HCC.[68]

Since the preventive vaccine was available in 1981, the implementation of universal vaccination in infants has played a critical role in the sharply declined prevalence.[57] Several erological markers of HBV infection, including HBsAg and anti-HBs, HBeAg and anti-HBe, and anti-HBc IgM and IgG, have being used in clinical diagnosis. Currently, the treatments for patients with chronic HBV infection include interferon-α and nucleoside analogues, however, they are limited by low rates of sustained response, side effects, and the emergence of drug resistance.[69] The key obstacle against curing chronic hepatitis B is the inability to eradicate or inactivate cccDNA.[49, 70] Thus, it is urgent to understand HBV-host interactions at the molecular level and to identify novel molecular targets for HBV therapy.

1.2.4 Modulation of HBV replication

HBV replication is regulated by many extracellular and intracellular factors, such as specific hormones, inflammatory cytokines, intracellular signaling pathways, and metabolic processes.[71-74] HBV gene expression can be modulated both in transcriptional or

posttranscriptional process.

The HBV cccDNA plays a key role in the viral life cycle and permits the persistence of infection.[49] cccDNA accumulates in hepatocyte nuclei and forms a stable minichromosome organized as a template for the transcription of viral mRNAs. Thus, HBV utilizes the cellular transcriptional machinery to produce all viral RNAs necessary for viral protein production and viral replication.[75, 76] Moreover, the acetylation status of cccDNA-bound histones is closely correlated with viremia levels, indicating that epigenetic mechanisms can regulate the transcriptional activity of the cccDNA.[76] Our previous data demonstrated that the ectopic expression of miRNAs, such like miR-1, miR-449a, resulted in a marked increase of HBV replication through up-regulated HBV transcription in hepatoma cells.[23, 28, 77]

Virus replication also relies on host cells. The ability of HBV replication mainly depends on the nature of the antiviral stimulus applied. Host cellular factors participate in HBV life cycle in almost every step from cccDNA formation, transcription, core particle formation and progeny secretion. The proliferation status of host cell also affect HBV replication.[23, 28] In addition, HBV replication can be controlled by a variety of cellular transcription factors, in particular, several nuclear receptors like farnesoid X receptor a (FXRA), hepatocyte nuclear factor 4a (HNF4A), liver X receptor (LXR), retinoid X receptor a (RXRA), and peroxisome proliferator activated receptor a/c (PPARA/G). [25]

Moreover, there are other cell pathways that contribute to control HBV replication, such as host innate immunity.[78] As the results shown previously, type I IFNs, proinflammatory cytokines, and chemokines play essential roles in controlling HBV infection. IFNs elicit an anti-viral response by triggering the JAK-STAT signaling pathway, followed by increasing the levels of IFN-stimulated genes (ISGs) expression, whose products exhibit antiviral effects.[79] At present, activation of innate immune response can act as therapeutic approaches for chronic hepatitis B infection.

Among the relevant intracellular pathways, the phosphatidylinositol 3-kinase (PI3K)/Akt signaling pathway is a major cellular pathway involved in regulating HBV infection.[80, 81] Guo et al. reported that HBV replication could be inhibited by activation of the PI3K/Akt signal pathway.[80] This mechanism is likely in part responsible for the reduced HBV replication observed in tumor cells, which can show activation of the PI3K/Akt pathway. Moreover, Hepatitis B surface antigen (HBsAg) synthesis may also be regulated through the PI3K/Akt/mTOR signaling pathway.[82]

HBV could also be regulated by metabolic processes, including autophagy.[83-86] Autophagy is also known as one of the host defense responses against infections. However, it has been

demonstrated that HBV induces autophagy and elicite this to facilitate its DNA replication. This process is mediated by HBx protein, which binds to and activates class III phosphatidylinositol-3-kinase (PI3KC3), an enzyme important for autophagy initiation.[87, 88] There is also evidence showing that the small HBV surface protein was required to induce autophagy formation by triggering unfolded protein responses.[89]

1.3 Autophagy

1.3.1 Autophagy formation

Macroautophagy (herein named simply as ‘‘autophagy’’), an evolutionarily conserved intracellular process, engulfs long-lived cytoplasmic macromolecules and damaged organelles and delivers them to lysosomes for degradation and recycling.[90] This process is essential for maintaining cellular homeostasis in response to multiple stress signals, including nutrient starvation, stress and pathological conditions.[91] There are two different autophagy pathways: one is selective autophagy by removing defective organelles, protein aggregates, cell reorganization upon differentiation, and intracellular parasites; the other is non-selective autophagy by removing ribosomes, organelles, and cytoplasma during starvation.

Complete autophagy involves the formation of a double membrane construction, known as autophagosome.[90, 91] The formation of autophagosomes is arised from a phagophore assembly site (PAS). The formation of the phagophore from the PAS requires the subsequent activity of the ULK1/2 (Atg1 in yeast) kinase complex and 2 ubiquitin-like conjugation systems, including the ATG12–ATG5-ATG16L1 complex and the phosphatidylethanolamine -conjugated LC3/Atg8. Next, the autophagosome travels through the cytoplasm to the endolysosomal system to form amphisomes or autolysosomes, and then degrade the contents (Figure 1.6). Within the lysosomes, the cargo of macromolecules, damaged organelles, and viral proteins in the autophagosome are degraded through lysosomal hydrolases.[92]

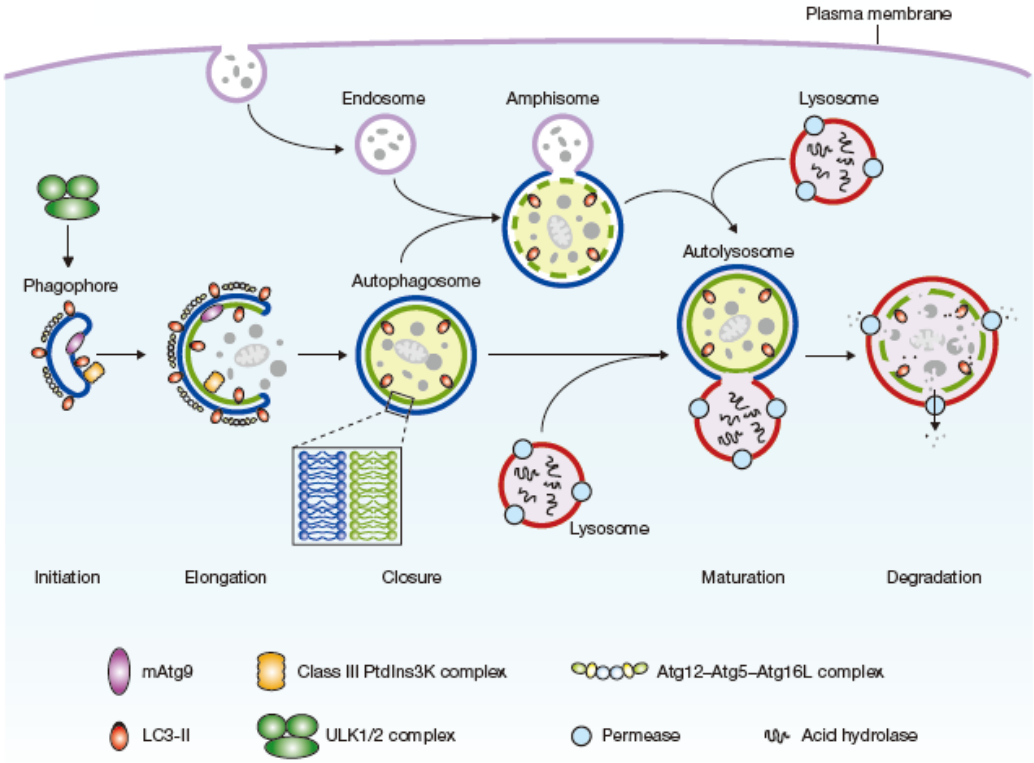

Figure 1.6 Schematic depiction of autophagy

Mammalian autophagy consists of the formation of the phagophore, the elongation and expansion of the phagophore, closure and completion of a double-membrane autophagosome, autophagosome maturation through docking and fusion with an endosome (known as an amphisome) and/or lysosome (known as an autolysosome), breakdown and degradation of the autophagosome inner membrane and cargo inside the autolysosome. The core molecular machinery has already been depicted. The ULK1 and ULK2 complexes are required for autophagy induction; class III PtdIns3K complexes are involved in autophagosome formation; mammalian Atg9 (mAtg9) potentially contributes to the delivery of membrane to the forming autophagosome and two conjugation systems, the LC3-II and Atg12-Atg5-Atg16L complex.[91]

1.3.2 Signaling regulation of autophagy

Autophagy is a complex process and involved in many signals pathway.[91] Autophagy is initiated by the ULK1 kinase complex and receives signal from mTOR complex.[93, 94] Once the mTOR kinase activity is inhibited, autophagosome formation occurs. This involves PI3kinaseIII which forms a complex with Beclin 1. Human Beclin 1 is the first identified mammalian gene to induce autophagy. Autophagosome formation also requires LC cleavage and protein conjugation systems that resemble ubiquitin (Atg proteins). LC3 (microtubule-associated protein 1 light chain 3) is one of the mammalian Atg8 homologues and present in two forms: LC3-I (cytosolic form) and LC3-II (membrane-bound form). On induction of autophagy, LC3-I was converted to LC3-II. The LC3 system is important for transport and maturation of the autophagosome. Once an autophagosome has matured, it fuses its external membrane with lysosomes to degrade its cargo.

Autophagy is regulated by a complex signalling network of various stimulatory and inhibitory inputs (Figure 1.7).[91] MTOR plays a central role in autophagy by integrating the class I PtdIns3K signalling and amino acid-dependent signalling pathways. In 1995, Meijer's group showed that an inhibitor of mTOR, rapamycin, could induce autophagy in rat hepatocytes and relieve the inhibitory effect of amino acids on autophagy.[95] They also demonstrated that amino acids stimulated the phosphorylation of ribosomal protein S6, an effect inhibited by rapamycin, providing a connection between amino acid-dependent and mTOR-dependent regulation. The mTOR signalling pathway is critical because of its ability to integrate the information from nutrient, metabolic and hormonal signals.[96]

Activation of insulin receptors stimulates the class I PtdIns3K complex and small GTPase Ras, leading to activation of the PtdIns3K-PKB-mTOR pathway.[97] PKB phosphorylates and inhibits the tuberous sclerosis complex 1/2 (TSC1-TSC2), leading to the stabilization of Rheb GTPase, which in turn activates mTOR, causing inhibition of autophagy. Subsequent studies demonstrated that activation of this pathway, by expressing an active form of PKB, or expressing a constitutively active form of PDK1, has an inhibitory effect on autophagy. Moreover, mTOR is a downstream target: rapamycin reverses the inhibition of autophagy that results from activation of the class I PtdIns3K pathway.[94, 98]

Energy depletion causes the AMP-activated protein kinase (AMPK) to be phosphorylated and activated by LKB1.[94] AMPK phosphorylates and activates TSC1-TSC2, leading to inactivation of mTOR and autophagy induction. p70S6K kinase is a substrate of mTOR that may negatively feed back on mTOR activity, ensuring basal levels of autophagy that are important for homeostasis.

Although mTOR was considered central to autophagy regulation, mTOR-independent pathways have been recently reported. Amino acids inhibit the Raf-1-MEK1/2-ERK1/2 signalling cascade, leading to inhibition of autophagy.[97] JNK1 and DAPK phosphorylate and disrupt the association of anti-apoptotic proteins, Bcl-2 and Bcl-XL, with Beclin 1, leading to the activation of the Beclin 1-associated class III PtdIns3K complex and stimulation of autophagy.[99, 100]

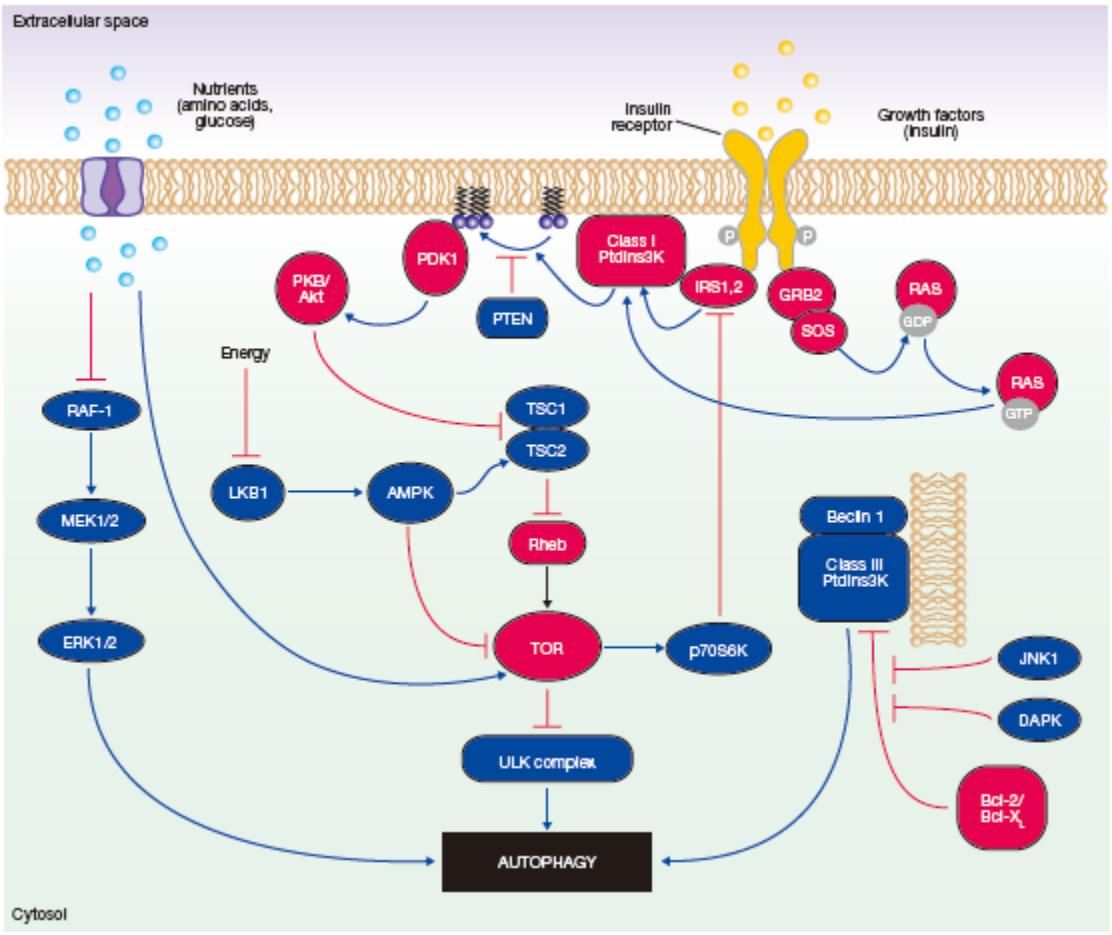

Figure 1.7 Signaling regulation of mammalian autophagy

Autophagy is regulated by a complex signaling network of various stimulatoryand inhibitory inputs. MTOR plays a central role in autophagy by integrating the class I PtdIns3K signalling and amino acid-dependent signalling pathways. Activation of insulin receptors stimulates the class I PtdIns3K complex and small GTPase Ras, leading to activation of the PtdIns3K-PKB-mTOR pathway. PKB phosphorylates and inhibits the TSC1-TSC2, leading to the stabilization of Rheb GTPase, which in turn activates mTOR, causing inhibition of autophagy. Amino acids inhibit the Raf-1-MEK1/2-ERK1/2 signalling cascade, leading to inhibition of autophagy. Energy depletion causes the AMPK to be phosphorylated and activated by LKB1. AMPK phosphorylates and activates TSC1-TSC2, leading to inactivation of mTOR and autophagy induction. JNK1 and DAPK phosphorylate and disrupt the association of anti-apoptotic proteins, Bcl-2 and Bcl-XL, with Beclin 1, leading to the activation of the Beclin 1-associated class III PtdIns3K complex and stimulation of autophagy. Beclin 1 is shown bound to the phagophore membrane.[91]

1.3.3 Autophagy and HBV

In recent years, some studies have reported that HBV could also be regulated by metabolic processes, including autophagy.[83-86] Autophagy, an evolutionarily conserved intracellular process, engulfs long-lived cytoplasmic macromolecules and damaged organelles and delivers them to lysosomes for degradation and recycling.[90] Complete autophagic process mainly involves the formation of autophagosomes, known as early autophagy, and their fusion with

lysosomes and cargo degradation in the lysosomes, known as late autophagy. The cargo of autophagosomes will subsequently be degraded by lysosomal enzymes.[101] Xie et al. reported that activation of PRKAA/AMPK promotes autolysosome-dependent degradation through stimulation of cellular ATP levels, which then leads to the depletion of autophagic vacuoles.[102]

Autophagy has been implicated in a number of cellular and developmental processes, including cell-growth control and programmed cell death.[91] Notably, the dysfunction of autophagy has been implicated in multiple diseases, including neurodegenerative diseases, muscle diseases, cancer, cardiac diseases, and infectious diseases. Autophagy can contribute to innate and adaptive immunity against intracellular microbial pathogens or their products.[103, 104]

However, this intracellular process can also be exploited by some viruses to benefit their replication, such as HBV, HCV, HIV, dengue virus, and influenza A virus.[87, 105-108] In recent years, HBV has been shown to induce partial autophagy to facilitate its own replication (Figure 1.7). Sir et al. reported that the hepatitis B x (HBx) protein interacts with class III phosphatidylinositol 3-kinase to enhance autophagosome formation, which in turn activates viral DNA replication.[87] Moreover, the results of Liu et al. revealed that HBx impaires lysosome maturation by inhibiting lysosomal acidification without disturbing autophagosome-lysosome fusion, which may be beneficial for HBV replication.[109] In addition, Li et al. reported that the small HBV surface protein triggers the unfolded protein responses and enhances the autophagic process without promoting protein degradation by the lysosomes, which is required for HBV envelopment but not for efficient HBV release.[89] Thus, cellular autophagy is closely related with HBV envelopment or its replication.

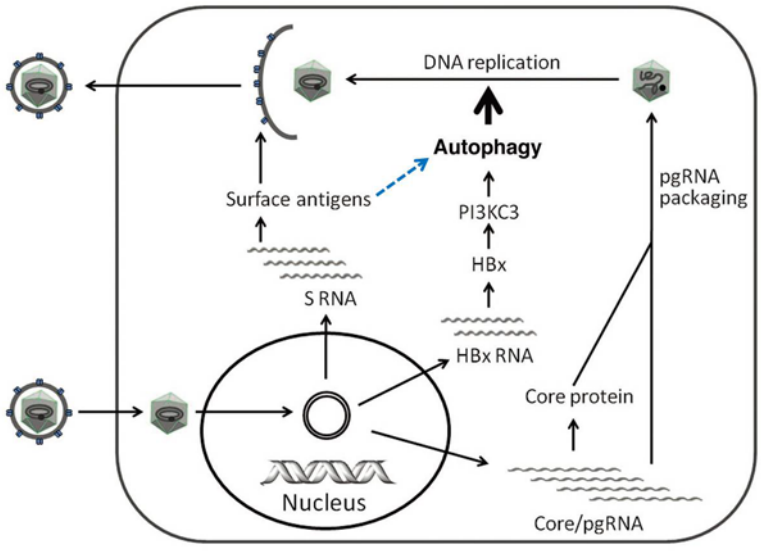

Figure 1.8 Autophagy in the life cycle of HBV

The HBx RNA directs the synthesis of HBx protein, which activates PI3KC3 to enhance autophagy, which in turn activates viral DNA replication. The S RNA codes for the viral surface antigens, which triggers the unfolded protein responses and enhances the autophagic process.[85]

1.4 Rab

1.4.1 Rab function

The Rab proteins are small GTPases that act as molecular switches, to control the formation, transport, tethering and fusion of vesicles in the secretory and endocytic pathways.[110, 111] More than 70 Rabs have been detected in humans, however, many of their functions remain unknown.[112] Previous papers revealed that impaired Rab cascades could cause alterations in the autophagic process leading to various human diseases.

All of the Rabs contain a conserved nucleotide binding domain, which is able to bind both GTP and GDP.[112] Rabs generally cycle between GTP-bound active and GDP-bound inactive forms (Figure 1.9). In their active state, Rab proteins recruit various effectors to the membrane, which they are attached to. Rabs have a low intrinsic hydrolase activity; their hydrolysis rate depends on GTPase-activating proteins (GAPs). These proteins can complement the catalytic site of Rabs, thereby promoting GTP hydrolysis. Inactive, GDP-bound Rabs are removed from their target membrane and kept soluble in the cytoplasm by GDP dissociation inhibitors (GDIs). Upon Rab activation, GDIs are removed mainly by GDI displacement factors (GDFs). Thereafter, guanine nucleotide exchange factors (GEFs) activate Rab proteins by stimulating the exchange of GDP to GTP. Active Rabs can stably attach to membrane surfaces via their C-terminal lipid (geranylgeranyl) anchor, provided by Rab escort proteins.

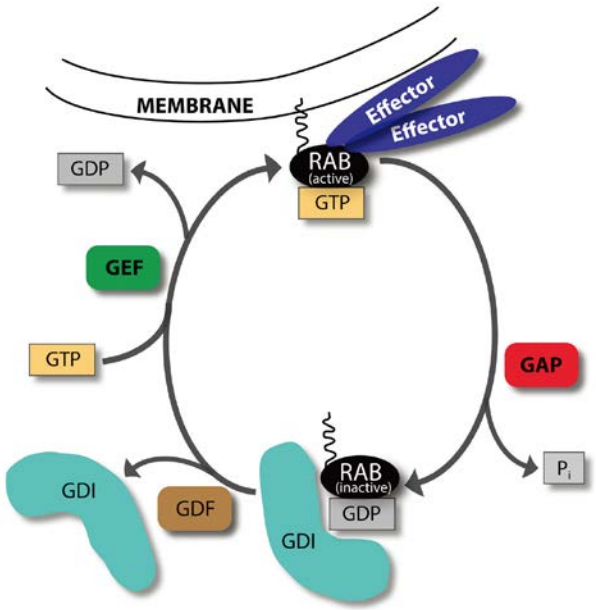

Figure 1.9 GTP-GDP exchange cycle of Rab proteins

Rabs cycle between GTP-bound active and GDP-bound inactive forms. In their active, membrane-attached state they recruit various effectors. GTPase-activating proteins (GAPs) increase the GTP hydrolysis rate, thereby inactivating Rabs. Inactive Rabs are sequestered in the cytosol by GDP dissociation inhibitors (GDIs). Upon Rab activation, GDI displacement factors (GDFs) can displace GDIs. Afterwards, guanine nucleotide exchange factors (GEFs) activate Rab proteins by changing GDP to GTP.[112]

1.4.2 Rab and autophagy

Rab5 and autophagy

Rab5 is a well-known marker of early or sorting endosomes (EEs). Active Rab5 recruits effector proteins, which play a role in maintaining, trafficking, cargo recycling, and maturation of EEs.[113] Rab5 is involved in vesicle fusion events through its effectors CORVET and EEA1/Vac1. Furthermore, Rab5 participates in the endosomal recruitment of PIK3C3/VPS34, which in turn produces phosphatidylinositol 3-phosphate (PtdIns3P) on the EE membrane.[114]

Moreover, Rab5 was found to be a regulator of the early steps of autophagosome formation.[111, 113, 115] Similar to its endosomal functions, Rab5 may have a role in the recruitment of the autophagic BECN1-PIK3C3 complex and subsequent PtdIns3P production on the phagophore membrane.[114] Previous work showed that Rab5 regulated the conjugation of ATG12 to ATG5 through its effector, PIK3C3, as a part of the autophagic BECN1 complex.[116] This study suggested a direct role for Rab5 in the process of autophagosome formation, since its effect on autophagy was not due to its endocytic roles or through the regulation of mTOR signaling. Moreover, both Rab5 and PIK3C3 were found to be required for the formation of autophagosomes during autophagy induced by the nonstructural protein 4B (NS4B) of hepatitis C virus.[114] Interestingly, recent studies showed that the catalytic subunit of the class IA phosphoinositide 3-kinase complex, PIK3CB/p110-β, facilitated the function of Rab5, however, loss of PIK3C3 led to impaired autophagy.[117]

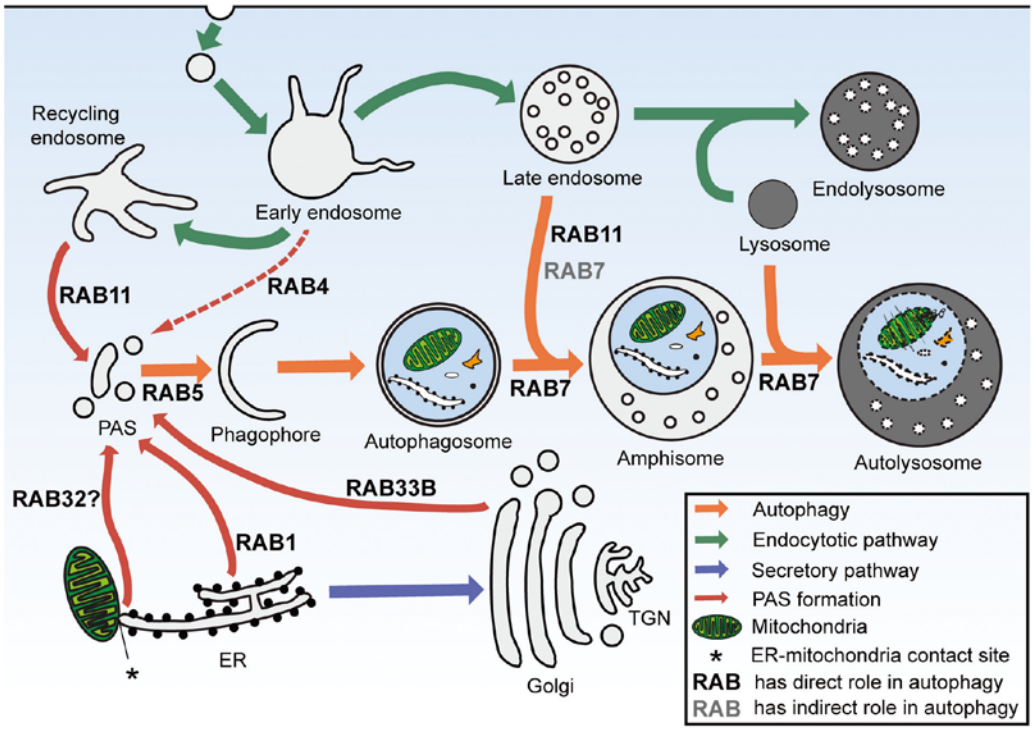

Figure 1.10 The functions of Rab proteins in autophagy

The schematic picture shows the interactions of autophagy with the endocytic and secretory pathways. Series of Rab small GTPases play a role in the earliest steps of autophagosome formation by providing various membrane sources for the PAS. RAB5 participates in this autophagic stage, through its interactions with the PIK3C3-BECN1 complex. Rab7 has both direct roles in the transport of autophagosomes and amphisomes and indirect roles in the fusion process of autophagosomes with late endosomes. ER, endoplasmic reticulum; TGN, trans-Golgi network; PAS, phagophore assembly site.[112]

Rab7 and autophagy

After cargo recycling, EEs mature into late endosomes (LEs).[118] During the maturation process, inactivated Rab5 is substituted by Rab7 on the endosomal membrane. Subsequently, Rab7 recruits its effectors, RILP (Rab-interacting lysosomal protein) and OSBPL1A/ORP1L (oxysterol-binding protein-like 1A), which are required for LE trafficking and fusion with lysosomes.[119]

Similar to its endosomal functions, Rab7 is required for fusion of autophagosomes with late endosomes or lysosomes. Previous studies revealed that Rab7 colocalizes with LC3, and silencing or overexpression of dominant negative Rab7 leads to an increase in size and number of autophagosomes due to impairing their fusion with lysosomes.[120, 121] Supporting these findings, a recent study revealed a similar role for Rab7 was in selective autophagy.[122] Although some results show that the homotypic fusion and vacuole protein sorting (HOPS) complex-associated SNAREs VTI1B and VAMP8 play a role in this fusion process, the HOPS member VPS16 was not found to be necessary for it.[123] In addition, other RAB7

effectors, UVRAG, KIAA0226/Rubicon, and RNF115 have a role in autophagosome maturation.[119, 124] Furthermore, Rab7 is also described in autophagosome formation through the effector PLEKHF1/Phafin1.[125]

However, it is possible that these Rab7 effector proteins have an indirect impact on the late stages of autophagy.[111, 113] There are several lines of evidence that closed autophagosomes fuse not only with lysosomes, but also with various populations of endosomes to form hybrid organelles called amphisomes. In many cell types amphisome formation seems to be essential for subsequent lysosomal fusion and degradation. Thus, in these cells the presence of mature endosomes is required for the completion of the autophagic process. Consequently, it is possible that impairment of autophagic maturation due to depletion of Rab7 or UVRAG is caused in fact by the lack of mature endosomes.[118, 119] Supporting this, recent studies showed that direct autophagosome-lysosome fusion is mediated independently of Rab7 and its effectors, by the SNARE protein STX17 (syntaxin 17).[126] All of these studies suggest that Rab7 effectors facilitating endosome maturation have a cell typedependent role in autophagy.

There are only a few studies revealing a role for Rab7 in other stages of autophagy.[111, 113] Rab7 is implicated at the formation of autophagosomes. Recent studies showed that Rab7 is required at the initial steps during the antibacterial autophagic response against GAS.[127] Their data showed that depletion of Rab7 led to a decrease in formation of GAS-containing autophagicvacuoles. A former paper indicated that mTOR regulates the process of autophagic lysosome reformation likely through Rab7.[120]

Collectively, the endosomal Rabs, including Rab5 and Rab7, have important functions in autophagy regulation. It is necessary to clarify and investigate the distinct roles of Rab5 and Rab7 cascades in orchestrating autophagy.

1.4.3 Rab and HBV

Previous studies have shown that autophagy can be exploited by HBV to facilitate their replication.[106, 107, 128, 129] Autophagy was recognized to have a significant impact on HBV replication, as well as viral envelopment.[87, 88, 130] However, the exact mechanisms of different autophagic phases affecting HBV production remain unclear.

Endosomal Rab5 and Rab7 have important functions in autophagy regulation. As revealed above, Rab5 and Rab7 are related to the formation or the degradation of early autophagic bodies and autophagosomes.[131, 132] Rab5 has been demonstrated to play an important role in autophagosome formation by inhibiting mTOR kinase activity or interacting with Beclin1 and Vps34 to form a complex.[114, 131] Previous studies have demonstrated that Rab5 is an NS4B-interacting protein that is crucial for HCV replication.[133]

However, Rab7 was demonstrated to play a central role in regulating endo-lysosomal membrane traffic.[110] Rab7 is required for the maturation of late endosomes (LEs)/MVBs as well as autophagosomes, directing the trafficking of cargos along microtubules, and participating in the fusion step with lysosomes. Moreover, previous reports have demonstrated that knockdown of Rab7 led to the blocking of the fusion of autophagosomes and lysosomes.[121] Thus, we hypothesized that HBV production is modulated either by the early autophagic process mediated by Rab5, or the late autophagic process mediated by Rab7.

2. Aims of the study

MiRNAs are highly conserved small noncoding RNAs which are widely expressed in multicellular organisms and participate in the regulation of various cellular processes, including autophagy and viral replication. Evidently, miRNAs are able to modulate host gene expression and thereby inhibit or enhance HBV replication. Our previous work has described that miRNAs has complex interconnections with HBV, such as miR-1, miR-125b, and miR-449a. We have found that the miR-99 family members are highly expressed in the liver tissue. Interestingly, the plasma levels of miR-99 family in the peripheral blood correspond with HBV DNA loads. As previous studies identified, the mRNA of IGF-1R, Akt, and mTOR as direct targets with binding sites for miR-99 family members. Moreover, it has been revealed that HBV replication can be regulated through the PI3K/Akt/mTOR signaling pathway, which plays a critical role to induce autophagy. In recent years, it has been found that cellular autophagy has a significant impact on HBV replication, as well as viral envelopment. This process can be exploited by HBV to facilitate its replication *in vitro* or *in vivo*. Thus, we addressed whether the miR-99 family regulated HBV replication and analyzed the underlying molecular mechanism. Next, we further explored the definite mechanisms of different autophagic phases affecting HBV production.

To elucidate these questions, we have investigated it as the following steps:

1. Detecting the levels of the miR-99 family expression in primary human hepatocytes and different hepatoma cells
2. Transfecting miR-99 family mimics with or without a HBV genome containing plasmid pSM2 into hepatoma cell lines to investigate whether miR-99 family could modulate HBV replication in hepatoma cells
3. Transfecting miR-99 family mimics into hepatoma cell lines to explore the molecular and cellular mechanism of miR-99 family modulating HBV replication in hepatoma cells
4. Treating the hepatoma cell lines and primary human hepatocytes with different autophagic inhibitors to investigate the effect on HBV production
5. Silencing or overexpression of Rab5 and Rab7 to investigate the effect of interfering the early or late autophagic phase on HBV production in hepatoma cell lines
6. Silencing of Rab5 and Rab7 to explore the definite mechanisms of different autophagic phases affect HBV production in hepatoma cell lines

3. Materials and methods

3.1 Materials

3.1.1 Plasmids

The HBV plasmid pSM2 was kindly provided by Prof. Hans Will as previously reported.[134] Plasmid GFP-LC3 was a gift from Prof. Jiming Zhang, Shanghai, China. Plasmid HBsAg expressing mCherry was a gift from Prof. Xinwen Chen, Wuhan, China. Plasmids GFP-Rab7 WT, GFP-Rab7 DN, GFP-Rab5 CA (Q79L) and GFP-Rab5 DN (Addgene, 35141) were all purchased from Addgene (Cambridge, MA, USA).

pGL3-HBV promoter report plasmids. The luciferase reporter plasmids containing HBV promoters were constructed by Dr. Xiaoyong Zhang.[23] The regions of HBV core promoter (nt1648-1853), HBV X promoter (nt1237-1375), SP1 promoter (nt2224-2784), SP2 promoter (nt2814-3123) were amplified from pSM2 plasmid and inserted into pGL3-basic vector between Mlu I and Bgl II restriction sites (Promega, Madison, WI) (Figure 3.1, adopted from Promega), resulting in the luciferase reporter vectors pSP1, pSP2, pCP and pXP, respectively. The Renilla luciferase report plasmid was purchased from Clontech.

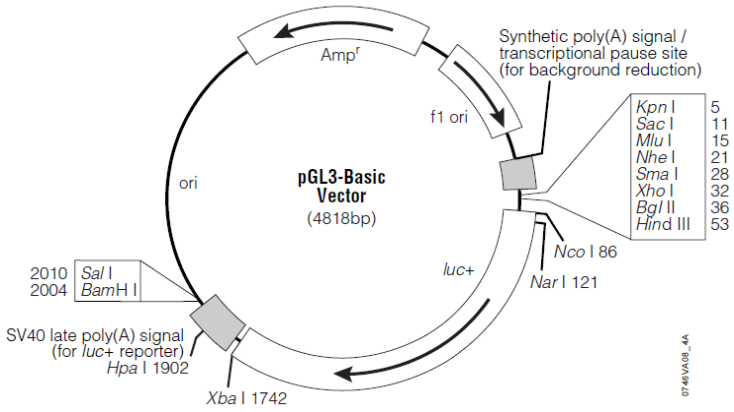

Figure 3.1 pGL3-basic vector circle map

p$^{MIR-REPORT}$ system. Full length of HBV genome sequence was generated from pSM2 plasmid by restriction enzyme SpeI digestion and cloned into the 3' UTR of luciferase gene of p$^{MIR-REPORT}$ vector (Invitrogen). Four partial fragments of the HBV sequence (nt2840-837, nt837-1840, and nt1830-2849) and HBV RNA 3' UTR sequence (nt1841-1964) were amplified from pSM2 plasmid, digested with restriction enzymes MluI and HindIII, and cloned into the 3' UTR of luciferase gene by Dr. Xiaoyong Zhang (Figure 3.2).[23]

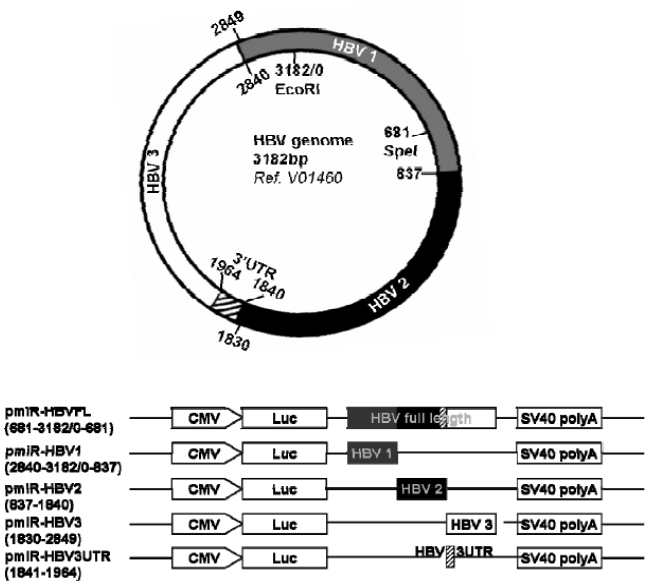

Figure 3.2 Luciferase reporter plasmids containing HBV fragments

3.1.2 Reagents

The list of the reagents used in the present study is shown as follows:

Name	Company
2-propanol	Roche
3-methyladenine (3-MA)	Sigma
4',6-Diamidino-2-phenylindole (DAPI)	Sigma
5× Green GoTaq™ Reaction Buffer	Promega
10× SDS-PAGE	Roche
10× TBE Buffer	Invitrogen
20× SSC Buffer	Invitrogen
30% Acrylamide Solution	BIO-RAD
Akti-1/2	Merck Millipore
Alpha-P32 (dCTP)	Hartmann Analytic GmbH
Amersham ECL Western Blotting Reagent	GE Healthcare
Amersham™ Rapid-hyb Buffer	GE Healthcare
Amersham Protran 0.45 NC	GE Healthcare
Chloroform	Sigma
CID1067700	Sigma
Dimethyl sulfoxide (DMSO)	Sigma
DMEM High Glucose medium	PAA Laboratories
DNAase I	Roche

D-PBS	Invitrogen
EcoR I and Buffer	New England BioLab
EDTA solution (pH 8.0)	AppliChem
Ethanol	AppliChem
Fetal Calf Serum (FCS)	Biochrom
Hydrochloric Acid	Sigma
HEPES Buffer Solution	PAA Laboratories
Illustra™ MicroSpin™ S-200 HR columns	GE Healthcare
Lipofectamine® 2000 Reagent	Invitrogen
LY294002	Merck Millipore
Insulin	Sigma
MEM Non Essential Amino Acids	PAA Laboratories
MHY1485	Selleckchem
NorthernMax®-Gly Sample Loading Dye	Thermofisher
Penicillin/Stretomycin	PAA Laboratories
PeqGOLD Protein-Marker Ⅳ	Peqlab
Positively Chgd. Nylon transfer membrane	GE Healthcare
Proteinase K	Qiagen
QIAprep Spin Miniprep Kit	Qiagen
QIAGEN Plasmid Midi Kit	Qiagen
QIAGEN Plasmid Maxi Kit	Qiagen
Rapamycin	Sigma
Red lysis & Loading Buffer	Cell Signaling
RNase A	Qiagen
Roti-phenol	Roche
RPMI 1640 medium	PAA Laboratories
Salmon Sperm DNA	Invitrogen
SmartLadder	Eurogentec
Sodium Acetate (3M, pH 5.5)	Ambion
Tris buffer (pH7.4 / 8.0 / 8.8)	AppliChem
TRIzol® Reagent	Invitrogen
Trypsin-EDTA	PAA Laboratories
Tween 20	Biochemica
William’s Medium E	Biotech GmbH

Yeast RNA	Ambion

3.1.3 Buffers

The list of buffers used in the present study is shown as follows:

Name	Component
Lysis buffer for HBV EcDNA extraction	50 mM Tris pH 7.4 1 mM EDTA 1% Nonidet P-40
Lysis buffer for HBV core particle extraction	10 mM Tris pH 7.5 1 mM EDTA 50 mM NaCl 8% sucrose 0.25% Nonidet P-40
Denaturation buffer	1.5 M NaCl 0.5 M NaOH
Neutralization buffer	2.0 M NaCl 1.0 M Tris-base 2.5% hydrochloric acid
12 % Separation gel (10 ml)	3.3 ml ddH_2O 4.0 ml 30% acrylamide 2.5 ml 1.5M Tris pH 8.8 100 µl 10% SDS 100 µl 10% AP 4 µl TEMED
5% Concentration gel (5 ml)	3.15 ml deionized water 720 µl 30 % acrylamide 540 µl 1.0 M Tris pH6.8 45 µl 10 % SDS 25 µl 10% AP 5 µl TEMED
10× Transfer buffer (1 l)	142.6 g Glycin 30 g Tris-base

3.1.4 Instruments

The list of all the instruments used in the present study is shown as follows:

Name	Company
-20 °C Freezer	AEG, Germany
-80 °C Freezer	Thermo Forma, Germany
Amersham Hybond^{TM}-N^{+}	GE Healthcare, USA
BIO WIARD KOJAIR	BIO-FLOW Technik, Germany
Bio Imaging System	Syngene, UK
Bin DER	BIOTron Labortechnik GmbH, Germany
CAWOMAT 2000 IR	CAWO photochemisches Werk GmbH, Germany
Centrifuge Avanti J-26Xpi	Beckman Coulter, Germany
Centrifuge 5415 R	Eppendorf, Germany
Centrifuge: Ultracentrifuge Optima L-70K	Beckman Coulter, Germany
CO_2 incubator	Thermo, Germany
Cyclone Storage Phosphor Screen	Packard, USA
Hybidization Oven/Sharker	Amersham Pharmacia, USA
Model 785 Vacuum Blotter	BIO-RAD, USA
Mini Protein Tetra Cell	BIO-RAD, USA
Mini Trans-Blot Cell	BIO-RAD, USA
Rotor-Gene Q	Qiagen, Germany
TopCount.NXT^{TM}	Packard, UK
Vacuum Regulator	BIO-RAD, USA

3.1.5 miRNAs

The sequences of all miRNAs and siRNAs used in the present study are shown as follows:

Name	Product Name	Company	Sequence 5' - 3'
miR-C	miRIDIAN® microRNA mimic negative control #1	GE Healthcare	UCACAACCUCCU AGAAAGAGUAA
miR-99a-5p	Syn-hsa-miR-99a-5p miScript miRNA Mimic	Qiagen	AACCCGUAGAUC CGAUCUUGUG
miR-99b-5p	Syn-hsa-miR-99b-5p miScript miRNA Mimic	Qiagen	CACCCGUAGAAC CGACCUUGCG

miR-100-5p	Syn-hsa-miR-100-5p miScript miRNA Mimic	Qiagen	AACCCGUAGAUC CGAACUUGUG
anti-miR-C	miScript Inhibitor Negative Control	Qiagen	-
anti-miR-99a-5p	Anti-hsa-miR-99a-5p miScript miRNA Inhibitor	Qiagen	AACCCGUAGAUC CGAUCUUGUG
anti-miR-99b-5p	Anti-hsa-miR-99b-5p miScript miRNA Inhibitor	Qiagen	CACCCGUAGAAC CGACCUUGCG
anti-miR-100-5p	Anti-hsa-miR-100-5p miScript miRNA Inhibitor	Qiagen	AACCCGUAGAUC CGAACUUGUG

3.1.6 siRNAs

The sequences of all siRNAs used in the present study are shown as follows:

Name	Product Name	Company	Target sequence
siR-C	Allstars Negative Control siRNA	Qiagen	Proprietary
siAkt	Hs_AKT1_6 FlexiTube siRNA	Qiagen	AACCAGGACCATGAG AAGCTT
simTOR	Hs_FRAP1_6 FlexiTube siRNA	Qiagen	CAGGCCTATGGTCGAG ATTTA
siSREBP1	Hs_SREBF1_5 FlexiTube siRNA	Qiagen	TGCGGAGAAGCTGCC TATCAA
siHIF1A	Hs_HIF1A_5 FlexiTube siRNA	Qiagen	AGGAAGAACTATGAA CATAAA
siIRF7	Hs_IRF7_1 FlexiTube siRNA	Qiagen	CCCGAGCTGCACGTTC CTATA
sip70S6K	Hs_RPS6KB1_5 FlexiTube siRNA	Qiagen	GGGAGTTGGACCATAT GAACT
si4E-BP1	Hs_EIF4EBP1_5 FlexiTube siRNA	Qiagen	TCGGAACTCACCTGTG ACCA
siULK1	Hs_ULK1_6 FlexiTube siRNA	Qiagen	TGCCCTTTGCGTTATAT TGTA
siATG13	Hs_KIAA0652_5 FlexiTube siRNA	Qiagen	AAGGCGGGAGTGACC GCTTAA
siFIP200	Hs_RB1CC1_7 FlexiTube siRNA	Qiagen	ACGCAAATCAGTTGAT

			GATTA
siATG5	Hs_APG5L_6 FlexiTube siRNA	Qiagen	AACCTTTGGCCTAAGA AGAAA
siRab5	Hs_RAB5A_5 FlexiTube siRNA	Qiagen	ATTCATGGAGACATCC GCTAA
siRab7	Hs_RAB7_5 FlexiTube siRNA	Qiagen	CACGTAGGCCTTCAAC ACAAT
siSNAP29	Hs_SNAP29_2 FlexiTube siRNA	Qiagen	CAGAAGATCGACAGC AACCTA
siVAMP8	Hs_VAMP8_2 FlexiTube siRNA	Qiagen	CCGACTAGGCGAATT CACTTA

3.1.7 Primers

The sequences of commercial used in the present study are shown as follows:

Name	Product Name	Company	Cat. No.
RNU6	Hs_RNU6-2_11 miScript Primer Assay	Qiagen	MS00033740
miR-100	Hs_miR-100_2 miScript Primer Assay	Qiagen	MS00031234
miR-99a	Hs_miR-99a_2 miScript Primer Assay	Qiagen	MS00032158
miR-99b	Hs_miR-99b_2 miScript Primer Assay	Qiagen	MS00032165
β-actin	Hs_ACTB_2_SG QuantiTect primer assay	Qiagen	QT01680476
ATG13	Hs_ATG13_1_SG QuantiTect Primer Assay	Qiagen	QT00054194
FIP200	Hs_RB1CC1_1_SG QuantiTect Primer Assay	Qiagen	QT00028021
ATG5	Hs_ATG5_1_SG QuantiTect Primer Assay	Qiagen	QT00073325

The synthesized primer pairs were used as follows:

HBV pgRNA: 5'-TGCCTCATCTGGTTCT-3' (sense) and 5'-CCCCAAWACCCATATA-3' (anti-sense); HBx: 5'-CCGTCTGTGCTCATCT-3' (sense) and 5'-TAATCTCCTCAACTCC -3' (anti-sense).

3.1.8 Antibodies

Antibodies against the following proteins were used:

Name	Source	Company
anti-HBcAg	Rabbit pAb	Abcam
Akt	Rabbit pAb	Cell Signaling

mTOR	Rabbit pAb	Cell Signaling
ULK1	Rabbit pAb	Abcam
p70S6 K	Rabbit pAb	Cell Signaling
anti-Rab5	Rabbit pAb	Cell Signaling
anti-Rab7	Rabbit pAb	Cell Signaling
anti-SNAP29	Rabbit pAb	Sigma
anti-VAMP8	Rabbit pAb	Sigma
anti-LAMP1	Rabbit pAb	Sigma
anti-p62	Rabbit pAb	Abcam
anti-LC3	Rabbit pAb	MBL International
anti-β-actin	Mouse mAb	Sigma
phospho-Rb	Rabbit pAb	Cell Signaling
phospho-Akt	Rabbit pAb	Cell Signaling
phospho-mTOR	Rabbit mAb	Cell Signaling
phospho-p70S6 K	Rabbit mAb	Cell Signaling
phospho-ULK1	Rabbit mAb	Cell Signaling

3.2 Methods

3.2.1 Cell culture and transfection

All cell cultures were maintained at 37 ºC in a humidified atmosphere containing 5% CO_2. The human hepatoma cell line HepG2.2.15, which harbors integrated dimers of the HBV genome (GenBank Accession Number: U95551) and shows a constantly detectable level of HBV replication, was cultured in RPMI-1640 medium (Gibco) with 10% fetal bovine serum (FBS), 100 U/ml penicillin, 100 μg/ml streptomycin (Gibco), and 500 μg/ml G418 (Merck Millipore). Another human hepatoma cell line Huh7 was grown in Dulbecco's Modified Eagle's Medium (Gibco) supplemented with 10% FBS. Primary hepatocytes were kindly provided by Dr. Ruth Broering, University Hospital Essen.

The cultivation and viral infection of PHHs are shown as follows:

(1) 2 day before HBV infection, separate the PHHs from patient and seed them into 12-well plate.

(2) 1 day before HBV infection, Wash the cells with PBS one time. PHHs were incubated with 20 μl HBV viron (2×10^{10} copies/ml, 1:50) and 1 ml WM1 medium (WM2 medium + PEG 8000) at 37 °C for 24 h.

(3) At the end of incubation (0 day post HBV infection), wash the cells with PBS 3 times.

Then PHHs were incubated with 1 ml WM2 medium.

(4) At 2, 4, 6, day post HBV infection, harvest the supernant, wash the cells with PBS 1 time, and change new medium with 1 ml WM2 medium.

(5) At 10 day post HBV infection, harvest the supernant to detect HBsAg and HBeAg, wash the cells with PBS 1 time, and change with 1 ml WM2 medium including autophagy inhibitors (including Rapamycin, CID, and CQ) for 48 h or for 72 h.

(6) At 13 day (72 h post treatment), collect the supernatant and cells for further detection.

Plasmids, miRNAs, or siRNAs were transfected into cells at indicated concentrations using the Lipofectamine 2000 transfection reagent (Invitrogen) according to the manufacturer's instructions. The protocol of transfection used in this study is as follows:

(1) 1 day before transfection, seed HepG2.2.15 cells into 6-well plate.

(2) Wash the cells with PBS once.

(3) Dilute 1.5 μl of 20 μM miR-100 mimics into 250 μl Opti-MEM.

(4) Dilute 4 μl Lipo2000 into 250 μl Opti-MEM, incubate them at RT for 5 min.

(5) Add 250 μl Opti-MEM (diluted with Lipo2000) into 250 μl Opti-MEM (diluted with miR-100), incubate at RT for 20 min.

(6) Discard the old medium from 6-well plate, and wash with PBS once.

(7) Add 1 ml Opti-MEM into each well, and then add 500 μl Lipo2000-miRNA complex (from step 5) drop by drop.

(8) 4-6 hours later, change new medium with 2 ml complete 1640 medium, then put the cells at 37 ºC in a humidified atmosphere.

3.2.2 Plasmid extraction

The transformation of plasmid into *E.coli* strains (DH5α, Invitrogen) was performed according to manufacturer's instructions.

(1) Thawed 50 μl aliquots of bacteria on ice, mixed gently with 2-3 μl of ligation mixture, and incubated on ice for 30 min.

(2) Heat shock at 42 °C for 30 s, followed by a subsequent incubation on ice for 2 min.

(3) Added 200 μl of SOC medium (Invitrogen, Switzerland) into the cells, and then shake at 37 °C for 2 h. Using a sterile spatula, the complete mixture was spread over an LB-agar plate containing a selective antibiotic (100 μg/ml of ampicillin or 50 μg/ml kanamycin).

(4) The plates were incubated at 37 °C overnight.

(5) One bacterial colony was picked up from the LB agar plate using a sterile pipette tip and transferred into the flask with LB-medium containing selective antibiotic.
(6) Prepare 2 ml culture LB medium for mini extraction of plasmid, 50 ml for midi extraction, and 250 ml for maxi extraction, respectively.
(7) Put the LB medium into the shaker, and incubate at 37 °C overnight.
(8) The plasmid DNA was extracted using Qiagen plasmids kits according to the manufacturer protocol. DNA concentration was quantified by spectrophotometric OD 260 nm measurement as follows:

Concentration [μg/μl] = OD 260 nm × dilution factor × 50

(9) Finally, purified plasmid DNA was confirmed by restriction enzyme digestion.

3.2.3 RNA extraction

Total cellular RNA was extracted by using Trizol reagent (Invitrogen, Switzerland), followed by digestion with the DNase Set (Roche, Switzerland). The protocol of RNA extraction in detail is as follows:

(1) Collect the cells in 12-well plate with 500 μl Trizol reagent by pipetting the cells up and down several times.
(2) Incubate the homogenized sample for 5 min at RT to permit complete dissociation of the nucleoprotein complex.
(3) Add 100 μl chloroform, and shake tubes vigorously by hand for 15 s.
(4) Incubate at RT for 2-3 min. Centrifuge at 12,000 g at 4 °C for 15 min.
(5) Transfer the aqueous phase to a new 1.5 ml EP tube, and add 250 μl isopropanol.
(6) Incubate at RT for 10 min. Centrifuge at 12,000 g at 4 °C for 10 min.
(7) Remove the supernatant from the tubes, and wash the RNA pellet with 100 μl 75% ethanol.
(8) Vortex the samples briefly, and centrifuge at 12,000 g at 4 °C for 5 min.
(9) Discard the supernatant, and air dry the RNA pellet for 5-10 min.
(10) Finally, elute the RNA into 50 μl RNase free water. Measure the concentration of RNA (1:50 dilution).
(11) The concentration of all samples is then diluted into 100 ng/μl by adding RNase free water, and then store in -80 °C or for real-time RT-PCR.

3.2.4 Real-time RT-PCR

Quantitative real-time RT-PCR

The levels of relative mRNA expression in cells were determined by quantitative real-time PCR analysis using commercial QuantiTect Primer Assays (Qiagen, Germany). Finally, the ratio of mRNA levels was normalized to internal control beta-actin.

The protocol of real-time RT-PCR for RNA is as follows:

Quantification of the mature miRNAs was performed by using QuantiFast SYBR Green RT-PCR kit (Qiagen). Reaction mixture as follows:

Component	**Volume (20 μl)**
2× SYBR Green RT-PCR Master Mix	10 μl
10× primers	2 μl
QuantiFast RT mix	0.2 μl
Template RNA	1 μl
RNase-free water	6.8 μl

cycler conditions:

1) 50 °C, 10 min for reverse transcription
2) 95 °C, 5 min for initial activation of hotstar Taq DNA polymerase
3) 95 °C, 10 s for denaturation
4) 60 °C, 30 s for annealing and extension step

   40 cycles for DNA (step 3 to 4)

Quantitative miScript real-time RT-PCR

The levels of relative mature miRNA expression were determined by quantitative miScript real-time PCR analysis using commercial miScript Primer Assay (Qiagen, Germany). Finally, the ratio of miRNA levels was normalized to internal control RNU6 expression. The protocol of miScript real-time RT-PCR is as follows:

Total RNA is extracted from cells by Trizol reagent as mentioned above.

1 μg total RNA is reverse-transcribed into cDNA according to miScript II RT Kit (Qiagen). The reverse-transcription master mixes on ice as follows:

Component	**Volume (20 μl)**
5× miScript HiSpec Buffer	4 μl
miScript Reverse Transcriptase Mix	1 μl
Template RNA	1 μl
RNase-free water	14 μl

cycler conditions:

37 °C for 60 min

95°C for 5 min

Quantification of the mature miRNAs was performed by miScript SYBR Green PCR kit (Qiagen). Reaction mixture as follows:

Component	Volume (20 µl)
2× SYBR Green RT-PCR Master Mix	10 µl
10× miScript Universal Primer	2 µl
10× miScript Primer Assay	2 µl
Template RNA	2 µl
RNase-free water	4 µl

Cycle parameter:

1) 95 °C for 15 min
2) 94 °C for 15 s for denaturation
3) 55 °C for 30 s for annealing
4) 70 °C for 30 s for extension

   40 cycles (step 2 to 3)

   For standard curve:

1) Dilute the synthetic miRNA mimics into 10^{10} copies/µl.
2) Prepare 20 µl reverse-transcription reaction as mentioned above, using 5 µl synthetic miRNA (10^{10} copies/µl) and 50 ng carrier bacterial RNA (yeast mRNA, 10 µg/µl).
3) Incubate at 37 °C for 60 min. Incubate at 95°C for 5 min to inactivate and place on ice.
4) Add 480 µl of 1 ng/µl bacterial carrier RNA to the 20 µl reaction. Mix gently by pipetting up and down and centrifuge briefly to yields the cDNA (10^8 copies/µl).
5) Using the diluted cDNA mix (10^8 copies/µl) and carrier RNA (1 ng/µl), prepare a series of standard curve (10^8, 10^7, 10^6, 10^5, 10^4, 10^3 copies/µl) to run real-time miScript RT-PCR by miScript SYBR Green PCR kit (Qiagen).

3.2.5 Analysis of HBV gene expression

Quantification of HBsAg and HBeAg

The levels of HBsAg and HBeAg in the culture medium were determined using the Architect System and the HBsAg and HBeAg CMIA kits (Abbott Laboratories, Germany) according to the manufacturer's instructions.

Quantification of HBV DNA

HBV progeny DNA was extracted from culture medium using the DNA Blood Mini Kit

(Qiagen) and quantified by quantitative real-time polymerase chain reaction (Invitrogen). HBV DNA was extracted from intracellular core particles in hepatoma cell lines and detected by quantitative real-time PCR or Southern blotting analysis (mention below).

The protocol of quantitative real-time PCR for quantification of total HBV DNA levels is as follows:

Purification of HBV DNA from culture medium:

(1) Pipette 20 μl QIAGEN Protease into the bottom of a 1.5 ml EP tube.
(2) Add 200 μl culture medium to the EP tube.
(3) Add 200 μl Buffer AL to the sample. Mix by pulse-vortexing for 15 s.
(4) Incubate at 56 °C for 10 min.
(5) Add 200 μl ethanol (96–100%) to the sample, and mix again by pulse-vortexing for 15 s.
(6) Carefully apply the mixture from step 5 to the QIAamp spin column without wetting the rim, close the cap, and centrifuge at 6,000 g for 1 min. Place the QIAamp spin column in a clean 2 ml collection tube, and discard the tube containing the filtrate.
(7) Carefully open the QIAamp spin column and add 500 μl Buffer AW1 without wetting the rim. Close the cap and centrifuge at 6,000 g for 1 min. Place the QIAamp spin column in a clean 2 ml collection tube, and discard the collection tube containing the filtrate.
(8) Carefully open the QIAamp spin column and add 500 μl Buffer AW2 without wetting the rim. Close the cap and centrifuge at full speed for 3 min.
(9) Place the QIAamp spin column in a new 2 ml collection tube and discard the collection tube with the filtrate. Centrifuge at full speed for 1 min.
(10) Place the QIAamp spin column in a clean 1.5 ml EP tube, and discard the collection tube containing the filtrate. Carefully open the QIAamp spin column and add 50 μl ddH_2O. Incubate at RT for 1 min, and then centrifuge at 6,000 g for 1 min.
(11) Store the samples at -20 °C or using as template for real-time PCR for detecting HBV progeny DNA directly.

Reaction mixture for real-time PCR:

Component	**Volume (20 μl)**
2× UDG mix	10 μl
Hope-forward prime	0.4 μl
Hope-reverse prime	0.4 μl
$MgCl_2$	0.8 μl
BSA	1 μl
Template	2 μl

Aqua	5.4 μl

cycler conditions:

(1) 95 °C, 15 s for denaturation

(2) 60 °C, 15 s for annealing

(3) 72 °C, 10 s for extension step

45 cycles (step 1 to 3)

3.2.6 Southern blotting analysis

HBV replicative intermediates from intracellular core particles were extracted from hepatoma cell lines and detected by Southern blotting, respectively. The encapsided HBV DNA in nucleocapsids was also detected by Southern blotting. However, HBV nucleocapsid in cell lysates was analyzed in a native agarose gel and then detected by western blotting analysis.

The protocol of Southern blotting for detecting HBV replication is as follows:

EcDNA extraction:

(1) 3 or 4 days post-transfection, wash the cells in 6-well plate with PBS 1 time.

(2) Add 800 μl iced lysis buffer and incubate on ice for 10 min.

(3) Collect the cell lysates into 2 ml EP tube, vortex vigorously for 15 s, and then incubate on ice for 10 min.

(4) Centrifuge at 13,200 rpm for 2 min.

(5) Transfer the supernatant to a new 2 ml EP tube, then add 8 μl of 1 M $MgCl_2$ and 8 μl of 10 mg/ml DNase I, mix gently, and incubate for 30 min at 37 °C.

(6) Shortly centrifuge, and add 40 μl of 0.5 M EDTA (pH 8.0) to a final concentration of 25 mM, mix by vortex.

(7) Shortly centrifuge, and add 80 μl 10% SDS, mix by vortex.

(8) Shortly centrifuge, and add 20 μl 20 mg/ml proteinase K.

(9) Incubate at 55 °C for 2 h.

(10) Phenol/chloroform extraction, vortex and static for 2 min, then centrifuge at 13,000 rpm at RT for 8 min.

(11) Suck up the first layer liquid and add 0.7 V of isopropanol, 0.1 V of 3 M NaAc (pH5.2) and 2 μl of 10 mg/ml yeast RNA, incubate over night at -20 °C.

(12) 13,200 rpm at 4 °C for 15 min, discard the supernatant carefully.

(13) Wash the pellet with 1 ml 75% ethanol, up and down 2 times gently without disrupt the whole pellet, centrifuge at 8,000 rpm at RT for 5 min. Discard the supernatant carefully, then air dry for 5-10 min.

(14) Dissolve the pellet in 15 μl TE buffer.

(15) Add 5 μl 5× green loading buffer, scrape on tube shelf and short centrifugate.

Run agarose gel:

(1) Prepare 1% agarose gel.

(2) Electrophoresis for 1.5-2 h at 50 V.

(3) Wash with ddH_2O one time, then denaturation for 30 min at RT with gentle agitation.

(4) Wash with ddH_2O one time, then neutralization for 30 min at RT with gentle agitation.

(5) Wash the agarose gels with ddH_2O one time, and then soak in 20× SSC.

(6) Transfer the membranes (from down to up including: white fiberboard, filter paper, Nylon membrane, green plastic membrane and the agarose gels), cover the cover. 13Hg for 2 h.

(7) Fix DNA on the membranes at 150 J/cm^2 2 times.

Hybridization probe preparation:

(1) Digest plasmid pSM2 (1 μg/μl) which contain HBV dimer by restriction enzyme EcoR I.

Component	**Volume (100 μl)**
EcoR I	1 μl
10× NEB 2	10 μl
pSM2	10 μl
Aqua	79 μl

(2) After digestion at 37 °C for 2 h, 25 μl 5× green loading buffer was added. Run 0.8% agarose gel at 130 V for 2 h to separate two bands (3.2 kb for HBV fragment and 2.7 kb for vector), and cut 3.2 kb band for agarose gel extraction.

(3) Agarose gel extraction to quantify the HBV fragment concentration and dilute into 25 ng/μl. The HBV fragments were put in -80 °C for long-term storage or used directly for Southern blotting hybridization.

Hybridization:

(1) Dilute 5 μl HBV DNA probe (5 ng/μl) into 41 μl TE in 1.5 ml tube.

(2) Mix and then denature at 95 °C for 5 min.

(3) Then snap cool the DNA by placing on ice for 5 min after denaturation.

(4) Prehybridize the membranes in 10 ml Rapid-Hyb buffer (Amersham) at 65 °C for 10-20 min.

(5) Centrifuge briefly the denatured DNA, and add into the reaction tube (GE Healthcare) which contains polymerase.
(6) Add 2 μl/reaction α-^{32}P dCTP into the reaction tube.
(7) Incubate at 37 °C for 10 min.
(8) Stop the reaction by adding 5 μl of 0.2 M EDTA.
(9) Loosen the cap of column 1/4 turn, snap off the bottom closure of the microspin columns, and centrifuge for 1 min at 3,000 rpm.
(10) Place the column in 1.5 ml tube with 100 μl of 10 mg/mL salmon sperm, and slowly apply the reaction sample to the resin.
(11) 3,000 rpm for 2 min.
(12) For use in hybridization, denature the labeled DNA by heating to 95 °C for 5 min, then snap cool on ice for 5 min.
(13) Add purified labeled DNA to the pre-hybridization solution by directly dropping into hybridization tube.
(14) Hybridize at 65 °C overnight.
(15) Wash the membranes with 50 ml wash buffer I (2× SSC + 0.1% SDS) at RT for 30 min 2 times.
(16) Wash the membranes with 50 ml wash buffer II (0.2× SSC + 0.1% SDS) at 65 °C for 30 min 2 times.

3.2.7 Northern blotting analysis

HBV transcripts were extracted from hepatoma cell lines and detected by northern blotting.

1. The protocol of northern blotting (Glyoxal method) for HBV transcription is as follows:

(1) Wash gel electrophoresis chamber, tray and combs with ddH_2O 3 times, with DEPC-water for 2 times. Then dry them in ventilate hood.
(2) Prepare 1.2% agarose gel.
(3) Weight 1.2 g agarose, and add 100 ml 1× Gly prep/Running Buffer.
(4) Boil them in microwave oven, cool to 50~60 °C, and then pour into chamber.
(5) Prepare RNA samples: 10 μl RNA (1 μg/μl) + 10 μl Glyoxal load Dye + 1 μl EB.
(6) Incubate at 50 °C for 30 min, and then put into ice for 10 min.
(7) Electrophoresis: Add 1× Gly prep/Running Buffer, 60 V at 4 °C for 4 h.
(8) Detect 18 s and 28 s quickly by Gel Imager.
(9) Transfer.
(10) Wash gel with DEPC water.

(11) Shake gently in 20× SSC (diluted by DEPC water) for 1 h.

(12) Prepare to put the positive-charged NC membrane into 20× SSC, and then do membrane transferring just like Southern blotting.

(13) Ultraviolet crosslinking like Southern blotting.

(14) Hybridization processes are just like Southern blotting.

3.2.8 Western blotting analysis

Western blotting analysis was performed to detect the relative protein expression. Briefly, after transfection or treatment, cells were washed with phosphate-buffered saline and lysised with 1× lysis buffer (Cell Signaling Technology, USA). Protein samples were resolved by sodium dodecyl sulfate-polyacrylamide gel electrophoresis and then electrotransferred to nitrocellulose membranes. The membranes were incubated with the indicated primary antibodies overnight at 4 ℃ after being blocked with 5% milk in 1× TBST. The membranes were washed with 1× TBST and incubated (as appropriate) with a secondary peroxidase-affiniPure Rabbit anti-mouse IgG antibody (Jackson ImmunoResearch West Grove, USA) or a peroxidase-affiniPure goat anti-rabbit IgG antibody (Jackson ImmunoResearch). Immunoreactive bands were visualized using an enhanced chemiluminescence system (GE Healthcare, UK).

The protocol of western blotting in detail is as follows:

(1) Aspirate culture media from 12-well plate, wash the cells with PBS, and aspirate it.

(2) Lyses the cells by adding 100 µl of 1× red lysis buffer (Cell Signaling). Scrape off the cells from the plate immediately, and transfer them to a new 1.5 ml centrifuge tube on ice.

(3) Heat the samples at 95 ℃ for 10 min; then cool on ice.

(4) Prepare four 12%-15% separate gel.

(5) Load protein samples into SDS-PAGE gel: 3 µl protein marker/well, 10 µl sample/well for purpose band, and 3 µl sample/well for beta-actin detection.

(6) Run at 100 V for 30 min firstly, and then change to 130 V for 1.5 h.

(7) Transfer to NC membrane, 250 mA for 1 h.

(8) Incubate the membranes in 5% milk at RT for 1 h.

(9) Wash the membranes with 1× TBST.

(10) Incubate the membranes in primary antibody (1:1000, by 0.25% milk in 1×TBST) at 4 ℃ overnight with gentle agitation.

(11) Wash the membranes with 1× TBST for 10 min 3 times.

(12) Incubate the membranes in 5 ml HRP-conjugated secondary antibody (1:15000, by 0.25% milk in 1× TBST) at RT with gentle agitation for 1 h.
(13) Wash the membranes with 1× TBST for 10 min 3 times.
(14) Put the membrane in plastic wrap and add 600 µl ECL buffer/membrane, then put into black-box for exposure.

3.2.9 Luciferase reporter gene assay

The Dual-Glo luciferase reporter assay (Promega) was used to detect the firefly luciferase activity and the internal control Renilla luciferase activity. The firefly luciferase reporter plasmids pSP1, pSP2, pCP, pXP (containing HBV promoters), and pmiR-HBV FL, pmiR-HBV1, pmiR-HBV2, pmiR-HBV3, and pmiR-HBV3'UTR (containing full length genome, and partial genome fragments) were generated previously as described [23].

The protocol of Dual-Glo luciferase reporter assay is as follows:

(1) 48 h post transfection, discard the culture medium, wash the cells with PBS once, and remove it.
(2) Add 75 µl PBS for each well.
(3) Add 75 µl Dual-Glo luciferase Reagent to each well.
(4) Punch the cells with tip into 96-well black plate from 24-well plate.
(5) Cap the plate and measure the firefly luminescence.
(6) Add 75 µl Dual-Glo stop reagent to each well and wait for at least 10 min then measure Renilla luminescence.
(7) Calculate the ratio of firefly to Renilla.

3.2.10 Microscopy image acquisition and quantification

For fluorescence staining, Huh7 cells were grown on cover slips and cotransfected with the plasmid GFP-LC3 and miRNAs or siRNAs. After transfection for 48 h, cells were fixed in 4% paraformaldehyde for 10 min, and permeabilized with 0.1% Triton X-100 for 10 min. The nuclei were stained with 4', 6-Diamidino-2-phenylindole (DAPI), and the distribution of the GFP-tagged LC3 protein was visualized with confocal microscope (LSM 710; Carl Zeiss) with objectives Plan-Apochromat 63×/1.40 oil Iris M27. Images were acquired by ZEN acquisition software (2012; Carl Zeiss) and analyzed by ImageJ software. The images were not manipulated other than contrast and brightness adjustments. For quantification of the number of the GFP-LC3 puncta, approximately 50 cells were recorded and analyzed by ImageJ software.[109]

The protocol of immunofluorescence staining in detail is as follows:

(1) Fix the cells with 200 µl 4% formaldehyde, incubate at RT for 10 min.
(2) Wash the cells with 200 µl PBS for 5 min 3 times.
(3) Incubate with 200 µl 0.1% Triton X-100 at RT for 10 min.
(4) Wash the cells with 200 µl PBS for 5 min 3 times.
(5) Block with 150 µl 5% FBS in PBS, at RT for 30 min.
(6) Wash the cells with 200 µl PBS for 5 min 3 times.
(7) Incubate with 150 µl first-antibody (1:200) at RT for 1 h.
(8) Wash the cells with 200 µl PBS for 5 min 3 times.
(9) Incubate with 150 µl second-antibody (1:200) with FITC-labeled at RT for 1 h.
(10) Incubate with 150 µl DAPI (1:1000) at RT for 10-15 min.
(11) Wash the cells with 200 µl PBS for 5 min 3 times.
(12) Add 1 drop fluorescent mounting medium (Dako) onto the slide. Cover with glass lip and seal with nail polish.

3.2.11 Statistical analysis

Statistical analyses were performed using Graph Pad Prism software version 6 (La Jolla, CA, USA). Analysis of variance with two-tailed Student's *t* test or by one- or two-factor ANOVA analysis was used to determine significant differences. Differences were considered as statistically significant when $P < 0.05$. All experiments were repeated independently at least 3 times.

4. Results

4.1 Low expression of mature miR-100 and miR-99a in hepatoma cells

Previous data have identified members of the miR-99 family, including miR-100, miR-99a, and miR-99b, as tumor suppressors.[135-138] Their expression levels in HCC tissue were lower than that observed in normal liver tissue.[137, 138]

To compare expression levels of miR-99 family members in normal human hepatocytes and hepatoma cells, we determined their expression levels in primary hepatocytes (PHHs) and 3 different hepatoma cell lines Huh7, HepG2, and HepG2.215 cells by quantitative miScript real-time reverse transcriptase polymerase chain reactions (RT-PCR). Mature miR-100 and miR-99a were expressed at approximately 20- and 50-fold higher levels in PHHs than in hepatoma cells, respectively (Figure 4.1, A and B). However, miR-99b expression was not decreased in hepatoma cells; indeed, it was significantly higher in HepG2.2.15 cells than in primary human hepatocytes. Collectively, these data suggest that the expression of the miR-99 family is strongly dysregulated in hepatoma cells, compared to that in PHHs.

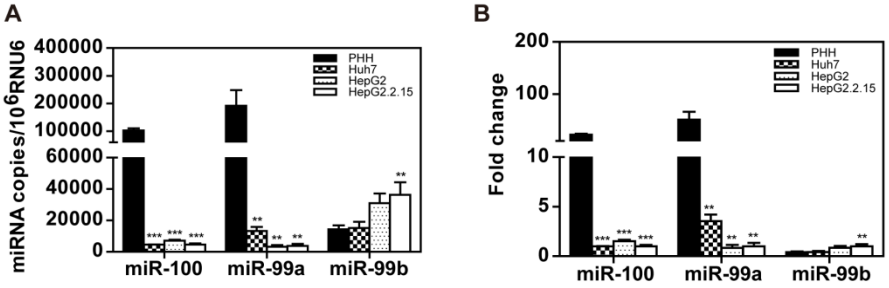

Figure 4.1 Low expression of mature miR-100 and miR-99a in hepatoma cells

The expression levels of miR-99 family members miR-100, -99a, and -99b in PHHs and hepatoma cell lines Huh7, HepG2, and HepG2.2.15 were determined by miScript real-time polymerase chain reaction. (A) The measured copy numbers of miR-100, -99a, and -99b were normalized to those of U6 snRNA (RNU6). RNU6 was used as an endogenous control. (B) The relative expression levels of miR-100, -99a, and -99b in cells compared to that of HepG2.2.15 (set as 1). The analyses were performed in triplicate. * $P < 0.05$, ** $P < 0.01$, *** $P < 0.001$.

4.2 The miR-99 family promotes HBV replication

4.2.1 The miR-99 family promotes HBV protein production, DNA replication and progeny secretion

Next, we investigated whether miR-99 family members regulated HBV replication in different hepatoma cells. Synthetic mimics of miR-100, miR-99a, and miR-99b were transfected into HepG2.2.15 cells at a final culture supernatant concentration of 40 nM. HBV replicative intermediates (HBV RIs) were isolated at day 4 post-transfection and analyzed by Southern blotting. As compared to transfection with a miRNA control (miR-C), the mount of

HBV RIs, HBV DNA in the supernatant, and HBsAg/HBeAg secretion significantly increased following ectopic expression of miR-99 family members (Figure 4.2, A). In Huh7 hepatoma cells, miR-99 family mimics could also promote HBV replication and gene expression if co-transfected with a replication competent clone of HBV plasmid pSM2 (Figure 4.2, B). Western blotting analysis of cell lysates indicated the hepatitis B core antigen (HBcAg) expression in HepG2.2.15 cells obviously increased after transfection with miR-99 family members (Figure 4.3).

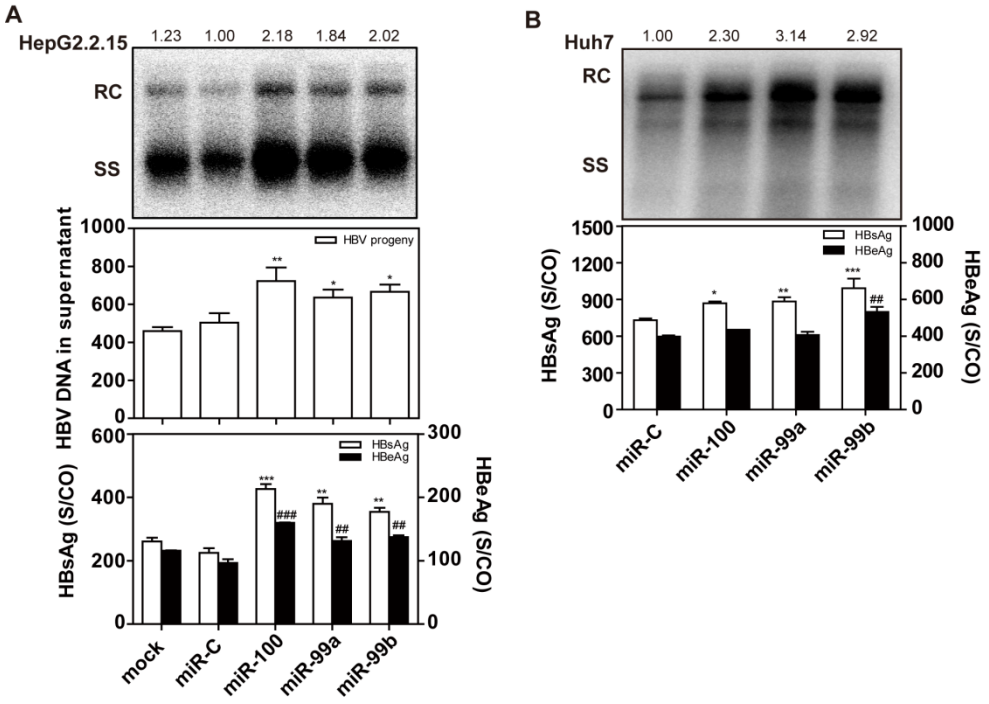

Figure 4.2 The miR-99 family promotes HBV DNA replication and gene expression

(A) HepG2.2.15 cells were transfected with miR-99 family mimics or a nonspecific miRNA control (miR-C) at a final concentration of 40 nM and harvested 96 h later. (B) Huh7 cells were co-transfected with 1.5 μg of pSM2 plasmid and miRNA mimics at a final concentration of 40 nM, and harvested after 72 h. HBV replicative intermediates inside the cells were isolated and detected by Southern blotting. HBV DNA levels in the supernatant were determined by quantitative real-time polymerase chain reaction. The levels of HBsAg and HBeAg in culture supernatant were determined by chemiluminescence immunoassay. S/CO = signal to cutoff ratio; RC, relaxed circular DNA; SS = single-stranded DNA. *, # $P < 0.05$; **, ## $P < 0.01$; ***, ### $P < 0.001$.

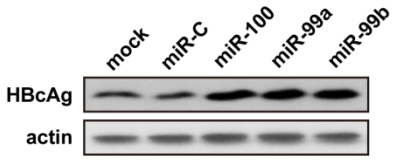

Figure 4.3 The miR-99 family promotes HBcAg expression

HepG2.2.15 cells were transfected with miR-99 family mimics or a nonspecific miRNA control (miR-C) at a final concentration of 40 nM, and cell lysates were harvested at 72 h post-transfection. The analysis of HBcAg expression was performed by western blotting. Beta-actin was used as the loading control.

4.2.2 The miR-99 family promotes HBV replication in dose dependence

Furthermore, HepG2.2.15 cells were transfected with different doses of miR-99 family mimics (at 10, or 40 nM) or miRNA control miR-C, and harvested after 96 h. The results revealed the miR-99 family members enhanced HBV replication and secreted HBsAg and HBeAg in a dose-dependent manner in HepG2.2.15 cells (Figure 4.4). Based on these results, subsequent experiments were performed mainly with HepG2.2.15 cells.

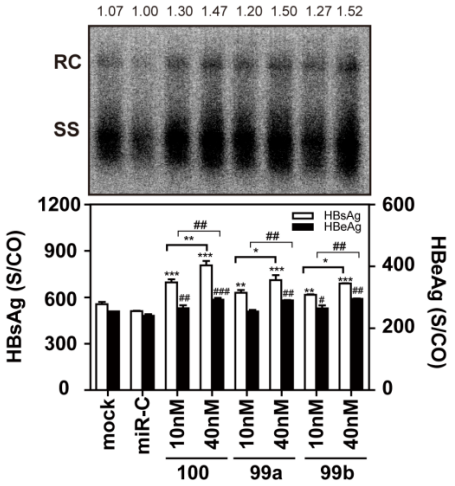

Figure 4.4 The miR-99 family promotes HBV DNA replication in dose dependence

HepG2.2.15 cells were transfected with different doses of miR-99 family mimics (at 10, or 40 nM) or miRNA control miR-C, and harvested after 96 h. HBV replicative intermediates inside the cells were isolated and detected by Southern blotting. The levels of HBsAg and HBeAg in the supernatant were determined by chemiluminescence immunoassay. S/CO = signal to cutoff ratio; RC, relaxed circular DNA; SS = single-stranded DNA. *, # $P < 0.05$; **, ## $P < 0.01$; ***, ### $P < 0.001$.

4.2.3 The miR-99 family inhibitors decrease HBV DNA replication and gene expression

Finally, the inhibitors of miR-100, miR-99a, and miR-99b could obviously inhibit the secretion of HBsAg and HBeAg and HBV replication in HepG2.2.15 cells (Figure 4.5), as they decreased the levels of miR-99 family expression (Figure 4.6). Together, these results support that the miR-99 family effectively promotes HBV replication, gene expression and progeny secretion.

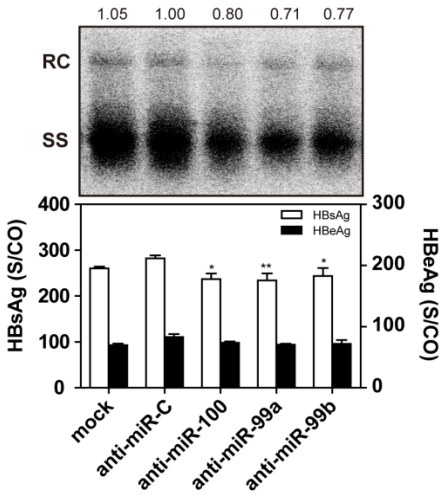

Figure 4.5 The miR-99 family inhibitors decrease HBV DNA replication and gene expression

HepG2.2.15 cells were transfected with miR-99 family inhibitors or a miRNA inhibitor control anti-miR-C at 40 nM, and harvested after 96 h. HBV replicative intermediates inside the cells were isolated and detected by Southern blotting. The levels of HBsAg and HBeAg in the supernatant were determined by chemiluminescence immunoassay. S/CO = signal to cutoff ratio; RC, relaxed circular DNA; SS = single-stranded DNA. * $P < 0.05$, ** $P < 0.01$, *** $P < 0.001$.

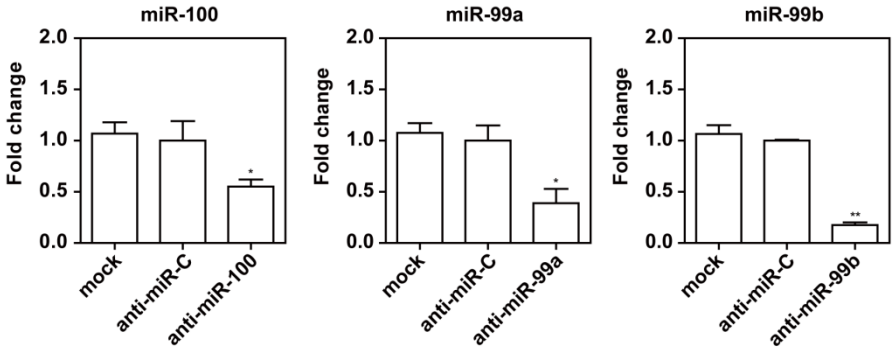

Figure 4.6 MiR-99 family inhibitors affect the expression of miR-99 family members

HepG2.2.15 cells were transfected with inhibitors of miR-100, -99a, -99b or control anti-miR-C at 40 nM, and harvested at 72 h. The levels of miR-99 family expression were determined by miScript real-time polymerase chain reaction with RNU6 as the normalization control. The relative expression levels of miR-100, -99a, and -99b were compared to that of anti-miR-C transfection (set as 1).

4.3 The miR-99 family enhances HBV replication through directly inhibiting the IGF-1R/PI3K/Akt/mTOR signaling pathway

4.3.1 The miR-99 family does not promote HBV transcription and promoter activity

Several cellular miRNAs have been shown to inhibit or enhance viral replication by directly targeting viral RNAs.[26, 139] Although HBV is a DNA virus, its transcripts might be targeted and modulated by cellular miRNAs.[25, 26] However, no potential binding site (UACGGGU) of the seed sequence of the miR-99 family members was found in the HBV genomic sequencing

the available prediction software packages (MiRanda, TargetScan, and Pictar) for studying miRNA-mRNA interactions.[8] In agreement, co-transfection of pMIR-REPORT plasmids harboring the full-length HBV genome or HBV genome fragments with miR-99 family mimics into HepG2.215 cells did not decrease the luciferase activities of different HBV fragments (Figure 4.7, A). Thus, we found no evidence for a direct interaction between HBV transcripts or the HBV genome with miR-99 family members, which may lead to regulation of HBV gene expression or replication.

Next, the effect of the miR-99 family members on the activities of HBV promoters was measured in Dual-Glo luciferase report assays. Consistently, we found that the luciferase activities of the HBV SP1, SP2, Core, and X promoters also were not significantly changed by ectopic expression of miR-99 family members (Figure 4.7, B).

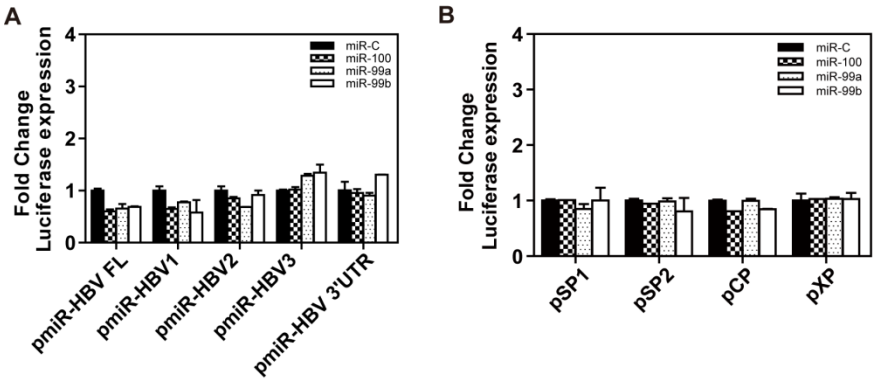

Figure 4.7 The miR-99 family does not promote HBV promoter activity

(A) HepG2.2.15 cells were co-transfected with miR-99 family mimics or control miR-C at 40 nM, pMIR-REPORT plasmids including pMIR-Luc, -HBV FL, -HBV1, -HBV2, -HBV3, or -HBV 3' UTR, and Renilla as an internal control for 48 h. Dual-Glo luciferase report assay was performed to measure the firefly and Renilla luciferase activities. The results were calculated by fold change, and normalized to the miRNA control samples. (B) HepG2.2.15 cells were co-transfected with miR-99 family mimics or control miR-C at 40 nM, HBV promoter luciferase reporters containing the regions of pSP1, pSP2, pCP, and pXP, and Renilla as an internal control. The determination of luciferase activities was described above. * $P < 0.05$, ** $P < 0.01$, *** $P < 0.001$.

The effect of miR-99 family members on the different steps of HBV life cycle was further examined. The levels of HBV RNA were separately determined by northern blotting (Figure 4.8, A) and real-time RT-PCR (Figure 4.8, B) in HepG2.2.15 cells. We observed that the levels of HBV RNA remained unchanged after transfection of miR-99 family members, indicating that these miRNAs did not promote HBV transcription, further implying that the miR-99 family enhanced HBV replication through some other mechanism(s).

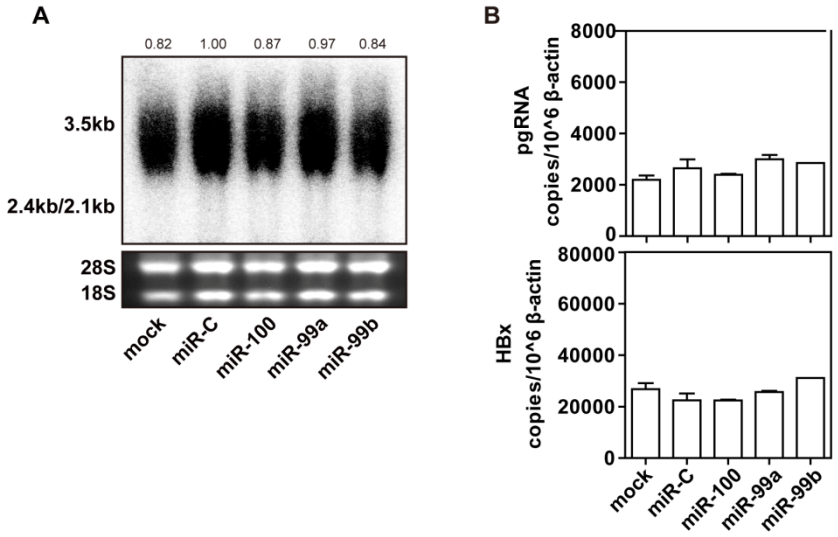

Figure 4.8 The miR-99 family does not promote HBV transcription

HepG2.2.15 cells were transfected with miR-99 family mimics or the miR-C control at 40 nM and harvested after 72 h. (A) HBV RNAs were detected by northern blotting analysis, using 28S and 18S RNAs as loading controls. (B) HBV pregenomic RNA (pgRNA) and HBx RNA levels were analyzed by real-time reverse transcriptase polymerase chain reaction, using primers matching to the pgRNA-specific region and HBx region (covering all transcripts), respectively. * $P < 0.05$, ** $P < 0.01$, *** $P < 0.001$.

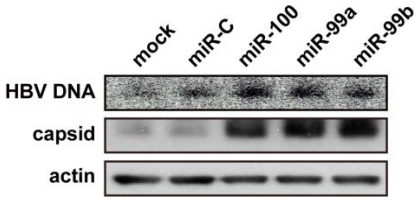

Figure 4.9 The miR-99 family promotes HBV capsid formation

HepG2.2.15 cells were transfected with miR-99 family mimics or the miR-C control at 40 nM and harvested after 72 h. Cell lysates from HepG2.2.15 cells were harvested at 72 h post transfection. Analysis of HBV nucleocapsid and the encapsidated HBV DNA was detected by western and Southern blotting, respectively. Beta-actin was used as the loading control.

Strikingly, ectopic expression of miR-99 family members strongly increased the amount of HBV capsid and capsid-associated HBV DNA detected by western and Southern blotting analysis, respectively (Figure 4.9). Taken together, these results suggest that the miR-99 family members promote HBV replication at post-transcriptional steps, such as capsid formation.

4.3.2 HBV replication is enhanced by inhibiting PI3K/Akt/mTOR signaling pathway

Previous studies have demonstrated that HBV replication and HBsAg production could be regulated through the PI3K/Akt/mTOR signaling pathway.[80, 140] Clearly, treatment of HepG2.215 cells for 48 h by using PI3K, Akt, and mTOR chemical inhibitors (LY294002,

Akti-1/2, and rapamycin, respectively) resulted in significant enhancement of HBV replication, as well as HBsAg and HBeAg secretion (Figure 4.10, A). In parallel, these 3 inhibitors decreased phosphorylation of Akt, mTOR, and p70S6K, respectively, without significant affecting total expression levels of these proteins (Figure 4.10, B). Moreover, HepG2.215 cells were transfected with specific siRNAs against Akt, mTOR or control siR-C. As we expected, HBV replication, as well as HBsAg and HBeAg secretion (Figure 4.11, A), was significantly increased when Akt or mTOR expression was silenced (Figure 4.11, B).

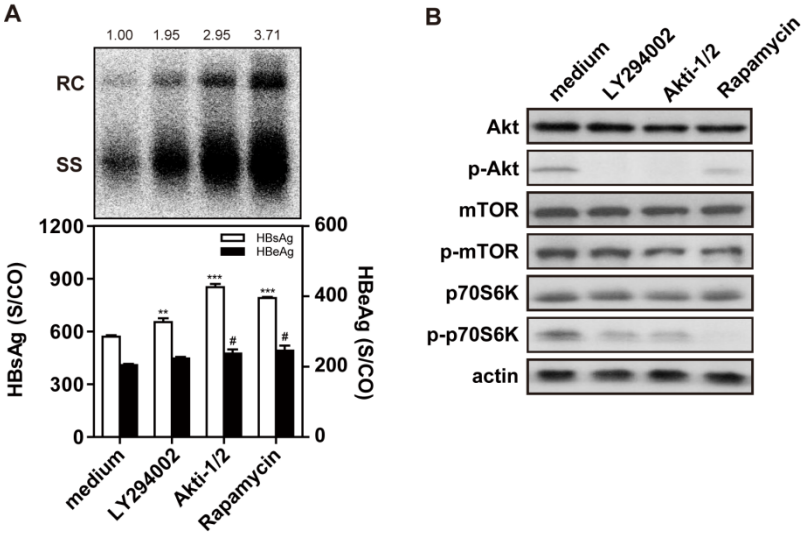

Figure 4.10 HBV replication is enhanced by inhibition of PI3K/Akt/mTOR signaling pathway

(A) HepG2.2.15 cells were treated with medium, 1 μM of PI3K inhibitor LY294002, 1 μM of Akt inhibitor Akti-1/2, or 1 μM of mTOR inhibitor rapamycin for 72 h, and harvested at 72 h post the treatment of inhibitors. The detection of HBV replicative intermediates, secreted HBsAg and HBeAg in the supernatant was performed as described above. (B) Western blotting analysis was performed to detect the total and phosphorylated forms of the Akt, mTOR, and p70S6K proteins, using beta-actin as the loading control. S/CO = signal to cutoff ratio; RC, relaxed circular DNA; SS = single-stranded DNA. *, # $P < 0.05$; **, ## $P < 0.01$; ***, ### $P < 0.001$.

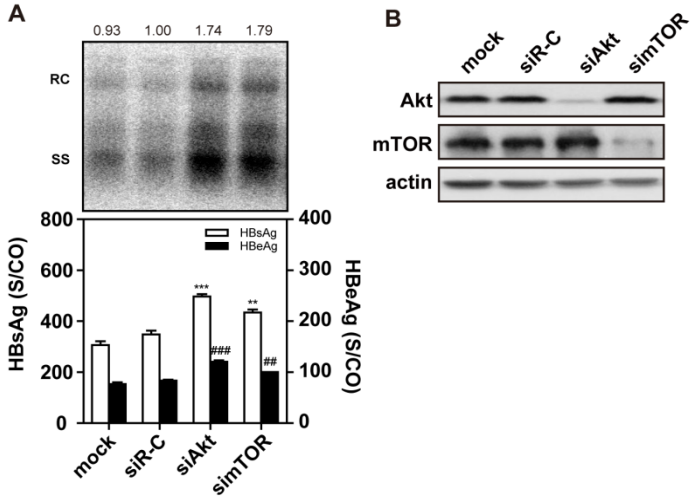

Figure 4.11 HBV replication is enhanced by silencing of Akt or mTOR

HepG2.2.15 cells were transfected with specific siRNAs against Akt, mTOR or the siRNA control at 20 nM, and harvested after 96 h post transfection. (A) The detection of HBV replicative intermediates, secreted HBsAg and HBeAg in the supernatant was performed as described above. (B) Western blotting analysis was performed to detect the expression of Akt and mTOR proteins, and beta-actin was used as the loading control. S/CO = signal to cutoff ratio; RC, relaxed circular DNA; SS = single-stranded DNA. *, # $P < 0.05$; **, ## $P < 0.01$; ***, ### $P < 0.001$.

4.3.3 The miR-99 family inhibits IGF-1R/PI3K/Akt/mTOR signaling pathway by directly targeting IGF-1R, Akt and mTOR

Previous studies have identified the mRNA of IGF-1R, Akt, and mTOR as direct targets with binding sites for miR-99 family members (Figure 4.12).[80, 82, 140-142] Thus, we tested whether ectopic expression of the miR-99 family could promote HBV replication by targeting the cellular IGF-1R/PI3K/Akt/mTOR signaling pathway. Firstly, we tested whether miR-99 family members could regulate IGF-1R, Akt and mTOR functions in hepatoma cells. HepG2.2.15 cells were transfected with miR-99 family mimics at a final culture supernatant concentration of 40 nM for 72 h, and total and phosphorylated IGF-1R, Akt, mTOR, and p70S6K proteins were detected by western blotting. As shown in Figure 4.13, the miR-99 family could significantly reduce the formation of total and phosphorylated forms of the IGF-1R, Akt, mTOR, and p70S6K proteins, in agreement with previous data obtained with other cell types.[143]

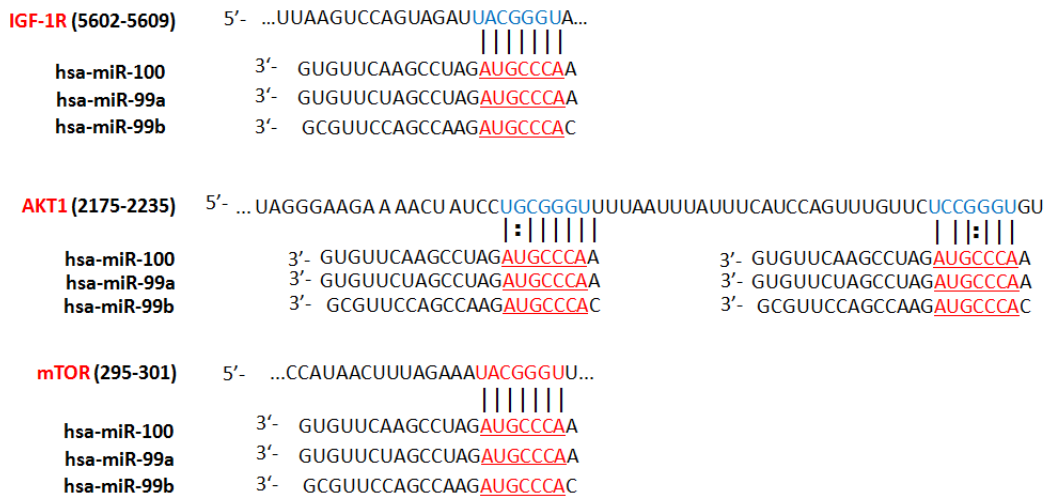

Figure 4.12 The direct targeting of miR-99 family members

MiR-99 family includes miR-100, miR-99a and miR-99b. They shared the same seed sequence and probably play a similar role in different cellular lives. They can directly target: IGF-1R, AKT1 and mTOR, and suppress their gene expression at post-transcriptional level.

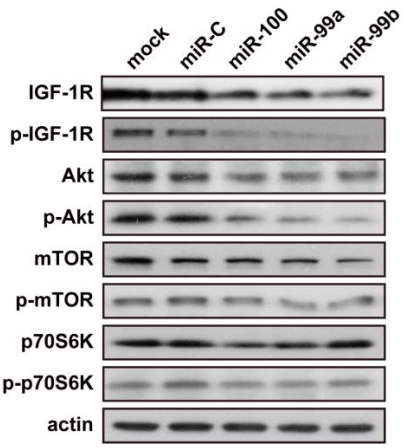

Figure 4.13 The miR-99 family inhibits IGF-1R/PI3K/Akt/mTOR signaling pathway

HepG2.2.15 cells were transfected with miR-99 family mimics or control miR-C at a final concentration of 40 nM and harvested at 72 h post transfection. Western blotting analysis was performed to detect the total and phosphorylated protein of the IGF-1R, Akt, mTOR, and p70S6K proteins.

4.3.4 The miR-99 family counteracts insulin-mediated activation of the PI3K/Akt/mTOR signaling pathway and downregulation of HBV replication

Many growth factors, such as insulin and epithelial growth factor, promote activation of PI3K/Akt/mTOR signaling in hepatic and hepatocellular cells.[144] Consistently, treatment of HepG2.2.15 cells with insulin at concentrations ranging from 1 to 10 μM for 72 h significantly reduced HBV replication in a dose-dependent manner (Figure 4.14). Compared to mock control with culture medium, insulin exposure also increased the levels of Akt and mTOR phosphorylation (Figure 4.15, A).

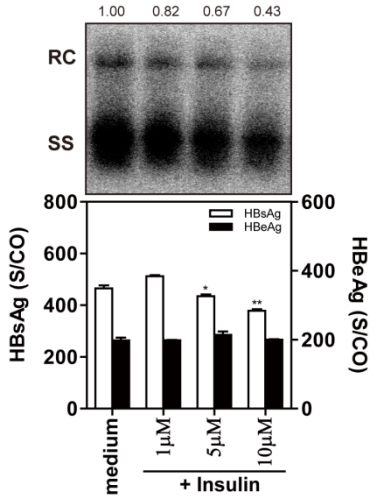

Figure 4.14 Insulin inhibits HBV replication in different dose

(A) HepG2.2.15 cells were treated with different doses of insulin (1, 5, and 10 μM) for 72 h. HBV RIs in cells were isolated and detected by Southern blotting. The levels of HBsAg and HBeAg in the supernatant were determined by chemiluminescent microparticle immunoassay. S/CO = signal to cutoff ratio; RC, relaxed circular DNA; SS = single-stranded DNA. * $P < 0.05$, ** $P < 0.01$, *** $P < 0.001$.

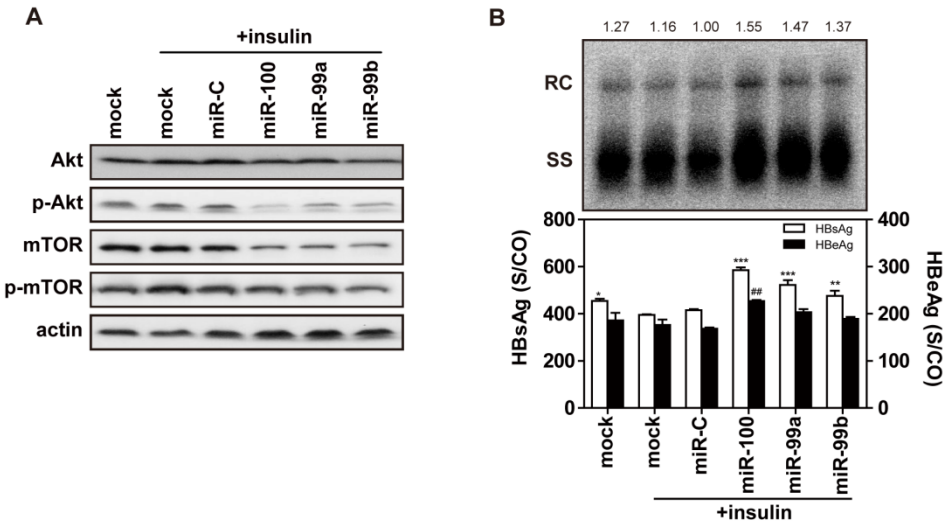

Figure 4.15 The miR-99 family counteracts insulin-mediated activation of the PI3K/Akt/mTOR signaling pathway and downregulation of HBV replication

(A) HepG2.2.15 cells were pre-transfected with miR-99 family mimics or control miR-C at 40 nM. At 24 h post-transfection, fresh medium containing 5 μM insulin was added, and the cells were grown an additional 72 h. Western blotting analysis was performed to detect the total or phosphorylated levels of the Akt, mTOR, and p70S6K proteins using beta-actin as a loading control. (B) HBV replicative intermediates inside the cells were isolated and detected by Southern blotting. The levels of HBsAg and HBeAg in the supernatant were determined by chemiluminescent microparticle immunoassay. S/CO = signal to cutoff ratio; RC: relaxed circular DNA; SS = single-stranded DNA. *, # $P < 0.05$; **, ## $P < 0.01$; ***, ### $P < 0.001$.

We investigated whether ectopic expression of miR-99 family members could inhibit the insulin-mediated activation of PI3K/Akt/mTOR signaling pathway and reverse the reduction of HBV replication. HepG2.2.15 cells were transfected with miR-99 family members at a final culture supernatant concentration of 40 nM. At 24 h post-transfection, the cells were exposed to insulin at a concentration of 10 μM for 72 h. Southern blotting analysis showed that treatment with insulin and miR-99 family members caused opposite effects on HBV replication and gene expression (Figure 4.15, B). Furthermore, ectopic expression of miR-99 family promoted HBV replication, as well as HBsAg and HBeAg production in the presence of insulin. In contrast, the induction of Akt and mTOR phosphorylation by insulin was markedly reduced by miR-99 family members, and also causing a significant decrease in total Akt and mTOR protein expression, as shown by western blotting analysis (Figure 4.15, A). Altogether, these findings suggest that the miR-99 family members counteract insulin-mediated activation of the PI3K/Akt/mTOR signaling pathway and downregulation of HBV replication.

4.4 The miR-99 family promotes HBV replication through mTOR/ULK1 signaling pathway-induced complete autophagy

4.4.1 The miR-99 family promotes HBV replication through mTOR/ULK1 signaling pathway-induced autophagy

The Akt/mTOR signaling pathway is known to regulate several downstream processes including protein synthesis, ribosome biogenesis, lipid synthesis, nutrient import, and autophagy.[94, 145, 146] To assess which biological process downstream of the Akt/mTOR signaling pathway may affect HBV replication, HepG2.2.15 cells were transfected with 6 selected small interfering RNAs (siRNAs) at a final concentration of 20 nM targeting the downstream effectors of the Akt/mTOR signaling pathway. HBV replication and gene expression in HepG2.2.15 cells were analyzed at 96 h post transfection. Compared to the control, HBV replication, as well as HBsAg/HBeAg secretion significantly decreased following knockdown of ULK1 expression (Figure 4.16). These findings suggested that autophagy mediates, at least in part, the regulatory function of Akt/mTOR pathway on HBV replication, consistent with data from previous studies showing that autophagy played a major role in regulating HBV replication.[87]

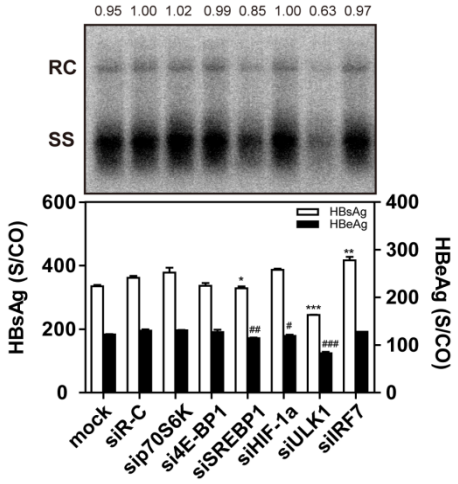

Figure 4.16 Knockdown of downstream genes of Akt/mTOR signaling affects HBV replication

HepG2.2.15 cells were transfected with specific siRNAs against p70S6K, 4E-BP1, SREBP1, HIF-1α, ULK1, or IRF7 mRNAs, or a control siRNA (siR-C) at 20 nM, and harvested after 96 h. The levels of secreted HBsAg and HBeAg in the supernatant were determined by chemiluminescent microparticle immunoassay. HBV replicative intermediates inside the cells were isolated and detected by Southern blotting. S/CO = signal to cutoff ratio; RC: relaxed circular DNA; SS = single-stranded DNA. *, # $P < 0.05$; **, ## $P < 0.01$; ***, ### $P < 0.001$.

Based on the results of the gene-silencing experiment, we asked whether the positive effect of miR-99 family members on HBV replication may be abolished by 3-MA, an inhibitor of autophagy. Consistent with previous findings, treatment with 3-MA alone significantly reduced HBsAg/HBeAg secretion, HBV replication, and capsid formation in HepG2.2.15

cells, but reverse results were obtained with rapamycin (Figure 4.17, A and B). The expression of green fluorescence protein (GFP) tagged LC3 was widely used to study autophagy. In this experiment, Huh7 cells were transfected with the GFP-LC3 plasmid, then treated with rapamycin or 3-MA, respectively. Indeed, rapamycin strongly promoted the formation of autophagic puncta, while 3-MA abolished it, as judged by using the immunofluorescence (IF) detection (Figure 4.17, C and D).

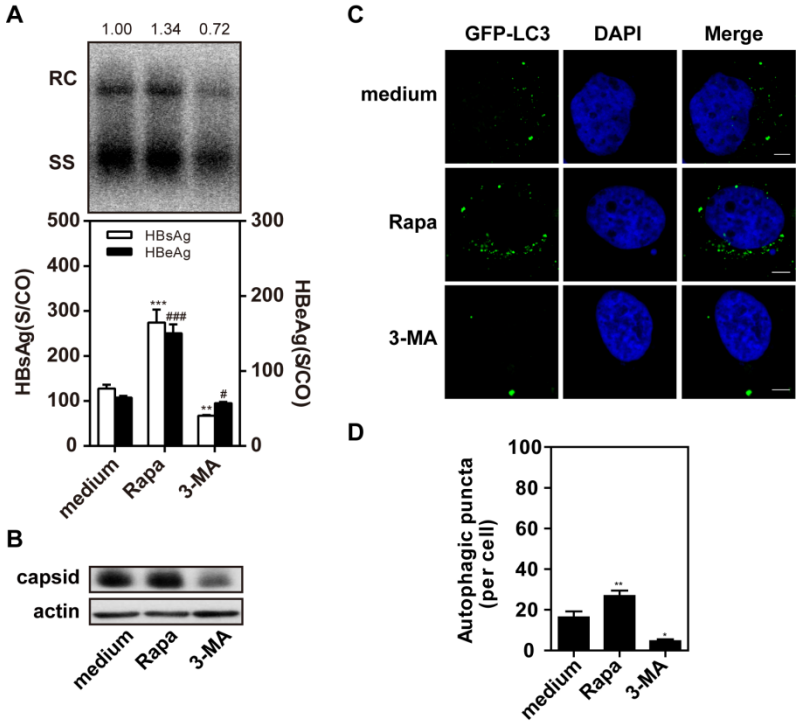

Figure 4.17 Rapamycin and 3-MA modulate HBV replication and autophagy

(A) HepG2.2.15 cells were treated with rapamycin at 1 μM or 3-MA at 10 mM for 48 h. The levels of secreted HBsAg and HBeAg in the supernatant were determined by chemiluminescent microparticle immunoassay. HBV replicative intermediates inside the cells were isolated and detected by Southern blotting. (B) The HBV capsids in cells were extracted and detected by western blotting, and beta-actin was used as the loading control. (C) Huh7 cells were transfected with the plasmid GFP-LC3, then treated with 100 nM rapamycin for 48 h or 10 mM 3-MA for 24 h. Then the cells were fixed and stained with 6-diamidino-2-phenylindole (DAPI). (D) Statistical analysis of the number of LC3-dots per cell was performed. Bars, 5 μm. S/CO = signal to cutoff ratio; RC: relaxed circular DNA; SS = single-stranded DNA. *, # $P < 0.05$; **, ## $P < 0.01$; ***, ### $P < 0.001$.

Thus, HepG2.2.15 cells were pre-transfected with 3 miR-99 family members or a control miRNA at a final concentration of 40 nM, and then treated with 3-MA for 48 h or MHY1485, an mTOR activator, for 72 h. Clearly, both the treatment of 3-MA (Figure 4.18, A) and MHY1485 (Figure 4.18, B) completely abolished the positive effect of the miR-99 family members on HBV replication. In contrast, treatment with rapamycin enhanced the effect of miR-99 family members on HBV replication in HepG2.2.15 cells (Figure 4.18, C).

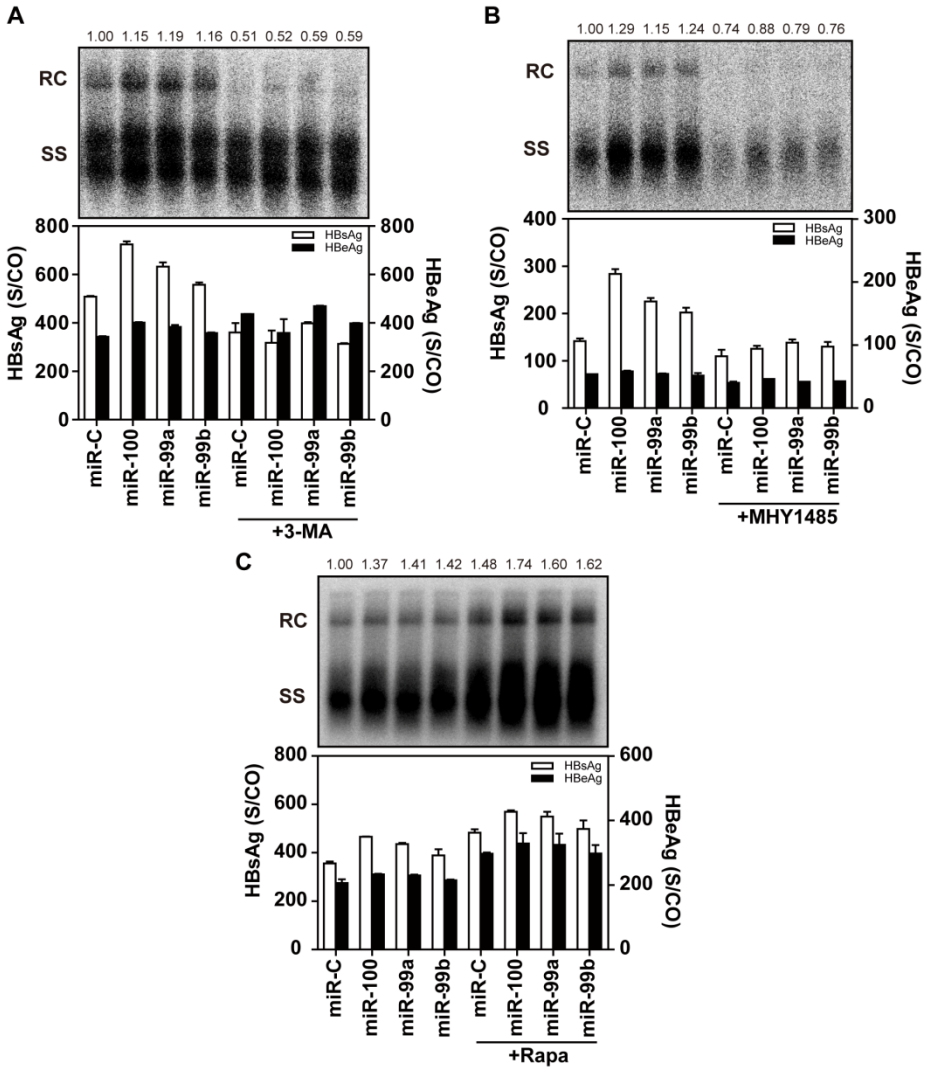

Figure 4.18 Autophagic inhibitors affect the enhancing effect of miR-99 family on HBV replication

HepG2.2.15 cells were pre-transfected with miR-99 family mimics or control miR-C at 40 nM, after which the cells were treated with 10 mM of 3-MA for 48 h (A), 1 μM of MHY1485 for 72 h (B), or 1 μM of rapamycin for 72 h (C). The levels of secreted HBsAg and HBeAg in the supernatant were determined by chemiluminescent microparticle immunoassay. HBV replicative intermediates inside the cells were isolated and detected by Southern blotting. S/CO = signal to cutoff ratio; RC: relaxed circular DNA; SS = single-stranded DNA. * $P < 0.05$, ** $P < 0.01$, *** $P < 0.001$.

4.4.2 The miR-99 family induces complete autophagy formation

Next, we examined whether miR-99 family members were indeed able to modulate autophagy in hepatoma cells. Interestingly, a recent report demonstrated that miR-100 could induce autophagy in HCC cells.[143] Thus, HepG2.2.15 cells were transfected with miR-99 family mimics or control miR-C and harvested after 72 h. Western blotting analysis confirmed that ectopic expression of the miR-99 family significantly elevated the level of autophagy marker LC3-II and promoted the degradation of cargo receptor SQSTM1/p62 (Figure 4.19, A and B).

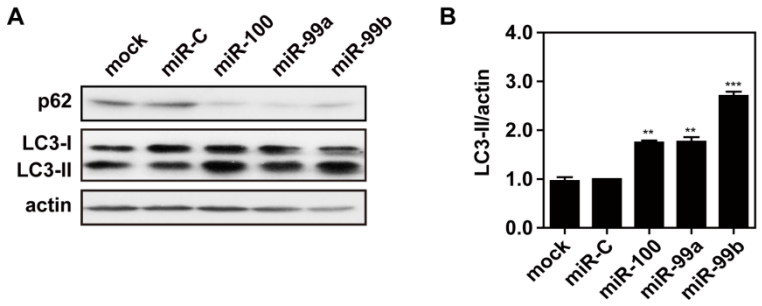

Figure 4.19 The miR-99 family induces complete autophagy formation

HepG2.2.15 cells were transfected with miR-99 family mimics or control miR-C at 40 nM and harvested after 72 h. (A) The levels of LC3 and p62 expression were detected by western blotting, with beta-actin as a loading control. (B) The LC3-II/beta-actin ratios of western blotting bands were quantified by densitometric analysis using ImageJ software. * $P < 0.05$, ** $P < 0.01$, *** $P < 0.001$.

Furthermore, Huh7 cells were cotransfected with 3 miR-99 family members or control miR-C and plasmid GFP-LC3, fixed, stained and finally subjected to confocal microscopy. In concordance with the western blotting results in HepG2.2.15 cells, the miR-99 family members strongly increased the formation of autophagic puncta in Huh7 cells (Figure 4.20, A and B).

In addition, Huh7 cells were transfected with plasmid GFP-LC3 and miRNAs, and then treated with 10 μM chloroquine (CQ), an inhibitor that prevented the acidification of lysosomes. Just as our hypothesis, ectopic expression of miR-99 family members could further increase the formation of autophagosomes in Huh7 cells, as CQ reduced autophagic degradation and preserved the formed autophagosomes (Figure 4.20, C and D). Collectively, all 3 miR-99 family members were capable of promoting autophagy in hepatoma cells; therefore, they likely enhance HBV replication by promoting autophagy.

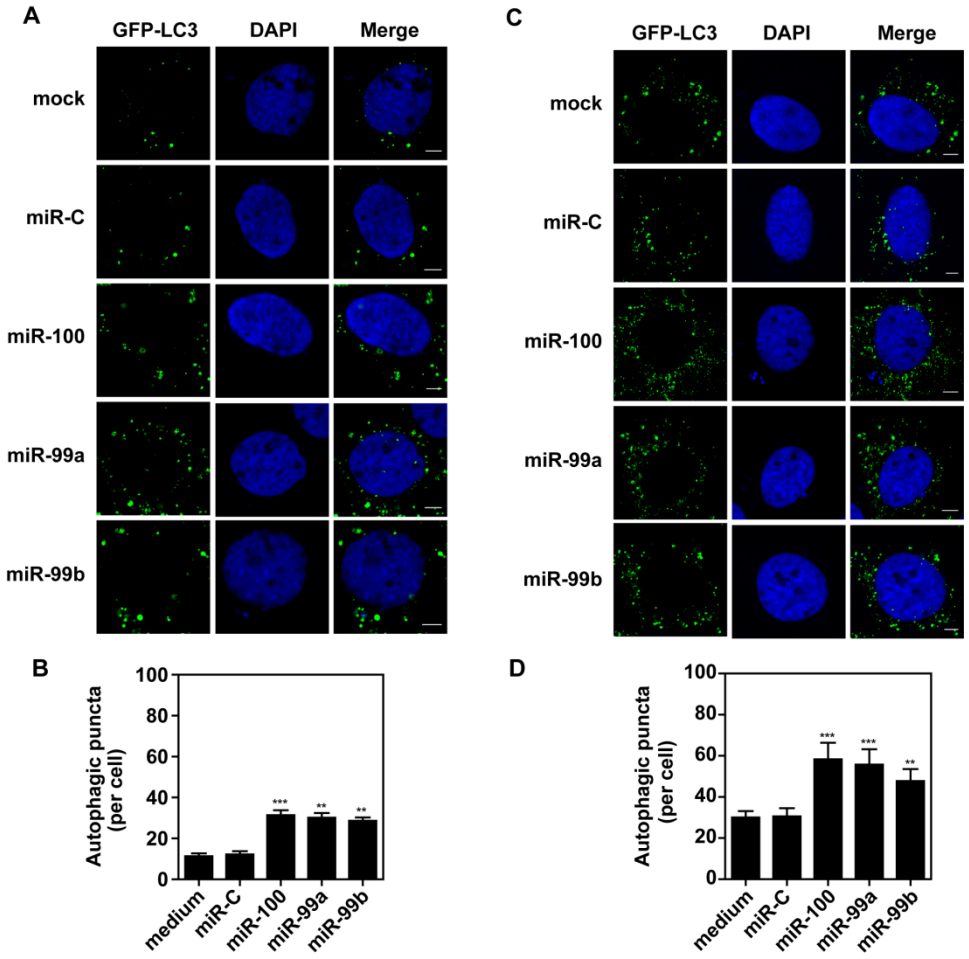

Figure 4.20 The miR-99 family promotes autophagosome formation

Representative images of Huh7 cells co-transfected with the GFP-LC3 plasmid and miR-99 family mimics or control miR-C at 40 nM, and then followed without (A) or with 10 μM CQ for 24 h (C). The cells were fixed and stained with DAPI. Bars, 5 μm. (B and D) Statistical analysis of the numbers of LC3 puncta per cell were performed, respectively. RC, relaxed circular DNA; SS = single-stranded DNA. * $P < 0.05$, ** $P < 0.01$, *** $P < 0.001$.

4.4.3 HBV can be regulated through the mTOR/ULK1 signaling pathway

As inhibition of mTOR activity led to the activation of autophagy via the ULK1-ATG13-FIP200 complex,[94, 98, 147] we addressed the question whether the ULK1 complex participate in miR-99 family-induced autophagy and enhancement of HBV replication. Firstly, we clarified the role of ULK1 on autophagic formation and HBV replication, as ULK1 plays a key role in the initiation of autophagosome formation.[148] HepG2.2.15 cells were transfected with miR-99 family mimics or control miR-C at a final concentration of 40 nM. Cell lysates were collected for western blotting analysis. We observed that ectopic expression of miR-99 family members resulted in ULK1 dephosphorylation in hepatoma cells (Figure 4.21). However, ULK1 silencing by specific siRNAs abolished the enhancing effect of the miR-99 family members on HBV replication,

and HBsAg/HBeAg secretion (Figure 4.22), suggesting that ULK1 is required for the action of the miR-99 family on HBV replication and gene expression.

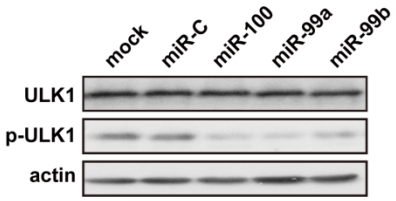

Figure 4.21 MiR-99 family promotes the dephosphorylation of ULK1

HepG2.2.15 cells were transfected with miR-99 family mimics or control miR-C at 40 nM and harvested after 72 h. Total and phosphorylated ULK1 protein levels were detected by western blotting, using appropriate antibodies. Beta-actin was used as a loading control.

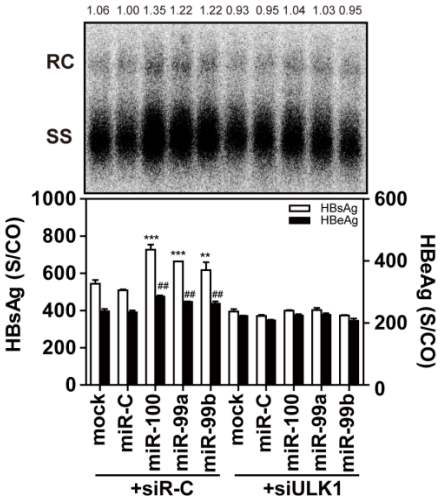

Figure 4.22 HBV replication can be regulated through mTOR/ULK1 signaling pathway

HepG2.2.15 cells were pre-transfected with specific siRNA against ULK1 or control siR-C at 20 nM. The cells were split into new 6-well plates at 24 h post-transfection. 24 hours later, the cells were transfected again with miR-99 family mimics or a miR-C control at 40 nM. HBV replicative intermediates inside the cells were isolated and detected by Southern blotting. The levels of HBsAg and HBeAg secretion in the supernatant were determined by chemiluminescent microparticle immunoassay. S/CO = signal to cutoff ratio; RC, relaxed circular DNA; SS = single-stranded DNA. *, # $P < 0.05$; **, ## $P < 0.01$; ***, ### $P < 0.001$.

Next, we examined the consequences of silencing of ULK1, FIP200, and ATG13, 3 factors forming the complex for involved autophagy initiation, for HBV replication. Thus, HepG2.2.15 cells were transfected with specific siRNA against ULK1, FIP200, ATG13, ATG5 or control siR-C at 20 nM, and harvested after 72 h. ATG5 was used as positive control, as it combined with ATG12 to form the ATG12 conjugation system and to regulate autophagic vesicle formation. The results revealed that the level of LC3-II expression significantly decreased, however, the degradation of p62 was blocked following silencing of these four targets (Figure 4.23, A and B). Meanwhile, the effectiveness of siRNA duplexes was verified by real-time RT-PCR (Figure 4.23, C).

Moreover, Huh7 cells were cotransfected with the GFP-LC3 plasmid and siRNAs, after which they were treated with 10 μM CQ for 24 h. Consistent with previous reports, we found that the frequencies of autophagic puncta of LC3 by confocal microscopy were significantly decreased by silencing of ULK1, FIP200, ATG13, or ATG5 (Figure 4.24, A and B).

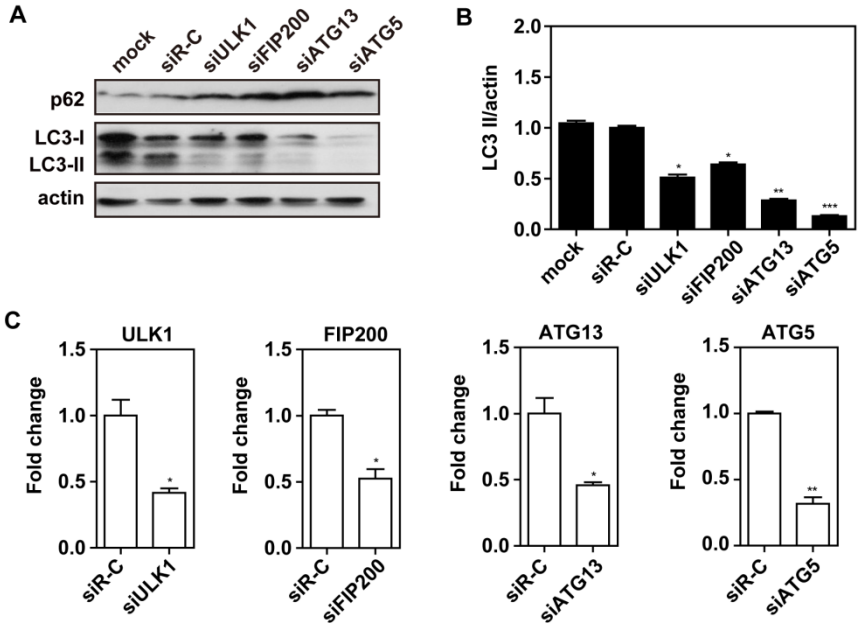

Figure 4.23 Silencing of ULK1-ATG13-FIP200 complex inhibits autophagy formation

(A) HepG2.2.15 cells were transfected with specific siRNA against ULK1, FIP200, ATG13, ATG5 or control siR-C at 20 nM, and harvested after 72 h. The levels of LC3 and p62 expression were by western blotting, and beta-actin was used as a loading control. (B) The LC3-II/beta-actin ratios of western blotting bands were quantified by densitometric analysis using ImageJ software. (C) The levels of the corresponding mRNAs were determined by real-time RT-PCR using specific primers. * $P < 0.05$, ** $P < 0.01$, *** $P < 0.001$.

We next sought to examine whether HBV replication was affected by silencing the components of the ULK1-ATG13-FIP200 complex. HepG2.2.15 cells were transfected with different specific siRNAs, and harvested at 96 h. As revealed in Figure 4.24 C, HBV replication, and HBsAg/HBeAg secretion into the supernatant were significantly decreased by knocking down ATG13 or ATG5 expression, however, the secretion of HBsAg and HBeAg was not significantly decreased by silencing of FIP200. Collectively, our data suggest that mTOR/ULK1 signaling pathway-induced complete autophagy is an important process that mediates the enhancing effect of miR-99 family members on HBV replication (Figure 4.25).

Besides HBV, previous studies have shown that autophagy can be exploited by some other viruses, such as hepatitis C virus, dengue virus, and influenza A virus, to facilitate their replication.[106, 107, 128, 129] However, the exact mechanisms of different phases of autophagic flux affecting virus production remain unclear.

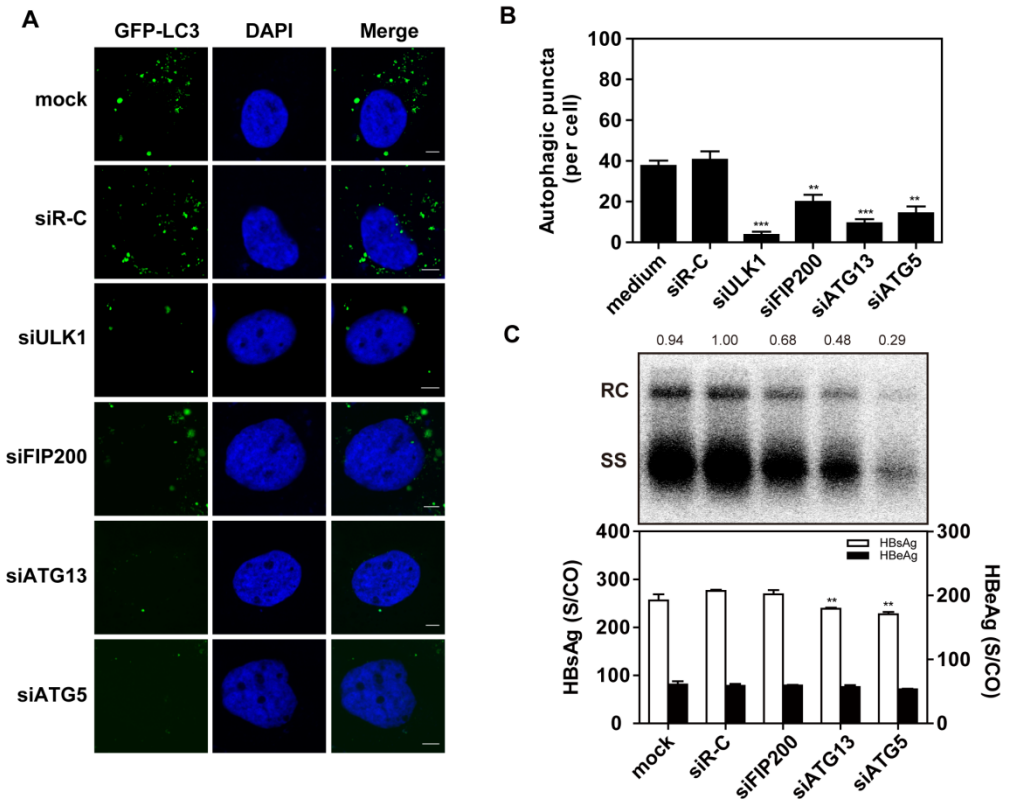

Figure 4.24 HBV replication can be regulated through ULK1-ATG13-FIP200 complex

(A) Representative images of Huh7 cells co-transfected with the plasmid GFP-LC3 and different specific siRNAs, and harvested after 48 h. The cells were fixed, and stained with DAPI. Bars, 5 μm. (B) Statistical analysis of the number of LC3 puncta per cell. (C) HepG2.2.15 cells were transfected with specific siRNAs against FIP200, ATG13, ATG5 or siRNA control at 20 nM, and harvested after 96 h. The detection of HBV replicative intermediates, secreted HBsAg and HBeAg in the supernatant was performed as described above. S/CO = signal to cutoff ratio; RC, relaxed circular DNA; SS = single-stranded DNA. * $P < 0.05$, ** $P < 0.01$, *** $P < 0.001$.

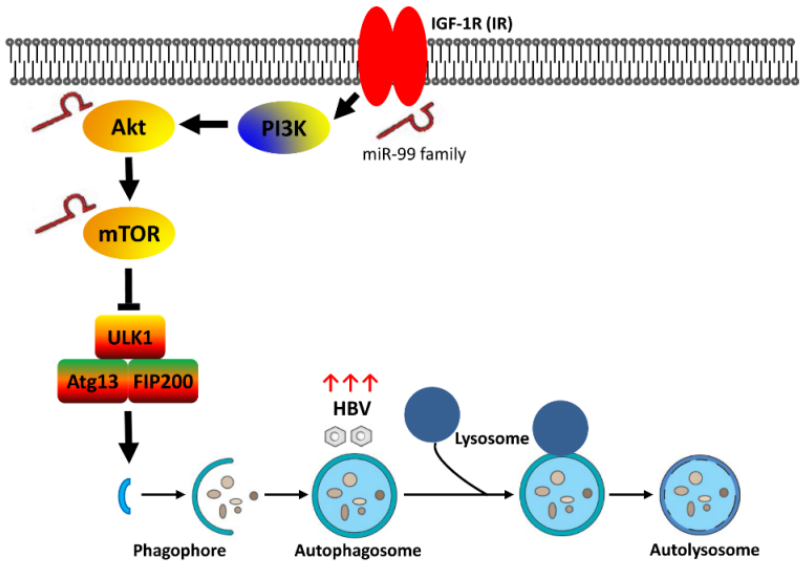

Figure 4.25 Proposed model whereby miR-99 family members regulate HBV replication through

IGF-1R/PI3K/Akt/mTOR/ULK1 signaling-induced autophagy

The miR-99 family members could decrease the levels of total and phosphorylated IGF-1R, Akt, and mTOR by directly targeting their mRNAs, and followed by ULK1 dephosphorylation, resulting in the initiation of autophagosome formation. Thus, ectopic expression of miR-99 family members could promote autophagosome formation through IGF-1R/PI3K/Akt/mTOR signaling pathway, and sequentially enhance HBV production.

4.5 Different autophagic phases inversely affects HBV production

4.5.1 Different autophagy inhibitors inversely affect HBV replication and HBsAg production

To further the effect of different phases on HBV production, Huh7 cells were transfected with the GFP-LC3 plasmid, and treated with the lysosome inhibitor CQ and Rab7 inhibitor CID1067700 (CID) for 48 h, or the PI3KC3 inhibitor 3-MA for 24 h.[130, 149] Immunofluorescence microscopy showed that the number of GFP-LC3 puncta was obviously increased following treatment with CQ and CID, but decreased by 3-MA (Figure 4.26, A and B). Western blotting analysis of cellular lysates revealed that both CQ and CID dramatically stimulated the conversion of light chain 3 (LC3)-I to LC3-II, indicating an increase in membrane-associated LC3. Moreover, both CQ and CID elevated the levels of autophagic cargo SQSTM1/p62 and hepatitis B core antigen (HBcAg) in HepG2.2.15 cells (Figure 4.26, C). Interestingly, 3-MA elevated the levels of p62 expression, but decreased the levels of LC3-II and HBcAg. These results suggest that autophagy inhibitors act on different autophagic phases to have different effects on HBV production.

To investigate the effects of different autophagy inhibitors on HBV production, analyses of secreted HBsAg, HBeAg and viral genomes from the supernatant, and intracellular HBsAg and viral genomes from the cell lysates were performed. Compared to control medium, the late autophagy inhibitors CQ and CID significantly increased the amount of secreted HBsAg and intracellular HBsAg as measured by chemiluminescent microparticle immunoassay (CMIA); however, 3-MA decreased their production (Figure 4.27, A and B). Further, the levels of HBV genomes in the supernatant and inside the cells determined by quantitative real-time PCR, and HBV replicative intermediates measured by Southern blotting were clearly increased (Figure 4.27, C and D).

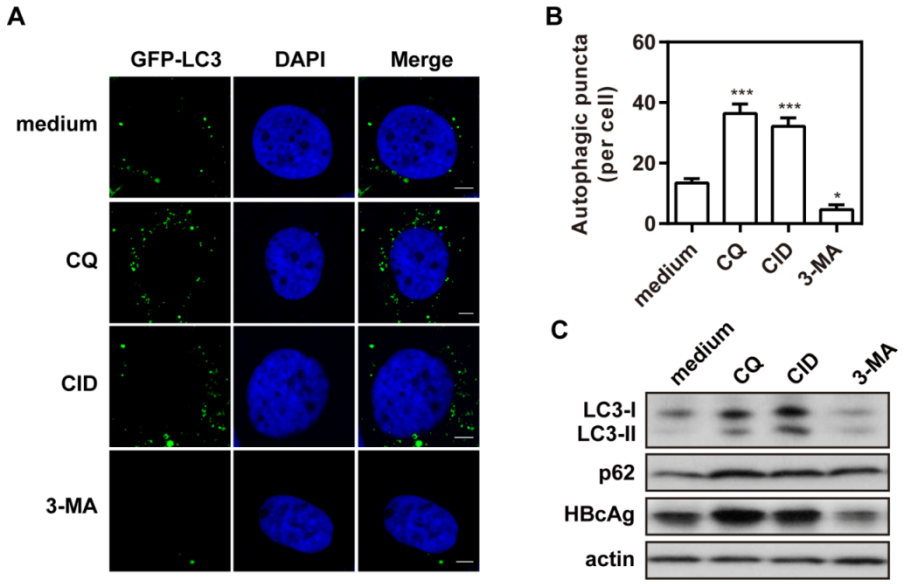

Figure 4.26 Different autophagy inhibitors affect autophagy process

(A) Huh7 cells were transfected with the green fluorescence protein (GFP)-LC3 plasmid (green), followed by treatment with autophagy inhibitors, 10 μM chloroquine (CQ) and 5 μM CID1067700 (CID) for 48 h, and 10 mM 3-MA for 24 h. The cells were fixed and stained with 6-diamidino-2-phenylindole (DAPI, blue). Bars, 5 μm. (B) Statistical analysis of the number of LC3 puncta per cell. (C) HepG2.2.15 cells were treated with autophagy inhibitors, 10 μM CQ and 5 μM CID for 48 h, and 10 mM 3-MA for 24 h. LC3, p62, and HBcAg expression was analyzed by western blotting. Beta-actin was used as a loading control. S/CO = signal to cutoff ratio; RC: relaxed circular DNA; SS = single-stranded DNA. * $P < 0.05$, ** $P < 0.01$, *** $P < 0.001$.

Moreover, the effects of different autophagy inhibitors on HBV production were detected in primary hepatocytes (PHHs). Western blotting showed that the levels of LC3-II expression were significantly elevated by late autophagy inhibitors CQ and CID in PHHs with HBV infection (Figure 4.28, A), but decreased by early autophagy inhibitors 3-MA. Analysis of secreted HBsAg and intracellular HBsAg showed that both CQ and CID significantly increased HBsAg production in PHHs; however, 3-MA decreased HBsAg production (Figure 4.28, B and C).

As the promotion of HBV replication may be mediated by its transcription, the effect of different autophagy inhibitors on HBV transcription was evaluated by real-time RT-PCR. Strikingly, quantification of HBV RNA revealed that all the autophagy inhibitors CQ, CID, and 3-MA did not affect the levels of HBV RNA in HepG2.2.15 cells, indicating that inhibition of different autophagic phases did not inhibit HBV transcription (Figure 4.29, A). In addition, the effect of different autophagy inhibitors on the activities of HBV promoters was measured by Dual-Glo luciferase report assays. Consistently, we observed that the luciferase activities of the HBV SP1, SP2, Core, and X promoters were not clearly changed by all the autophagy inhibitors (Figure 4.29, B).

These data demonstrate that inhibition of different autophagic phases using various autophagy inhibitors may inversely affect HBV replication and HBsAg production.

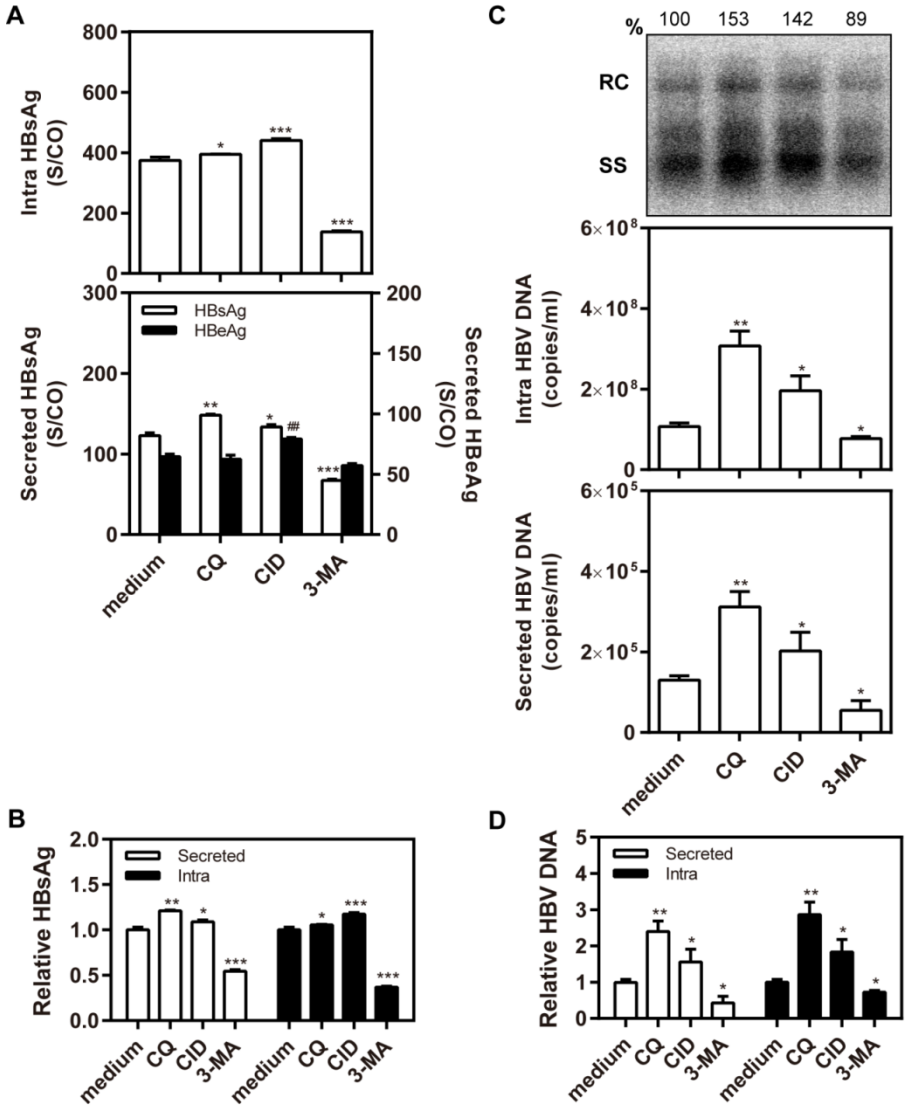

Figure 4.27 Different autophagy inhibitors affect HBV production in Hep2.2.15 cells

HepG2.2.15 cells were treated with autophagy inhibitors, 10 μM chloroquine (CQ) and 5 μM CID1067700 (CID) for 48 h, and 10 mM 3-MA for 24 h. (A) Analysis of secreted HBsAg and HBeAg from the supernatant and intracellular HBsAg from cell lysates was performed by chemiluminescent microparticle immunoassay. (B) The graph shows the relative values of HBsAg from the supernatant and cell lysates. (C) The levels of HBV genomes in the supernatant and inside the cells were determined by quantitative real-time polymerase chain reaction. Hepatitis B virus replicative intermediates inside the cells were isolated and measured by Southern blotting. (D) The graph shows the relative values of secreted and intracellular viral genomes. S/CO = signal to cutoff ratio; RC: relaxed circular DNA; SS = single stranded DNA. *, # $P < 0.05$; **, ## $P < 0.01$; ***, ### $P < 0.001$.

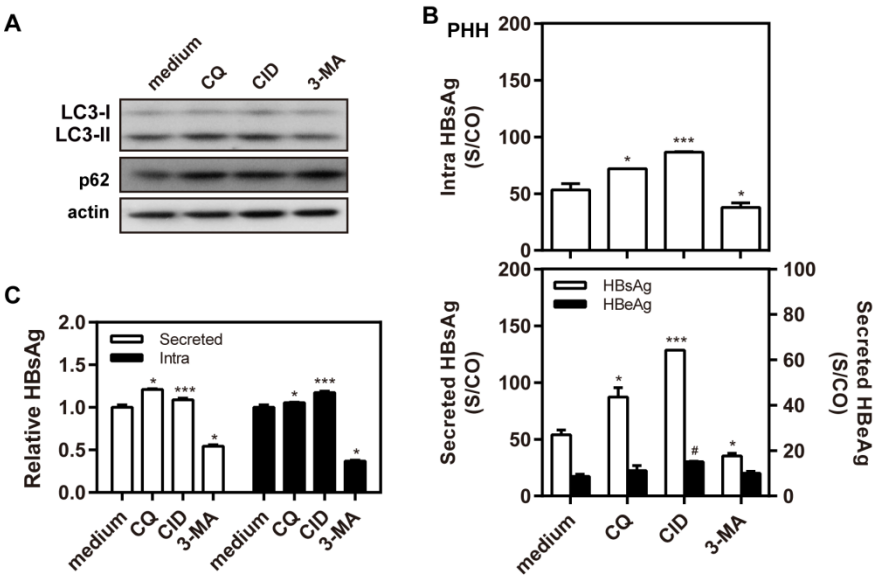

Figure 4.28 Different autophagy inhibitors affect HBV production in primary hepatocytes

Primary hepatocytes with HBV infection were treated with the autophagy inhibitors, 10 μM CQ and 5 μM CID for 48 h, and 10 mM 3-MA for 24 h. (A) LC3 and p62 expression was analyzed by western blotting, with beta-actin used as a loading control. (B) Analysis of secreted HBsAg and HBeAg in the supernatant and intracellular HBsAg from cell lysates in HBV-infected PHHs was performed by chemiluminescent microparticle immunoassay. (C) The graph shows the relative values of HBsAg from the supernatant and cell lysates. S/CO = signal to cutoff ratio. * $P < 0.05$, ** $P < 0.01$, *** $P < 0.001$.

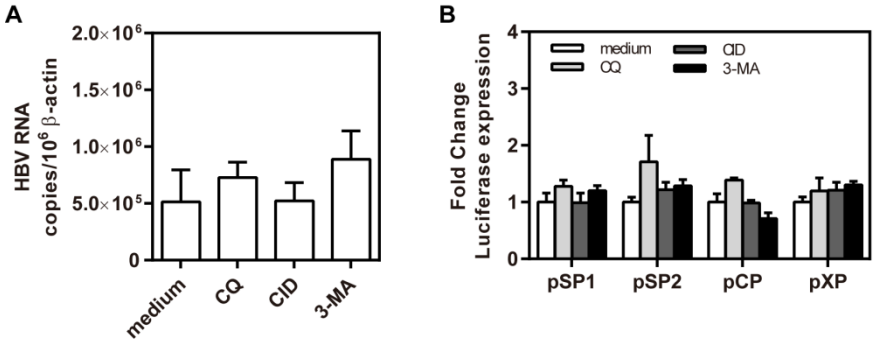

Figure 4.29 Different autophagy inhibitors affect HBV transcription and promoter activity

(A) HepG2.2.15 cells were treated with autophagy inhibitors, 10 μM chloroquine (CQ) and 5 μM CID1067700 (CID) for 48 h, and 10 mM 3-MA for 24 h. HBV pregenomic RNA (pgRNA) levels were analyzed by real-time reverse transcriptase polymerase chain reaction using primers specific for the pgRNA-specific region. (B) Huh7 cells were transfected with luciferase reporters containing the HBV promoter regions pSP1, pSP2, pCP, and pXP, and Renilla as an internal control for 48 h. Firefly and Renilla luciferase activities were analyzed by Dual-Glo luciferase reporter assay. Relative luciferase expression was calculated by fold-change and normalized to control medium treated samples.

4.5.2 Silencing of Rab5 decreases HBV replication and HBsAg production

Rab5, a member of the small GTPase family, has been demonstrated to play an important role

in autophagy and is crucial for HCV replication.[114] Thus, we investigated whether silencing of Rab5 could regulate autophagosome formation in hepatoma cells. First, immunofluorescence microscopy showed that silencing of Rab5 decreased the number of GFP-LC3 puncta (Figure 4.30, A and B). Western blotting analysis of cellular lysates confirmed that silencing of Rab5 decreased the levels of LC3-II using specific siRNA compared to the siRNA control in Huh7 cells; however, the autophagic cargo receptor p62 and HBcAg were increased (Figure 4.30, C). Strikingly, decreased expression of Rab5 strongly decreased the amount of HBV capsid and capsid-associated HBV DNA detected by western blotting and Southern blotting analyses, respectively. These results suggest that silencing of Rab5 decrease HBV production by inhibiting the formation of early autophagy.

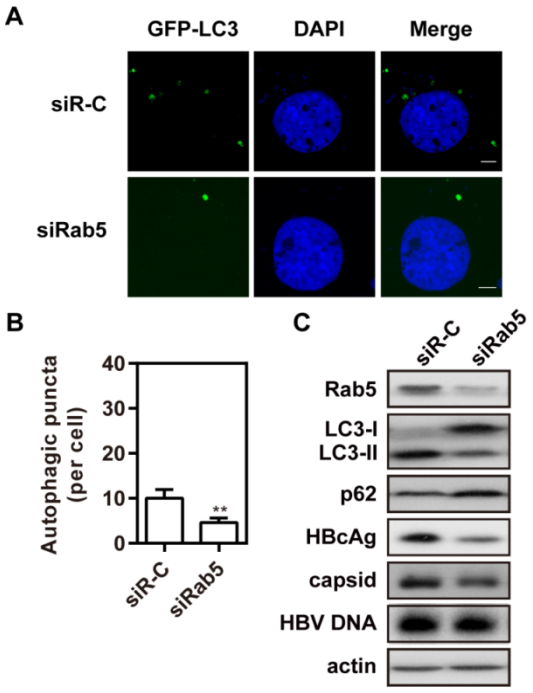

Figure 4.30 Silencing of Rab5 blocks autophagy formation

(A) Huh7 cells were cotransfected with GFP-LC3 plasmid (green) and specific small interfering RNAs against Rab5 (siRab5) or control siRNA (siR-C) at 20 nM and harvested after 48 h. The cells were fixed and stained with DAPI (blue). (B) Statistical analysis of the number of LC3 puncta per cell. (C) Huh7 cells were cotransfected with pSM2 plasmid and specific siRab5 or control siRNA (siR-C) at 20 nM and harvested after 72 h. Analysis of encapsidated HBV DNA was performed by Southern blotting. Rab5, LC3, p62, HBcAg, and viral nucleocapsid expression was analyzed by western blotting. Beta-actin was used as a loading control. S/CO = signal to cutoff ratio. * $P < 0.05$, ** $P < 0.01$, *** $P < 0.001$.

To confirm that silencing of Rab5 decreases the levels of secreted and intracellular HBV production, secreted HBsAg and HBeAg in the supernatant and intracellular HBsAg from cell lysates were quantified by CMIA in Huh7 cells. The results revealed that silencing of Rab5 obviously decreased the levels of secreted HBsAg in the supernatant and intracellular HBsAg, but there was no significant effect on secreted HBeAg (Figure 4.31, A and B). Quantification

of HBV DNA by quantitative real-time PCR revealed that silencing of Rab5 significantly decreased the levels of intracellular HBV DNA in Huh7 cells. Moreover, Southern blotting confirmed that silencing of Rab5 decreased HBV replication (Figure 4.31, C and D).

Next, we examined the consequences of silencing Rab5 on HBV replication in HepG2.2.15 cells. The cells were transfected with specific siRab5 and harvested after 96 h. In concordance with the results of HBsAg in Huh7 cells, the results showed that silencing of Rab5 obviously decreased the levels of secreted HBsAg in the supernatant and intracellular HBsAg, but there was no significant effect on secreted HBeAg (Figure 4.32, A and B). Quantification of HBV DNA by quantitative real-time PCR revealed that silencing of Rab5 significantly decreased HBV DNA in the supernatant and inside the cells. Moreover, Southern blotting analysis confirmed that silencing of Rab5 decreased HBV replicative intermediates (Figure 4.32, C and D).

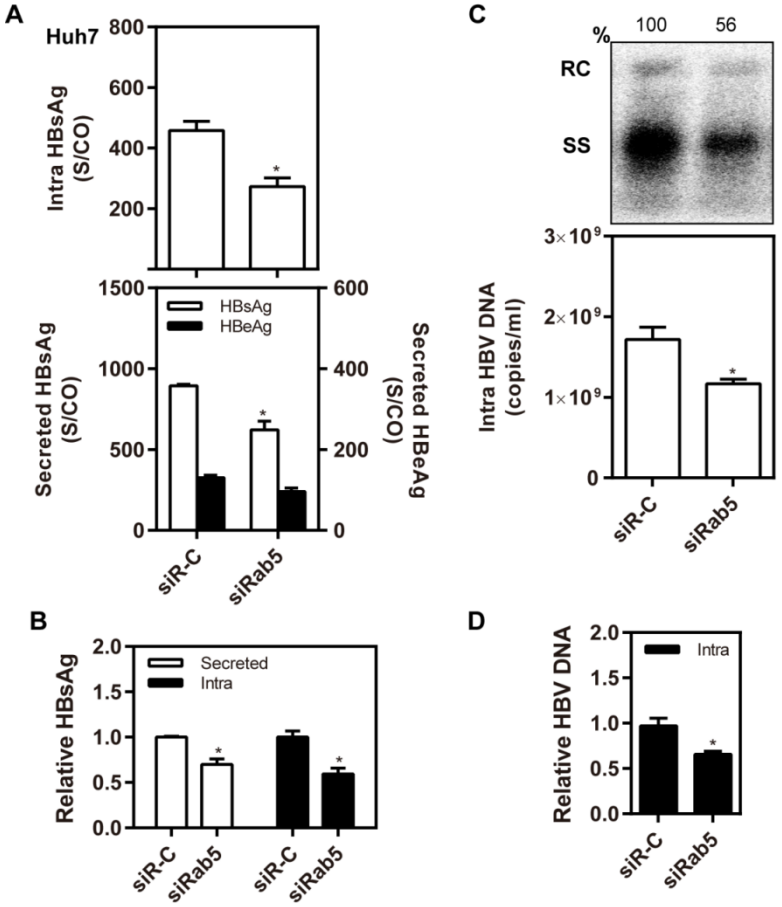

Figure 4.31 Silencing of Rab5 decreases HBV production in Huh7 cells

Huh7 cells were cotransfected with pSM2 plasmid and specific siRab5 or control siRNA (siR-C) at 20 nM and harvested after 72 h. (A) Analysis of secreted HBsAg and HBeAg in the supernatant and intracellular HBsAg from cell lysates was performed by chemiluminescent microparticle immunoassay. (B) The graph shows the relative values of HBsAg from the supernatant and cell lysates. (C) The levels of HBV genomes inside the cells were determined by quantitative real-time polymerase chain reaction. Analysis of HBV replicative intermediates was performed by Southern blotting. (D) The graph shows the relative values of intracellular viral genomes.

S/CO = signal to cutoff ratio; RC: relaxed circular DNA; SS = single-stranded DNA. * $P < 0.05$, ** $P < 0.01$, *** $P < 0.001$.

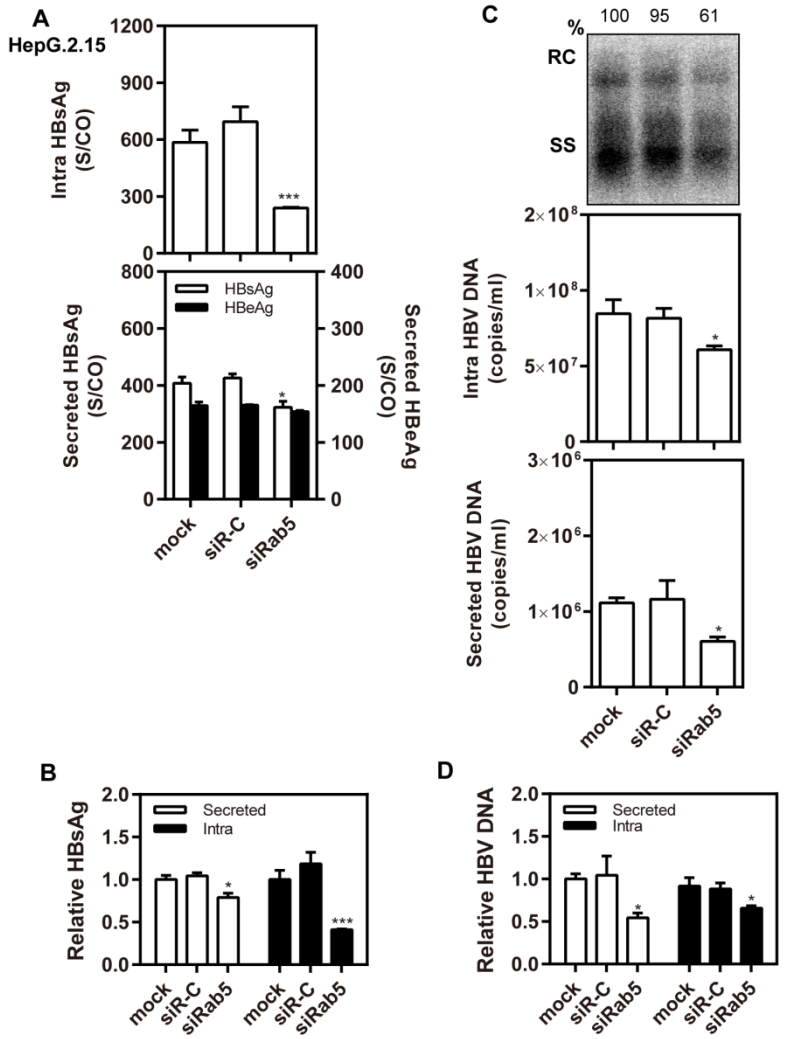

Figure 4.32 Silencing of Rab5 decreases HBV production in HepG2.2.15 cells

HepG2.2.15 cells were transfected with specific siRab5 or control siRNA (siR-C) at 20 nM and harvested after 96 h. (A) Analysis of secreted HBsAg and HBeAg in the supernatant and intracellular HBsAg from cell lysates was performed by chemiluminescent microparticle immunoassay. (B) The graph shows the relative values of HBsAg from the supernatant and cell lysates. (C) The levels of HBV genomes inside the cells were determined by quantitative real-time polymerase chain reaction. Analysis of HBV replicative intermediates was performed by Southern blotting. (D) The graph shows the relative values of secreted and intracellular viral genomes. S/CO = signal to cutoff ratio; RC: relaxed circular DNA; SS = single-stranded DNA. * $P < 0.05$, ** $P < 0.01$, *** $P < 0.001$.

Moreover, we test the consequences of silencing of Rab5 in different HBsAg expressive abundance. Huh7 cells were cotransfected with an expression vector with HBsAg high expression (HK-188) or with HBsAg low expression (HBs-2-S), and specific siRab5 or control siRNA. The results revealed that silencing of Rab5 obviously decreased the levels of secreted HBsAg in the supernatant and intracellular HBsAg from cell lysates with HBsAg

low expression (Figure 4.33, A and B), but there was no significant effect on HBsAg high expression (Figure 4.33, C and D). These data confirm that silencing of Rab5 leads to different consequences of HBsAg production in different HBsAg expressive abundance.

As the promotion of HBV replication may be mediated by its transcription, the effect of silencing of Rab5 on HBV transcription was evaluated by real-time RT-PCR. Strikingly, quantification of HBV RNA revealed that silencing of Rab5 did not affect the levels of HBV RNA in HepG2.2.15 cells, indicating that silencing of Rab5 did not inhibit HBV transcription (Figure 4.34, A). In addition, the effect of silencing of Rab5 on the activities of HBV promoters was measured by Dual-Glo luciferase report assays. Consistently, we observed that the luciferase activities of the HBV SP1, SP2, Core, and X promoters were not clearly changed by silencing of Rab5 (Figure 4.34, B). These data suggest that silencing of Rab5 decrease HBV production neither through inhibiting HBV transcription nor through inhibiting HBV promoter activities.

Taken together, these data demonstrate that silencing of Rab5 decreases the amount of secreted and intracellular HBsAg, as well as the levels of secreted HBV DNA and intracellular HBV replication.

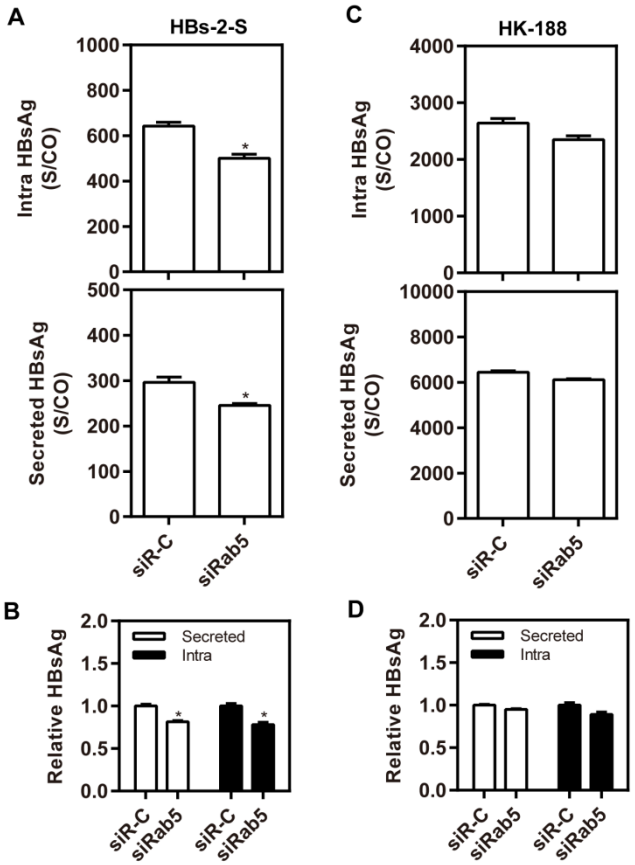

Figure 4.33 Silencing of Rab5 affects HBsAg production in different HBsAg expressive abundance

Huh7 cells were cotransfected with an expression vector (A) with HBsAg low expression (HBs-2-S) or (C) with HBsAg high expression (HK-188), and specific siRab5 or control siRNA (siR-C) at 20 nM, and harvested after

72 h. Secreted HBsAg in the supernatant and intracellular HBsAg from cell lysates were analyzed by chemiluminescent microparticle immunoassay. (B and D) The graphs show the relative values of HBsAg from the supernatant and cell lysates. * $P < 0.05$; ** $P < 0.01$; *** $P < 0.001$.

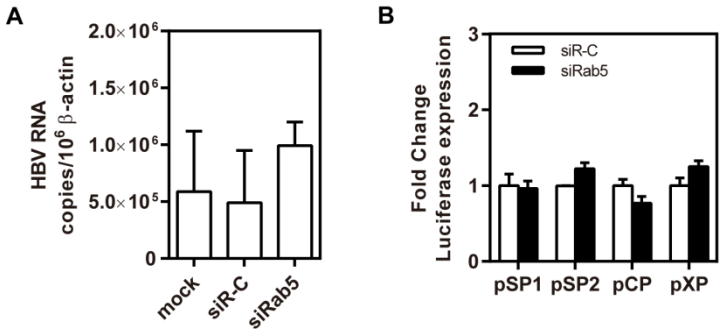

Figure 4.34 Silencing of Rab5 does not inhibit HBV transcription and promoter activity

HepG2.2.15 cells were transfected with specific siRab5 or control siRNA (siR-C) at 20 nM and harvested after 72 h. (A) Analysis of HBV pregenomic RNA (pgRNA) levels was performed by real-time reverse transcriptase polymerase chain reaction, using primers specific for the pgRNA-specific region. (B) Luciferase reporters containing the HBV promoter regions pSP1, pSP2, pCP, and pXP were co-transfected with specific siRab5 or control siRNA (siR-C) at 20 nM into Huh7 cells. At 48 h post-transfection, firefly and Renilla luciferase activities were analyzed by Dual-Glo luciferase report assay. Relative luciferase expression was calculated by fold-change, and normalized to control medium treated samples.

4.5.3 Activation of Rab5 promotes HBV replication and HBsAg production

To clarify the effect of Rab5 on autophagosome formation, Huh7 cells were cotransfected with GFP-LC3 plasmid and an expression vector carrying Rab5 (Flag-Rab5) or control vector (pcDNA5), and GFP-LC3 puncta were detected by immunofluorescence microscopy. The results revealed that overexpression of Rab5 increased the number of GFP-LC3 puncta (Figure 4.35, A and B). Western blotting analysis confirmed that overexpression of Rab5 dramatically stimulated the conversion of LC3-I to LC3-II, but decreased the levels of autophagic cargo p62 and HBcAg (Figure 4.35, C).

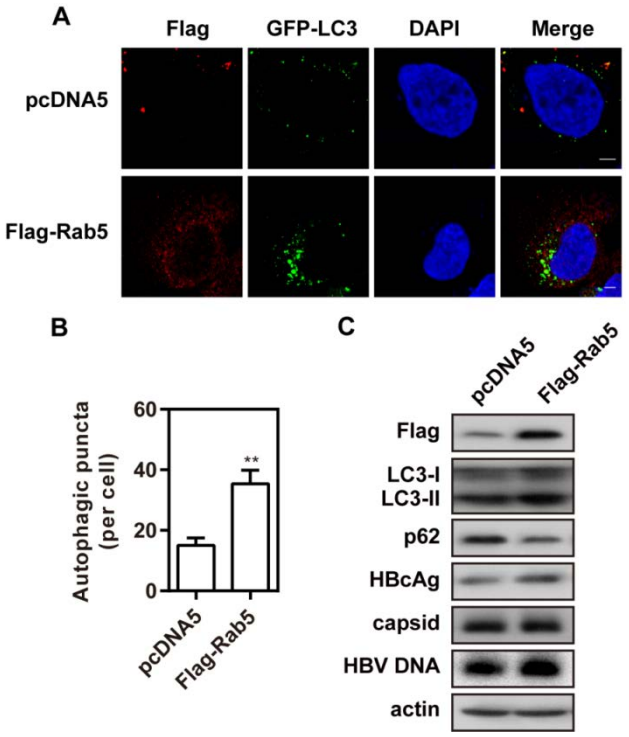

Figure 4.35 Overexpression of Rab5 promotes autophagy formation

(A) Huh7 cells were cotransfected with GFP-LC3 plasmid (green) and an expression vector carrying Rab5 (Flag-Rab5) or control vector (pcDNA5) and harvested after 48 h. The cells were fixed, incubated with primary antibody anti-HA, and then stained with Alexa Fluor 594 (red) conjugated anti-rabbit secondary antibody IgG. (B) Statistical analysis of the number of GFP-LC3 puncta per cell. (C) Huh7 cells were cotransfected with pSM2 plasmid and Flag-Rab5 or control vector pcDNA5 and harvested after 72 h. Analysis of encapsidated HBV DNA was performed by Southern blotting. Rab5, LC3, p62, HBcAg, and viral nucleocapsid expression was analyzed by western blotting, with beta-actin used as a loading control. * $P < 0.05$; ** $P < 0.01$; *** $P < 0.001$.

Because previous studies demonstrated that Rab5 is crucial for HCV replication, we examined the effect of Rab5 on HBV formation. As expected, overexpression of Rab5 strongly increased HBV capsid according to western blotting, and capsid-associated HBV DNA according to Southern blotting analysis in Huh7 cells (Figure 2.10, C). Furthermore, the results of CMIA revealed that overexpression of Rab5 clearly increased secreted HBsAg levels in the supernatant and intracellular HBsAg, but there was no significant effect on secreted HBeAg (Figure 4.36, A and B). Quantification of HBV DNA by quantitative real-time PCR revealed that overexpression of Rab5 significantly increased the levels of intracellular HBV DNA. In addition, Southern blotting analysis confirmed that overexpression of Rab5 enhanced HBV replication (Figure 4.36, C and D).

Next, we examined the effect of defective activation of Rab5 on HBV replication. Huh7 cells were cotransfected with the pSM2 plasmid and an expression vector carrying constitutively active Rab5 (Rab5 CA), dominant negative Rab5 (Rab5 DN), or control vector pEGFP-N1, and harvested after 72 h. Secreted HBsAg and HBeAg in the supernatant and

intracellular HBsAg from cell lysates were quantified as described above. The results revealed that overexpression of mutant Rab5 clearly decreased the levels of secreted HBsAg in the supernatant and intracellular HBsAg; however, overexpression of constitutively active Rab5 strongly increased their relative expression (Figure 4.37, A and B). Quantification of HBV DNA by quantitative real-time PCR revealed that overexpression of mutant Rab5 significantly decreased intracellular HBV DNA levels in Huh7 cells. In addition, Southern blotting analysis confirmed that overexpression of mutant Rab5 decreased the levels of HBV replication (Figure 4.37, C and D).

Taken together, these data reveal that activation of Rab5 increased the amount of secreted and intracellular HBsAg, as well as secreted HBV DNA levels and intracellular HBV replication.

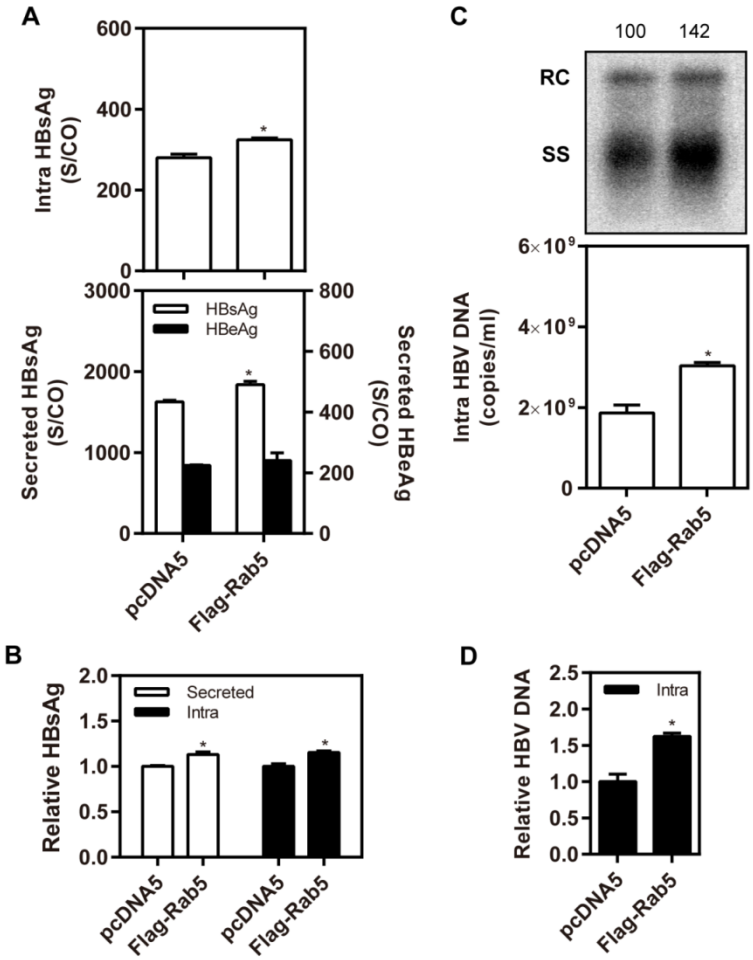

Figure 4.36 Overexpression of Rab5 increases HBV production

(A) Huh7 cells were cotransfected with pSM2 plasmid and Flag-Rab5 or control vector pcDNA5 and harvested after 72 h. Analysis of encapsidated HBV DNA was performed by Southern blotting. Rab5, LC3, p62, HBcAg, and viral nucleocapsid expression was performed by western blotting, with beta-actin as a loading control. (B) The levels of secreted HBsAg and HBeAg in the supernatant and intracellular HBsAg from cell lysates were detected by CMIA. (C) The graph shows the relative values of HBsAg from the supernatant and cell lysates. The levels of HBV genomes inside the cells were detected by quantitative real-time PCR analysis. Analysis of HBV

replicative intermediates was performed by Southern blotting. (D) The graph shows the relative values of intracellular viral genomes. S/CO = signal to cutoff ratio; RC: relaxed circular DNA; SS = single-stranded DNA. *, # $P < 0.05$; **, ## $P < 0.01$; ***, ### $P < 0.001$.

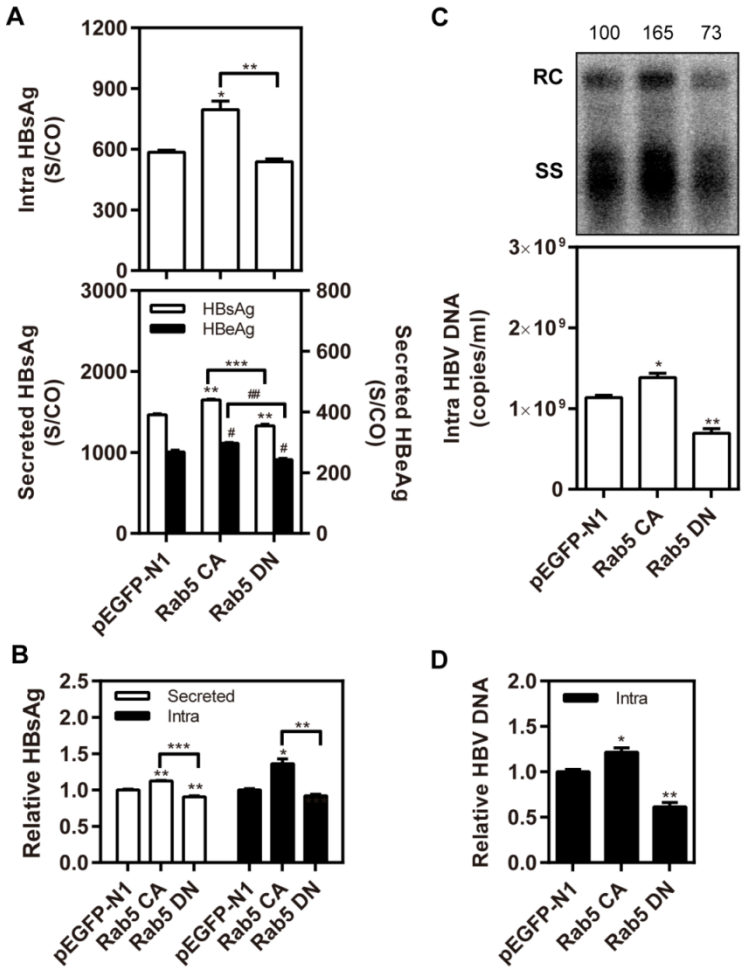

Figure 4.37 Activation of Rab5 increases HBV production

Huh7 cells were cotransfected with pSM2 plasmid and an expression vector carrying constitutively active Rab5 (Rab5 CA), dominant negative Rab5 (Rab5 DN), or control vector pEGFP-N1 and harvested after 72 h. (A) Analysis of secreted HBsAg and HBeAg in the supernatant and intracellular HBsAg from cell lysates was performed by chemiluminescent microparticle immunoassay. (B) The graph shows the relative values of HBsAg from the supernatant and cell lysates. (C) The levels of HBV genomes inside the cells were determined by quantitative real-time polymerase chain reaction. Analysis of HBV replicative intermediates was performed by Southern blotting. (D) The graph shows the relative values of secreted and intracellular viral genomes. S/CO = signal to cutoff ratio; RC: relaxed circular DNA; SS = single-stranded DNA. * $P < 0.05$; ** $P < 0.01$; *** $P < 0.001$.

4.5.4 Silencing of Rab5 decreases HBV production by interfering with autophagosome formation

To determine the exact mechanism of Rab5 affecting HBV formation, we analyzed the effect of inhibiting early autophagic phase on autophagosome formation. Colocalization of

GFP-LC3 with HBs-Cherry was evaluated by confocal microscopy in Huh7 cells. First, the results showed that knockdown of Rab5 decreased the number of GFP-LC3 puncta (Figure 4.38, A and B). Further confocal microscopy analysis showed that silencing of Rab5 slightly decreased the colocalization of GFP-LC3 with HBs-Cherry, while treatment with CQ strongly increased colocalization. These data indicate that inhibition of autophagosome formation by silencing of Rab5 decreased intracellular HBsAg.

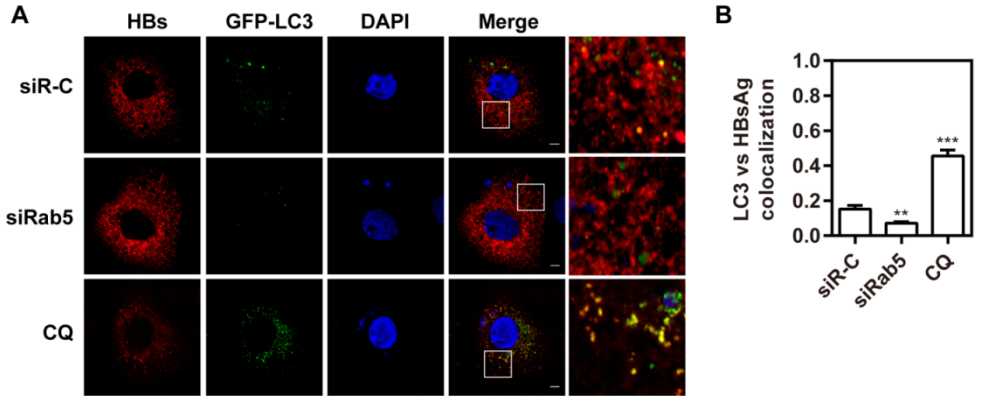

Figure 4.38 Silencing of Rab5 decreases the colocalization of LC3 and HBsAg

(A) Huh7 cells were transfected with HBsAg plasmid with expressing mCherry (red). At 24 h post-transfection, the cells were split and cotransfected with GFP-LC3 plasmid (green) and specific siRab5 or control siRNA (siR-C) at 20 nM and harvested after 48 h. The cells were fixed and stained with DAPI (blue). The colocalization of LC3 and HBsAg was measured by confocal microscopy. Bars, 5 μm. (B) Statistical analysis of the colocalization coefficient of LC3 and HBsAg. * $P < 0.05$, ** $P < 0.01$, *** $P < 0.001$.

The results were further confirmed by silencing of ULK1 or Rab5, followed by treatment with rapamycin or 3-MA. Quantification of secreted HBsAg in the supernatant and intracellular HBsAg from cell lysates revealed that rapamycin further increased the levels of secreted and intracellular HBsAg in HepG2.2.15 cells, but did not significantly increase following silencing of ULK1 (Fig. 4.39) or Rab5 (Fig. 4.40). However, 3-MA further decreased the levels of secreted and intracellular HBsAg, with no significant difference following silencing of Rab5 compared to the siRNA control. Thus, these data indicate that silencing of Rab5 decreases the levels of secreted and intracellular HBsAg by blocking the autophagosome formation.

Taken together, these data demonstrate that silencing of Rab5 decreases HBV production and secretion by interfering with autophagosome formation.

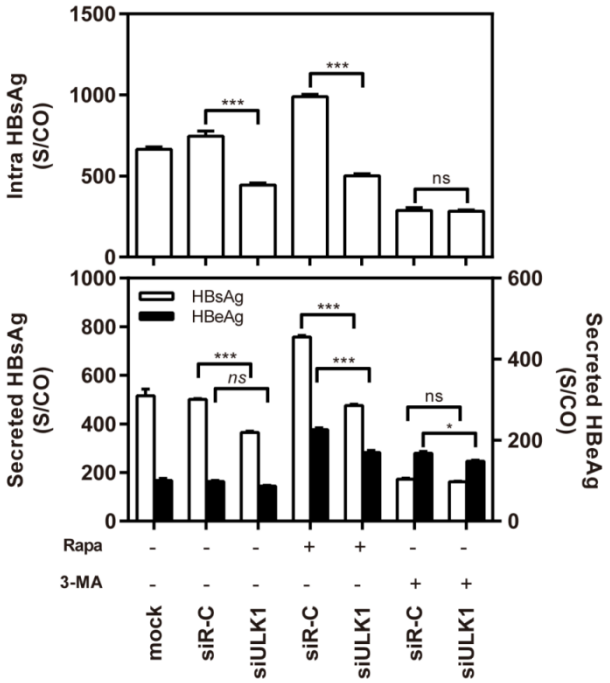

Figure 4.39 Silencing of ULK1 decreases HBV production by interfering with early autophagy

HepG2.2.15 cells were transfected with specific siULK1 or control siRNA (siR-C) at 20 nM. At 24 h post-transfection, the cells were treated with 2 μM rapamycin (Rapa), or 10 mM 3-MA for 48 h. The levels of secreted HBsAg and HBeAg in the supernatant and intracellular HBsAg from cell lysates were determined by chemiluminescent microparticle immunoassay. S/CO = signal to cutoff ratio. *, # $P < 0.05$; **, ## $P < 0.01$; ***, ### $P < 0.001$; ns, not significant.

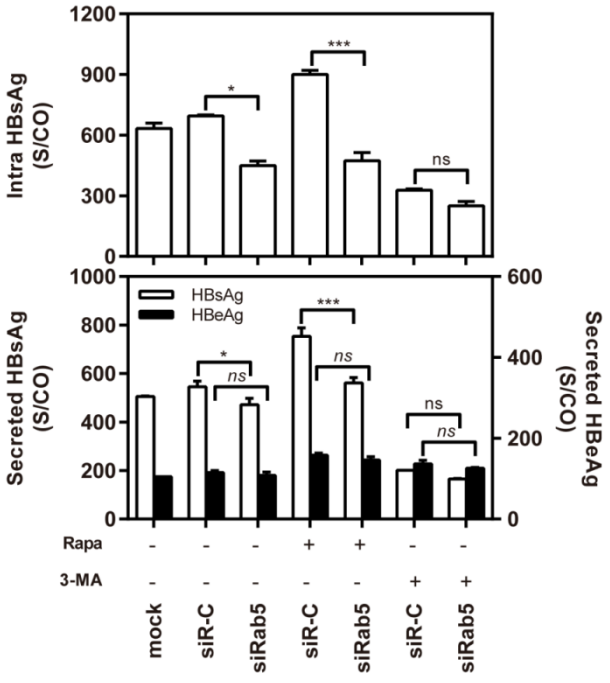

Figure 4.40 Silencing of Rab5 decreases HBV production by interfering with early autophagy

HepG2.2.15 cells were transfected with specific siRab5 or control siRNA (siR-C) at 20 nM. At 24 h post-transfection, the cells were treated with 2 μM rapamycin (Rapa) or 10 mM 3-MA for 48 h. The levels of secreted HBsAg and HBeAg in the supernatant and intracellular HBsAg from cell lysates were determined by

chemiluminescent microparticle immunoassay. S/CO = signal to cutoff ratio. *, # $P < 0.05$; **, ## $P < 0.01$; ***, ### $P < 0.001$; ns, not significant.

4.5.5 Silencing of Rab7 promotes HBV replication and HBsAg production

HBV is known to hijack steps of the autophagic pathway by inhibiting autophagic degradation through impairing lysosomal maturation or dampening autophagy maturation via negative regulation of Rab7 expression. During the maturation process of EEs, inactivated Rab5 is substituted by Rab7 on the endosomal membrane. Subsequently, Rab7 may recruit its effectors, RILP and OSBPL1A/ORP1L, followed by directing the LE trafficking and participating in the fusion step with lysosomes. Thus, we investigated whether autophagic degradation of autophagosome -lysosome fusion is the major target of HBV.

We observed that silencing of Rab7 increased the number of GFP-LC3 puncta by immunofluorescence microscopy in Huh7 cells (Figure 4.41, A and B). Western blotting analysis of cellular lysates confirmed that silencing of Rab7 elevated the levels of autophagic cargo LC3-II and p62 by specific siRab7 compared to the siRNA control (Figure 4.41, C). As expected, decreased expression of Rab7 strongly increased HBcAg and HBV capsid levels detected by western blotting, and increased the levels of capsid-associated HBV DNA detected by Southern blotting analysis. These data demonstrate that silencing of Rab7 promotes HBV production by modulating the autophagosome-lysosome fusion process.

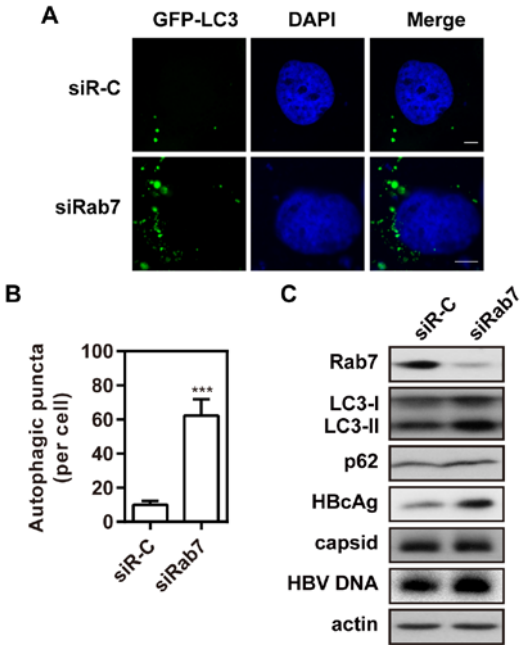

Figure 4.41 Silencing of Rab7 blocks the degradation of autophogosomes

Huh7 cells were cotransfected with GFP-LC3 plasmid (green) and specific small interfering RNAs against Rab7 (siRab7) or control siRNA (siR-C) at 20 nM and harvested after 48 h. (A) The cells were fixed and stained with DAPI (blue). The GFP-LC3 puncta were measured by confocal microscopy. Bars, 5 μm. (B) Statistical analysis of the number of LC3 puncta per cell. (C) Huh7 cells were cotransfected with pSM2 plasmid and specific siRab7

or control siRNA (siR-C) at 20 nM and harvested after 72 h. Analysis of encapsidated HBV DNA was performed by Southern blotting. Rab7, LC3, p62, HBcAg, and viral nucleocapsid expression was analyzed by western blotting. Beta-actin was used as a loading control. * $P < 0.05$, ** $P < 0.01$, *** $P < 0.001$.

It was previously reported that CID is a potent Rab7 inhibitor; thus, we evaluated its effect on HBV replication in HepG2.2.15 cells. In the present study, CID treatment led to an increase in secreted HBsAg and HBV replicative intermediates (Figure 4.42). As we hypothesized, silencing of Rab7 increased the levels of secreted and intracellular HBV. CMIA analysis revealed that silencing of Rab7 strongly increased the levels of secreted HBsAg in the supernatant and intracellular HBsAg, but there was no significant effect on secreted HBeAg (Figure 4.43, A and B). Moreover, silencing of Rab7 increased intracellular HBV DNA levels according to quantitative real-time PCR and HBV replicative intermediates according to Southern blotting analysis (Figure 4.43, C and D).

Next, we sought to confirm that knockdown of Rab7 affects HBV replication in HepG2.2.15 cells. The cells were transfected with specific siRab7 and harvested after 96 h. In concordance with the previous results in Huh7 cells, the data revealed that silencing of Rab7 clearly increased the levels of secreted HBsAg in the supernatant and intracellular HBsAg (Figure 4.44, A and B). Quantification of HBV DNA by quantitative real-time PCR revealed that silencing of Rab7 significantly increased the levels of HBV DNA in the supernatant and inside of the cells. Moreover, Southern blotting analysis further confirmed that silencing of Rab7 promoted HBV replication (Figure 4.44, C and D).

Moreover, we test the consequences of silencing of Rab7 in different HBsAg expressive abundance. Huh7 cells were cotransfected with an expression vector with HK-188 or HBs-2-S, and specific siRab7 or control siRNA. The results revealed that silencing of Rab7 obviously increased the levels of secreted HBsAg in the supernatant and intracellular HBsAg from cell lysates with HBsAg low expression (Figure 4.45, A and B). Silencing of Rab7 also significantly increased intracellular HBsAg levels with HBsAg high expression, but there was no significant effect on secreted HBsAg (Figure 4.45, C and D). These results confirm that silencing of Rab7 leads to different consequences of HBsAg production in different HBsAg expressive abundance.

Finally, the effect of silencing of Rab7 on HBV transcription was evaluated by real-time RT-PCR. The results showed that silencing of Rab7 did not affect HBV RNA levels in HepG2.2.15 cells (Figure 4.46, A). In addition, the effect of silencing of Rab7 on the activities of HBV promoters was measured by Dual-Glo luciferase report assays. Consistently, we observed that the luciferase activities of the HBV SP1, SP2, Core, and X promoters were not significantly changed by silencing of Rab7 (Figure 4.46, B). These data suggest that silencing

of the Rab7 increase HBV production neither through promoting HBV transcription nor through promoting HBV promoter activities.

These data demonstrate that silencing of Rab7 increases secreted and intracellular HBsAg levels, as well as secreted HBV DNA levels and intracellular HBV replication.

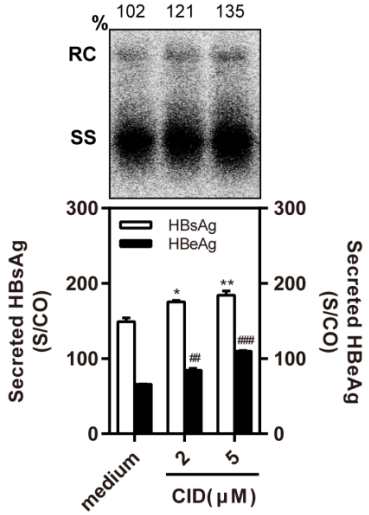

Figure 4.42 Rab7 inhibitor increases HBV production in different dose

HepG2.2.15 cells were treated with different doses of CID1067700 (CID, 0, 2 μM, or 5 μM) and harvested after 48 h. Analysis of HBV replicative intermediates was performed by Southern blotting. Analysis of secreted HBsAg and HBeAg in the supernatant and intracellular HBsAg from cell lysates was performed by chemiluminescent microparticle immunoassay. S/CO = signal to cutoff ratio; RC: relaxed circular DNA; SS = single-stranded DNA. *, # $P < 0.05$; **, ## $P < 0.01$; ***, ### $P < 0.001$.

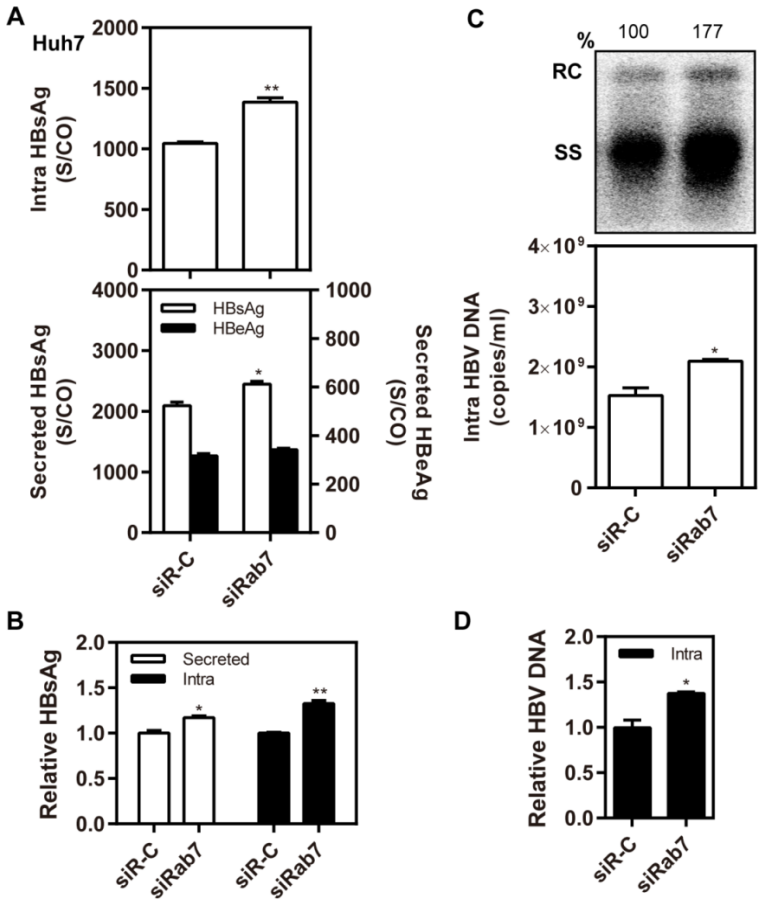

Figure 4.43 Silencing of Rab7 promotes HBV replication and HBsAg production in Huh7 cells

Huh7 cells were cotransfected with pSM2 plasmid and specific siRab7 or control siRNA (siR-C) at 20 nM and harvested after 72 h. (A) Analysis of secreted HBsAg and HBeAg in the supernatant and intracellular HBsAg from cell lysates was performed by chemiluminescent microparticle immunoassay. (B) The graph shows the relative values of HBsAg from the supernatant and cell lysates. (C) The levels of HBV genomes inside the cells were determined by quantitative real-time polymerase chain reaction. Analysis of HBV replicative intermediates was performed by Southern blotting. (D) The graph shows the relative values of intracellular viral genomes. S/CO = signal to cutoff ratio; RC: relaxed circular DNA; SS = single-stranded DNA. * $P < 0.05$; ** $P < 0.01$; *** $P < 0.001$.

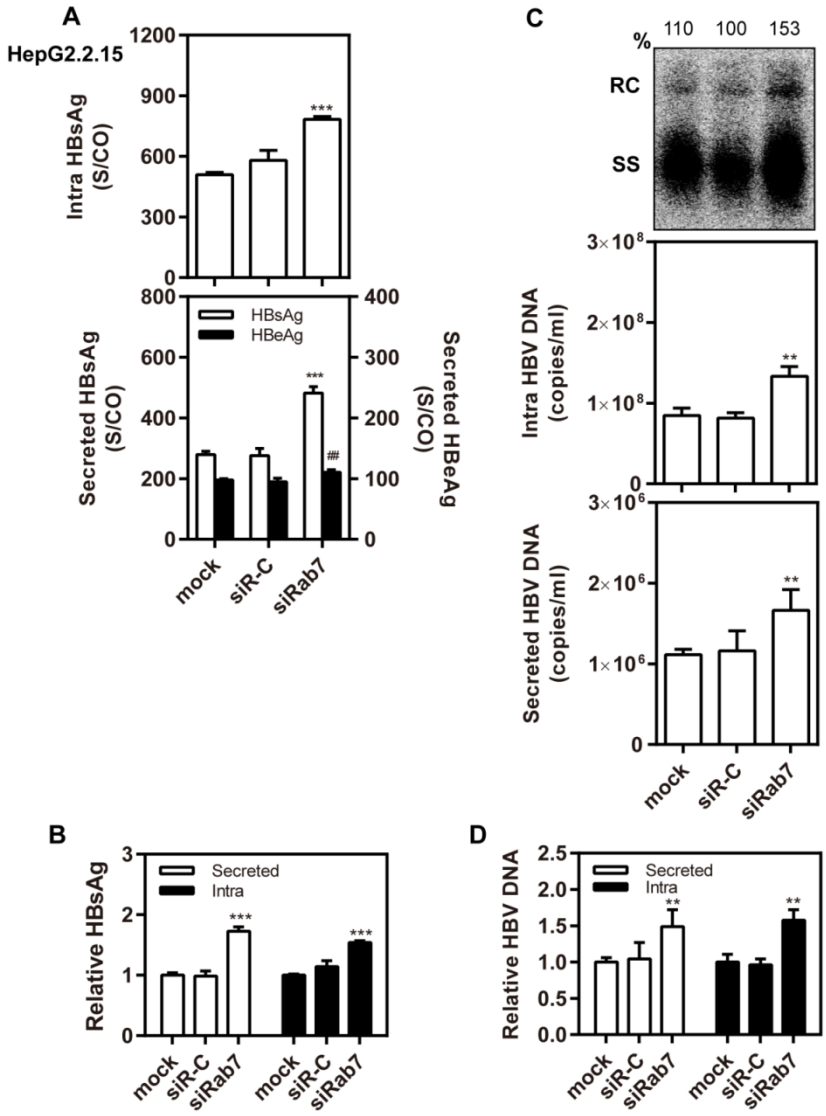

Figure 4.44 Silencing of Rab7 promotes HBV replication and HBsAg production in HepG2.2.15 cells

HepG2.2.15 cells were transfected with specific siRab7 or control siRNA (siR-C) at 20 nM and harvested after 96 h. (A) Analysis of secreted HBsAg and HBeAg in the supernatant and intracellular HBsAg from cell lysates was performed by chemiluminescent microparticle immunoassay. (B) The graph shows the relative values of HBsAg from the supernatant and cell lysates. (C) The levels of HBV genomes inside the cells were determined by quantitative real-time polymerase chain reaction. Analysis of HBV replicative intermediates was performed by Southern blotting. (D) The graph shows the relative values of secreted and intracellular viral genomes. S/CO = signal to cutoff ratio; RC: relaxed circular DNA; SS = single-stranded DNA. *, # $P < 0.05$; **, ## $P < 0.01$; ***, ### $P < 0.001$.

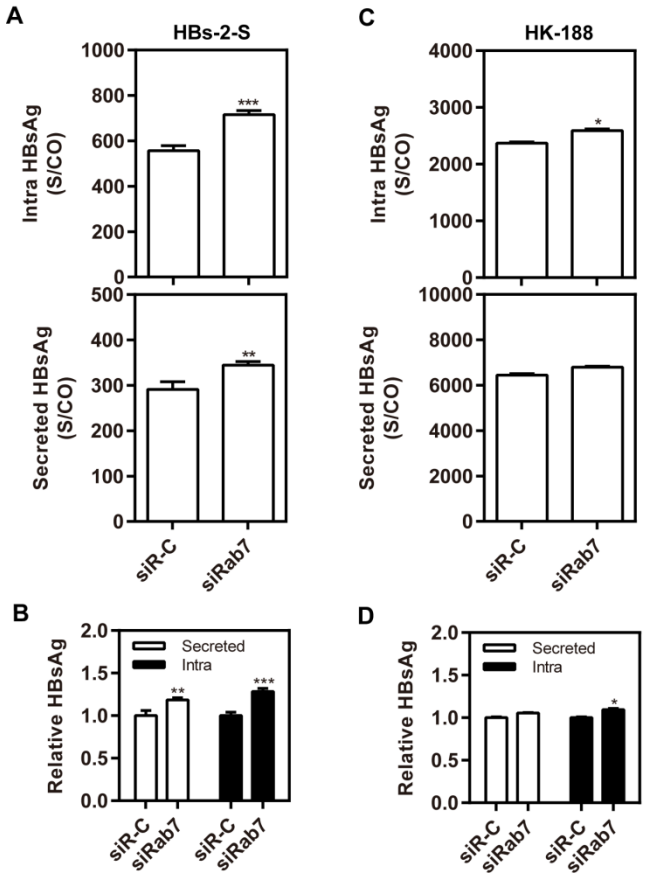

Figure 4.45 Silencing of Rab7 affects HBsAg production in different HBsAg expressive abundance

Huh7 cells were cotransfected with an expression vector with (A) with HBsAg low expression (HBs-2-S) or (C) HBsAg high expression (HK-188), and specific siRab7 or control siRNA (siR-C) at 20 nM, and harvested after 72 h. Secreted HBsAg in the supernatant and intracellular HBsAg from cell lysates were analyzed by chemiluminescent microparticle immunoassay. (B and D) The graphs show the relative values of HBsAg from the supernatant and cell lysates. * $P < 0.05$; ** $P < 0.01$; *** $P < 0.001$.

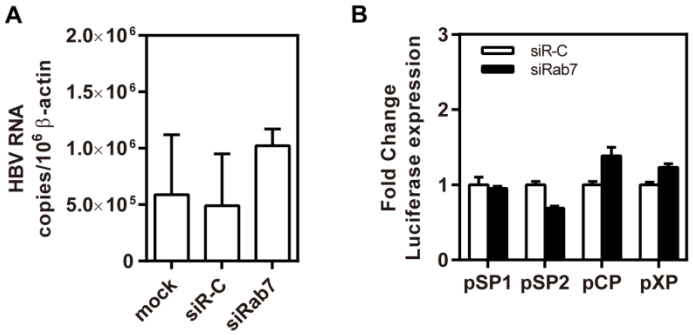

Figure 4.46 Silencing of Rab7 does not promote HBV transcription and promoter activity

HepG2.2.15 cells were transfected with specific siRab7 or control siRNA (siR-C) at 20 nM and harvested after 72 h. (A) Analysis of HBV pregenomic RNA (pgRNA) levels was performed by real-time reverse transcriptase polymerase chain reaction, using primers specific for the pgRNA-specific region. (B) Luciferase reporters containing the HBV promoter regions pSP1, pSP2, pCP, and pXP were co-transfected with specific siRab7 or control siRNA (siR-C) at 20 nM into Huh7 cells. At 48 h post-transfection, firefly and Renilla luciferase activities were analyzed by Dual-Glo luciferase report assay. The relative luciferase expression was calculated by

fold-change, and normalized to control medium treated samples. S/CO = signal to cutoff ratio. *, # $P < 0.05$; **, ## $P < 0.01$; ***, ### $P < 0.001$.

4.5.6 Activation of Rab7 inhibits HBV replication and HBsAg production

To investigate the effect of Rab7 activation on autophagosome formation, Huh7 cells were cotransfected with the GFP-LC3 plasmid and an expression vector carrying wild-type Rab7 (Rab7 WT), dominant negative Rab7 (Rab7 DN), or control vector pEGFP-N1, and harvested at 48 h. The puncta of internal LC3 were measured by immunofluorescence microscopy. The results revealed that overexpression of wild-type Rab7 increased the number of GFP-LC3 puncta (Figure 4.47, A and B), but decreased following inactivation of Rab7 with the Rab7 DN plasmid. Western blotting analysis confirmed that overexpression of Rab7 dramatically degraded the autophagic cargo LC3-II and p62 and decreased the levels of HBcAg (Figure 4.47, C).

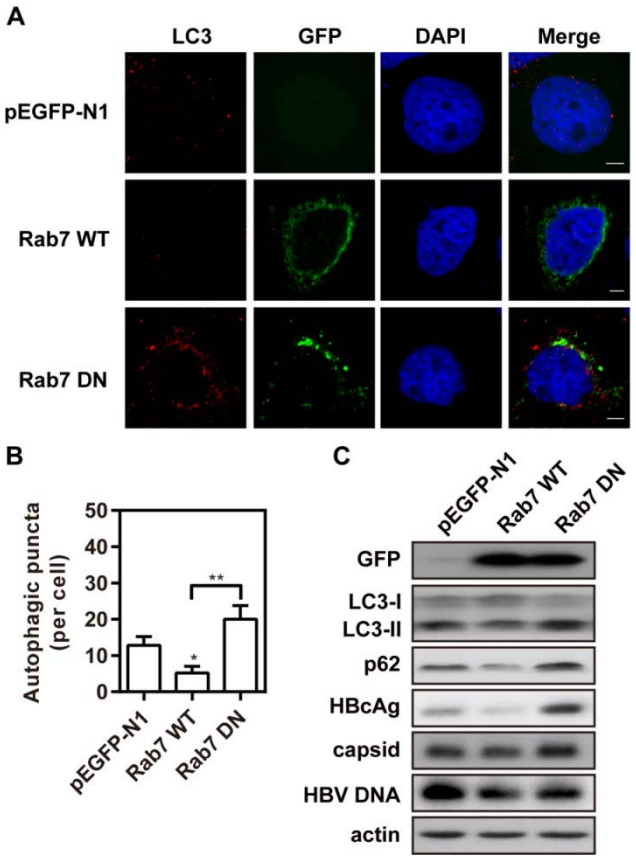

Figure 4.47 Activation of Rab7 promotes autophagic degradation

Huh7 cells were transfected with an expression vector carrying wild type Rab7 (Rab7 WT), dominant negative Rab7 (Rab7 DN) or control vector (pEGFP-N1) and harvested after 48 h. The cells were fixed, incubated with anti-LC3, and then stained with Alexa Fluor 594 (red) - conjugated anti-rabbit secondary antibody IgG. The nuclei were stained with DAPI (blue). Rab7 is visualized in green. (A) The GFP-LC3 puncta were measured by confocal microscopy. Bars, 5 μm. (B) Statistical analysis of the number of GFP-LC3 puncta per cell. (C) Huh7 cells were cotransfected with pSM2 plasmid and Rab7 WT, Rab7 DN, or control vector pEGFP-N1 and

harvested after 72 h. Analysis of encapsidated HBV DNA was performed by Southern blotting. LC3, p62, HBcAg, and viral nucleocapsid expression was analyzed by western blotting, with beta-actin as a loading control. * $P < 0.05$; ** $P < 0.01$; *** $P < 0.001$.

As Rab7 has different functions in vehicle transport and is particularly an essential component of autophagosome-lysosome fusion, we tested the effect of Rab7 on HBV formation in Huh7 cells. The data showed that activation of Rab7 decreased the amount of HBV capsid detected by western blotting and increased the levels of capsid-associated HBV DNA detected by Southern blotting analysis. Moreover, activation of Rab7 clearly decreased the levels of secreted HBsAg in the supernatant and intracellular HBsAg (Figure 4.48, A and B). Quantitative real-time PCR analysis revealed that activation of Rab7 decreased intracellular HBV DNA levels. In addition, Southern blotting analysis confirmed that activation of Rab7 inhibited HBV replicative intermediates (Figure 4.48, C and D).

Collectively, these data reveal that activation of Rab7 decreased the amount of secreted and intracellular HBsAg, as well as secreted HBV DNA levels and intracellular HBV replication by affecting the autophagic degradative process.

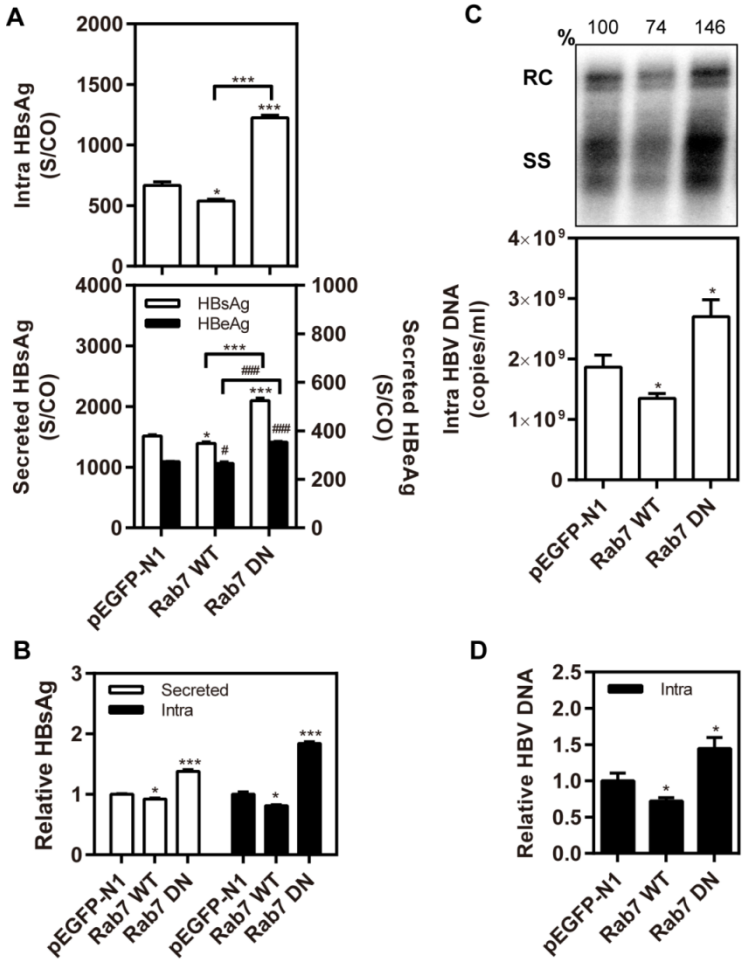

Figure 4.48 Activation of Rab7 inhibits HBV replication and HBsAg production

Huh7 cells were cotransfected with pSM2 plasmid and Rab7 WT, Rab7 DN, or control vector pEGFP-N1 and harvested after 72 h. Analysis of encapsidated HBV DNA was performed by Southern blotting. (A) The levels of

secreted HBsAg and HBeAg in the supernatant and intracellular HBsAg from cell lysates were determined by chemiluminescent microparticle immunoassay. (B) The graph shows the relative values of HBsAg from the supernatant and cell lysates. (C) The levels of HBV genomes inside the cells were determined by quantitative real-time polymerase chain reaction. Analysis of HBV replicative intermediates was performed by Southern blotting. (D) The graph shows the relative values of intracellular viral genomes. S/CO = signal to cutoff ratio; RC: relaxed circular DNA; SS = single-stranded DNA. *, # $P < 0.05$; **, ## $P < 0.01$; ***, ### $P < 0.001$.

4.5.7 Silencing of Rab7 promotes HBV production by interfering with autophagosome and lysosome fusion

To investigate the detailed mechanism of modulation of HBV formation mediated by Rab7, we analyzed the effect of Rab7 on the autophagosome formation. Colocalization of GFP-LC3 with HBs-Cherry was examined by confocal microscopy in Huh7 cells. We observed that silencing of Rab7 increased the number of GFP-LC3 puncta (Figure 4.41, A). Additional confocal microscopy results showed that silencing of Rab7 led to increase colocalization of GFP-LC3 with HBs-Cherry, showing a similar effect as CQ (Figure 4.49, A and B). These data indicate that blocking autophagic degradation caused by silencing of Rab7 leads to a decrease in intracellular HBsAg.

Because autophagic cargo degradation is the final step, we mainly focused on lysosomal function or autophagosome-lysosome fusion resulting from silencing of Rab7. Previous reports showed that knockdown of Rab7 had no obvious effect on the degradation of formed autophagosomes, but impaired autophagosome-lysosome fusion. Thus, the colocalization of LAMP1 with HBs-Cherry was further analyzed. The colocalization coefficient was markedly decreased by silencing of Rab7, but markedly elevated by treatment with CQ (Figure 4.49, C and D). These results indicate that degradation of HBsAg results from impaired of autophagosome-lysosome fusion.

Finally, after transfection with a specific siRab7 and siRNA control, the results were further confirmed by treatment with rapamycin, CQ, or 3-MA. Quantification of secreted HBsAg in the supernatant and intracellular HBsAg from cell lysates revealed that rapamycin further increased the levels of secreted and intracellular HBsAg with or without silencing of Rab7 in HepG2.2.15 cells (Figure 4.50). However, CQ did not further increase the levels of secreted and intracellular HBsAg after silencing of Rab7 compared to the siRNA control. Moreover, 3-MA decreased the levels of secreted and intracellular HBsAg after silencing of Rab7, but the difference was not significant. Thus, these data strongly indicate that silencing of Rab7 increases the levels of secreted and intracellular HBsAg by interfering with autophagosome and lysosome fusion.

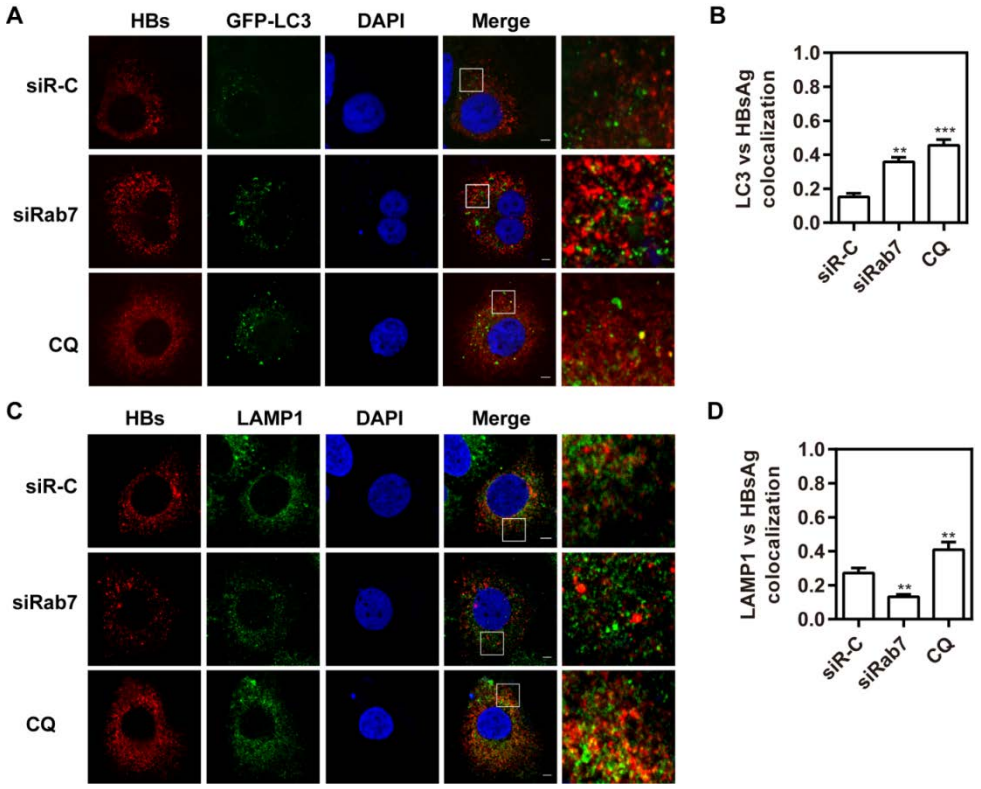

Figure 4.49 Silencing of Rab7 decreases the interaction of lysosomes with HBsAg

(A) Huh7 cells were transfected with HBsAg plasmid with expressing mCherry. At 24 h post-transfection, the cells were split and cotransfected with GFP-LC3 plasmid and specific siRab7 or control siRNA (siR-C) at 20 nM and harvested after 48 h. The cells were fixed and stained with DAPI (blue). The colocalization of LC3 (green) and HBsAg (red) was measured by confocal microscopy. Bars, 5 μm. (B) Statistical analysis of the colocalization coefficient of LC3 and HBsAg. (C) Huh7 cells were cotransfected with HBsAg plasmid with expressing mCherry and specific siRab7 or control siRNA (siR-C) at 20 nM and harvested at 48 h. The cells were incubated with anti-LAMP1, then stained with Alexa Fluor 488 - conjugated anti-rabbit secondary antibody IgG. The colocalization of LAMP1 (green) and HBsAg (Red) was measured by confocal microscopy. Bars, 5 μm. (D) Statistical analysis of the colocalization coefficient of LAMP1 and HBsAg. * $P < 0.05$; ** $P < 0.01$; *** $P < 0.001$; ns, not significant.

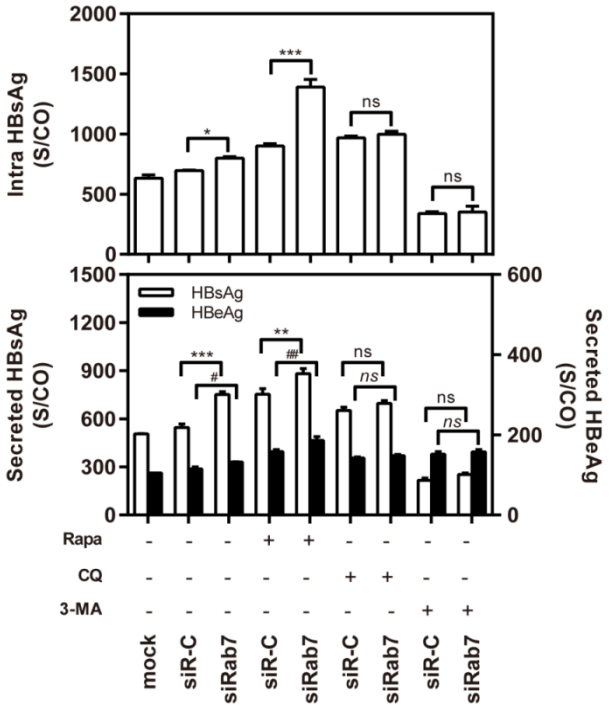

Figure 4.50 Silencing of Rab7 increases HBV production by interfering with late autophagy

HepG2.2.15 cells were transfected with specific siRab7 or control siRNA (siR-C) at 20 nM. At 24 h post-transfection, the cells were treated with 2 μM rapamycin (Rapa), 10 μM chloroquine (CQ), or 10 mM 3-MA for 48 h. The levels of secreted HBsAg and HBeAg in the supernatant and intracellular HBsAg from cell lysates were determined by chemiluminescent microparticle immunoassay. S/CO = signal to cutoff ratio. *, # $P < 0.05$; **, ## $P < 0.01$; ***, ### $P < 0.001$; ns, not significant.

As shown in Figure 4.51, HBV was captured and segregated by autophagosome compartments, which are used for HBV replication and morphogenesis. Small GTPase Rab5 participates in the earliest steps of autophagosome formation and is used for HBV replication and HBsAg production. Additionally, partial virus, including HBV capsid and HBsAg, are degraded by the fusion of autophagosomes and lysosomes. Another small GTPase Rab7 controls the process of autophagosome with lysosome fusion. Thus, our findings suggest that HBV replication and HBsAg production require the early autophagic process, but will be degraded to a significant extent in the autophagosome compartments.

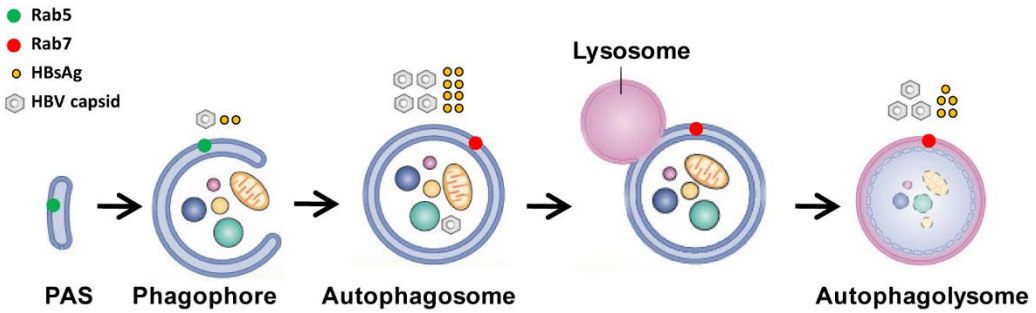

Figure 4.51 Proposed model depicting different autophagic phases inversely modulate HBV replication

A small GTPase, Rab5, participates in the earliest steps of autophagosome formation by providing various

membrane sources for the PAS through its interactions with the PIK3C3-BECN1 complex. HBV may be captured and segregated by autophagosome compartments, which are used for HBV replication and morphogenesis. Furthermore, HBV can exist in autophagosome compartments through certain mechanisms to evade degradation by lysosomes. Additionally, partial HBV may be degraded following the fusion of autophagosomes and lysosomes. Rab7 has different roles in the transport of autophagosomes and MVBs, particularly controlling the fusion process of autophagosomes with lysosomes. Thus, silencing of Rab7 led to accumulation of autophagosomes/MVBs and a subsequent increase in the amount of intracellular and released virus as a result of decreased viral transport to the lysosomes.

5 Discussion

In the present study, we found that the miR-99 family members were able to promote HBV replication in hepatoma cells upon ectopic expression. All 3 members of the miR-99 family targeted components of the IGF-1R/PI3K/Akt/mTOR signaling pathway and negatively regulated this pathway. Among the downstream pathways under the control of the PI3K/Akt/mTOR signaling pathway, autophagy may play a major role in regulating HBV replication. Transfecting hepatocytes with miR-99 family members clearly promoted autophagy. Blocking the initiation of autophagy by 3-MA abolished the enhancing effect of the miR-99 family member on HBV replication. Based on the available data, we conclude that the miR-99 family promoted HBV replication via the IGF-1R/PI3K/Akt/mTOR/ULK1 -autophagy axis.

5.1 Low expression of mature miR-100 and miR-99a in hepatoma cells

It is interesting that miR-99b is lowly expressed in PHHs, however, much more abundantly expressed than miR-100 and -99a in HepG2.2.15 cells. This observation could result from that fact that these 3 miRNAs are transcribed and supposedly regulated independently. The 3 miR-99 family members are derived from different pri-miRNA transcripts. The locations of the coding sequences of miR-100, -99a, and -99b are on the Chromosome 11, NC_000011.10 (122152229..122152308, complement), Chromosome 21, NC_000021.9 (16539089.. 16539169) and Chromosome 19, NC_000019.10 (51692612..51692681), respectively. This explains why the level of miR-99b was increased while that of miR-99a and -100 decreased in hepatoma cells. While the level of miR-99b was increased in hepatoma cells, it did apparently not compensate the loss of miR-100 and -99a expression. Thus, ectopic expression of the miR-99 family members could target the cellular mRNAs with the corresponding seed sequence sharing by all the 3 miRNAs, finally with similar effect on the cellular gene expression and signaling as well as on HBV replication.

5.2 The miR-99 family promotes HBV replication through mTOR/ULK1 signaling pathway-induced complete autophagy

Data from several studies have demonstrated that HBV can promote the autophagy in hepatoma cells.[87-89, 109, 150, 151] Sir et al. found that the HBx protein was able to bind to PI3KC3 and enhance its enzymatic activity, an enzyme critical for the initiation of autophagy.[87] The HBx was also found to upregulate Beclin1 expression and thereby sensitize cells to induce autophagy by starvation.[150] Furthermore, Liu et al. showed that HBV- or HBx protein-induced autophagosome formation was accompanied by unchanged mTOR activity and decreased

degradation of autophagic cargo proteins.[109] The HBx protein may prevent lysosomal acidification, in turn leading to reduced lysosomal degradative capacity and the accumulation of immature lysosomes, possibly through interaction with V-ATPase, affecting its lysosomal targeting. The repressive effect of HBx on lysosomal function inhibits autophagic degradation and may be linked to the development of HBV-associated HCC.[109, 152] In addition, Li et al. showed that HBsAg was required for HBV-stimulated autophagy.[89]

Autophagy was recognized to have a significant impact on HBV replication.[87, 88, 130] Independent research consistently demonstrated that autophagy inhibition strongly reduced HBV replication in hepatic cells.[87, 89] Moreover, Tian et al. demonstrated that a deficiency in autophagy strongly reduced HBV replication in a transgenic mouse model.[88] According to the available results, autophagy enhances HBV replication at the late stage, likely after at a step of capsid formation and viral assembly. Li et al. provided evidence that autophagy was required for HBV envelopment, although it was not necessary for HBV release.[89] In agreement with previous reports, our results demonstrated that the miR-99 family positively regulated HBV replication at the post-transcriptional level. The regulation of HBV promoter activity was not affected by ectopic expression of miR-99 family members. The levels of HBV replicative intermediates, capsids, and secreted HBsAg/HBeAg in hepatoma cells markedly increased following the transfection of miR-99 family members. Early reports suggested that inhibition of the PI3K/Akt/mTOR signaling pathway could promote HBV transcription.[80] In agreement with proposed mechanism, PI3K, Akt, and mTOR chemical inhibitors decreased the levels of phosphorylated Akt and mTOR protein expression in HepG2.2.15 cells. However, miR-99 family members decreased the levels of both total and phosphorylated IGF-1R, Akt, mTOR, and p70S6K protein expression but in a different extent compared to the chemical inhibitors. Our results suggest that miR-99 family members had likely milder inhibition on the IGF-1R/PI3K/Akt/mTOR signaling pathway than the chemical inhibitors.

Bioinformatics analysis of HBV genomic sequences and testing with reporter plasmids suggested that miR-99 family members did not directly act on HBV mRNAs. Recent data have shown that cellular miRNAs have the potential to inhibit or stimulate viral replication in host cells by directly targeting the HBV genome or indirectly by targeting cellular genes.[23, 27, 153, 154] The miR-99 family has been shown to play an important role in many cellular and biological functions. MiR-99 family members were reported to target many cellular genes like IGF-1R, Akt, mTOR, Ago2, and several components of the TGF-β signaling pathway.[155-157] The regulation of these important cellular pathways by the miR-99 family was clearly

essential for controlling cell growth.[136, 137] As shown previously, miR-99 family expression was reduced in primary human hepatocellular carcinoma, compared with that observed in matching normal liver tissues.[137] We showed in the present study that miR-99 family members are expressed in PHHs and hepatoma cells. However, the expression levels of miR-99 family members in hepatoma cells were strongly reduced, compared with their expression levels in primary hepatocytes. Consequently, the dysregulation of cellular processes might decrease the ability of hepatocytes or hepatoma cells to support HBV replication. Consistent with this possibility, previous data showed that the loss of differentiation status of hepatocytes might greatly reduce the ability of cells to support HBV replication.[23, 158, 159] Li et al. showed that replication of woodchuck hepatitis virus and viral antigen expression were gradually decreased in early pre-neoplastic cell line ages.[160] In general, HBV replication is low or absent in HCC tissues, which are associated with the de-differentiation of hepatocytes. We demonstrated that the ectopic expression of miRNAs (like miR-1) in hepatoma cells could promote cell differentiation and restore, at least partially, the hepatocyte phenotype.[23]

5.3 Different autophagic phases inversely affects HBV production

As reported in previous studies, HBV is captured and segregated by the autophagosome /endosome compartments, which are used for HBV replication and morphogenesis.[89, 161, 162] Moreover, HBV can exist in autophagosome compartments through special mechanisms that help HBV evade degradation by lysosomes.[89, 109] Thus, autophagy may be involved in different steps of the HBV life cycle.[87-89]

The complete autophagic process mainly involves the formation of autophagosomes, known as early autophagy, and their fusion with lysosomes and cargo degradation in the lysosomes, known as late autophagy. We found that inhibition of different autophagic phases by chemical inhibitors led to opposite consequences on HBV replication and HBsAg production. Consistent with previous reports,[109, 163] we found that the late autophagy inhibitor CQ increased the number of GFP-LC3 puncta in Huh7 cells as detected by immunofluorescence microscopy and the levels of autophagic cargo, LC3-II and p62, as shown by western blotting analysis in Huh7 cells. The main reason may be that CQ can block the autophagic degradation by inhibiting the lysosomal acidification.[102, 109] As expected, another late autophagy inhibitor CID inactivated Rab7 to cause a similar effect on autophagy by disturbing autophagosome-lysosome fusion without inhibiting lysosomal acidification.[149] Thus, both late autophagy inhibitors significantly increased the amount of secreted and

intracellular HBsAg and the levels of HBV genomes in the supernatants and inside the cells. However, the early autophagy inhibitor 3-MA decreased the expression of LC3-II and increased p62 expression. 3-MA inhibited secreted and intracellular HBsAg and the HBV genomes.[163] These data indicate that early autophagic flux is required for HBV production, and the late step is required for viral degradation.

As endosomal Rab5 and Rab7 are related to the formation or degradation of early autophagic bodies and autophagosomes, they were evaluated in this study to determine their roles in HBV production. Because previous studies found that HBV infection strongly depended on Rab5 and Rab7 expression, HBV transport from early to mature endosomes may be a required step in the viral life cycle. Moreover, the well-known marker of EEs, Rab5, was reported to regulate the autophagosome formation by inhibiting mTOR kinase activity or by forming the complex interacting with Beclin1 and Vps34.[114, 131] As the small GTPase Rab5 is related to the formation early autophagic bodies and autophagosomes, it is an excellent target to study their roles in HBV production. Our data showed that Rab5 was required for autophagosome formation in the early autophagy process, and it may serve as a critical regulator in HBV production. Previous studies showed that Rab5 was crucial for HCV replication, and thus it may have a similar function in an HBV-transfected hepatoma cell system. Consistent with our previous findings determined by silencing the components of the ULK1 complex or using the inhibitor 3-MA, HBV replication and HBsAg production were significantly decreased by silencing of Rab5. Furthermore, overexpression of mutant Rab5 clearly decreased the levels of secreted and intracellular HBsAg and HBV DNA, while overexpression of constitutively active Rab5 was strongly increased. As previously reported, the mechanism may be that Rab5 controls the formation of autophagosomes by inhibiting mTOR kinase activity or by forming a complex that interacts with Beclin1 and Vps34.

Regrettably, the detailed mechanisms of early autophagic phase to promote HBV replication or envelopment remain unknown.[87] HBV envelopment is thought to occur at post-ER/pre-Golgi membranes, where cytosolic nucleocapsids are packaged inside a lipid envelope integrated with viral envelope proteins.[162, 164-166] The following reasons may explain elevated HBV replication or envelopment in early autophagic phase. First, the autophagy pathway may enhance HBV replication or envelopment by sequestering the necessary restriction factor(s).[102, 109] Moreover, autophagosomes provide a physical scaffold for HBV replication or envelopment.[87, 163] Finally, autophagosome membranes may be as a source of membranes for viral envelopment. [89, 161, 162]

During the maturation process of EEs, inactivated Rab5 is substituted by Rab7 on the

endosomal membrane. Subsequently, Rab7 recruits its effectors, RILP and OSBPL1A/ORP1L, directs the LE trafficking, and participates in the fusion step with lysosomes.[121, 167, 168] Thus, we hypothesized that HBV production is modulated by the late autophagic process mediated by Rab7. Our data revealed that silencing of Rab7 significantly enhanced HBV replication and HBsAg production. In contrast, activation of Rab7 clearly decreased the levels of HBV production. These data suggest that the delivery of viral capsids and HBsAg to lysosomes facilitate their degradation. Confocal microscopy revealed that degradation of HBsAg resulted from impaired autophagosome-lysosome fusion, followed by an increase in the levels of HBV replication and HBsAg production.

In addition to Rabs, the vesicular transport and membrane fusion is also generally controlled by soluble *N*-ethylmaleimide-sensitive factor attachment protein receptors (SNAREs), including HOPS complex, STX17, SNAP29, and VAMP8.[169] Previous studies showed that the tethering gene SNAP29 bridged lysosomal VAMP8 and autophagosomal Stx17 to mediate autophagosome-lysosome fusion.[126] The phosphoprotein (P) of human parainfluenza virus type 3 (HPIV3) is necessary and sufficient to inhibition autophagosome degradation by binding to SNAP29 and inhibiting its interaction with syntaxin17. Thus, this thereby prevented the two host SNARE proteins from mediating autophagosome-lysome fusion, and resulted in increased virus production.[170] To confirm the function of late autophagy, silencing or overexpression of the tethering genes, SNAP29 and VAMP8, showed a similar effect on HBV replication and HBsAg as Rab7 (Data not shown). This effect may be contributed to the critical function of tethering genes on autophagosome and lysosome fusion. Thus, our findings indicate that HBV replication and HBsAg production require early autophagic phase mediated by Rab5, but HBV is degraded to a significant extent in autophagosome compartments, which is mediated by Rab7.

Taken together, our results demonstrated that the miR-99 family promotes HBV replication post-transcriptionally through IGF-1R/PI3K/Akt/mTOR/ULK1 signaling-induced complete autophagy. It suggests that more miRNAs may capable of facilitating HBV replication in hepatoma cells by promoting cell differentiation. Thus, the understanding of interactions between host miRNAs and HBV will continue to grow by incorporating new miRNAs and studying their new functions, which will potentially yield new insights of therapeutic relevance.

6 Summary

In our present study, we investigated the influence of the miR-99 family members on HBV replication and gene expression. We found that ectopic expression of miR-99 family members could markedly increase HBV replication, progeny secretion, and antigen expression in hepatoma cells. However, miR-99 family members showed no effect on modulating HBV transcription and HBV promoter activities, suggesting that they may regulate HBV replication through other mechanisms. Consistent with bioinformatic analysis and recent reports, we further found that ectopic expression of miR-99 family attenuated IGF-1R/Akt/mTOR signaling pathway and repressed insulin-stimulated activation in hepatoma cells. Moreover, the experimental data revealed that the miR-99 family promoted the formation of autophagosomes through inhibiting the phosphorylation of ULK1, followed with the autophagic degradation of cargo receptor SQSTM1/p62. Thus, these results implied that the miR-99 family enhanced HBV replication through mTOR/ULK1 signaling induced complete autophagy. We further explored the definite mechanisms of different autophagic phases affecting HBV production. Consistent with our findings by silencing the components of ULK1 complex or using autophagic inhibitor 3-MA, HBV replication and HBsAg production were significantly decreased by silencing of Rab5. In contrast, silencing of Rab7 significantly enhanced HBV replication and HBsAg production, while activation of Rab7 obviously decreased the levels of HBV production. Thus, these data indicated that the delivery of HBV capsids and HBsAg to lysosomes could facilitate their degradation.

Taken together, our results demonstrated that the miR-99 family promotes HBV replication post-transcriptionally through IGF-1R/PI3K/Akt/mTOR/ULK1 signaling-induced complete autophagy. We provide new evidence that HBV replication and HBsAg production requires early autophagic process, but may be degraded to a significant extent in the autophagosome compartment.

7 Zusammenfassung

In der vorliegenden Arbeit wurde der Einfluss der miR-99 Familienmitglieder auf die Replikation des Hepatitis B Virus (HBV) und die virale Genexpression untersucht. Es konnte gezeigt werden, dass alle drei Mitglieder sowohl die HBV-Replikation, die Progenesekretion als auch die Antigenexpression in Hepatom-Zellen deutlich erhöhen. Die miR-99 Familie hatte jedoch weder Auswirkung auf die Transkription noch auf die Promotoraktivitäten von HBV. Dies lässt vermuten, dass die miR-99 Familienmitglieder die HBV-Replikation durch andere Mechanismen regulieren. Übereinstimmend mit bioinformatischen Analysen und jüngsten Publikationen konnte festgestellt werden, dass die ektopische Expression der miR-99 Familie den IGF-1R/Akt/mTOR-Signalweg und die unterdrückte Insulin-stimulierte Aktivierung in Hepatom-Zellen abschwächte. Darüber hinaus zeigten die Daten, dass die miR-99 Familie die Bildung von Autophagosomen durch Hemmung der Phosphorylierung von ULK1 fördert und den Autophagie-vermittelten Abbau des Kargorezeptors SQSTM1/p62 antreibt. Daraus lässt sich schließen, dass die miR-99 Familie die HBV-Replikation durch die vom mTOR/ULK1 Signalweg vollständig induzierte Autophagie verstärkte. Des Weiteren wurde untersucht, durch welchen Mechanismus die Produktion von HBV während der verschiedenen Phasen der Autophagie reguliert wird. Übereinstimmend mit vorherigen Ergebnissen wurde sowohl die HBV-Replikation und als auch die HBsAg-Produktion durch *Silencing* der Komponenten des ULK1-Komplexes oder unter Verwendung des autophagischen Inhibitors 3-MA signifikant durch die Degradation von Rab5 vermindert. Das *Silencing* von Rab7 hingegen steigerte die HBV-Replikation und die HBsAg-Produktion signifikant. Umgekehrt verringerte die Aktivierung von Rab7 offensichtlich die Replikation von HBV. Daraus lässt sich schlussfolgern, dass die Abgabe von HBV-Kapsiden und HBsAg an Lysosomen ihren Abbau ermöglichen könnte.

Die HBV-Replikation wird von der miR-99 Familie post-transkriptional via Autophagie gefördert, welche durch den IGF-1R/PI3K/Akt/mTOR/ULK1-Signalweg vollständig induziert wird. Die HBV-Replikation und die HBsAg-Produktion werden scheinbar durch einen frühen autophagischen Prozess gefördert. Ab einem bestimmten Niveau werden diese jedoch möglicherweise in den Autophagosomen abgebaut.

8 References

1. Bartel DP. MicroRNAs: genomics, biogenesis, mechanism, and function. Cell 2004; 116:281-97.
2. Law PT, Wong N. Emerging roles of microRNA in the intracellular signaling networks of hepatocellular carcinoma. J Gastroenterol Hepatol 2011; 26:437-49.
3. Goodall EF, Heath PR, Bandmann O, Kirby J, Shaw PJ. Neuronal dark matter: the emerging role of microRNAs in neurodegeneration. Front Cell Neurosci 2013; 7:178.
4. Ambros V. The functions of animal microRNAs. Nature 2004; 431:350-5.
5. Kloosterman WP, Wienholds E, Ketting RF, Plasterk RH. Substrate requirements for let-7 function in the developing zebrafish embryo. Nucleic Acids Res 2004; 32:6284-91.
6. Saxena S, Jonsson ZO, Dutta A. Small RNAs with imperfect match to endogenous mRNA repress translation. Implications for off-target activity of small inhibitory RNA in mammalian cells. J Biol Chem 2003; 278:44312-9.
7. Rottiers V, Naar AM. MicroRNAs in metabolism and metabolic disorders. Nat Rev Mol Cell Biol 2012; 13:239-50.
8. Griffiths-Jones S, Saini HK, van Dongen S, Enright AJ. miRBase: tools for microRNA genomics. Nucleic Acids Res 2008; 36:D154-8.
9. Singaravelu R, O'Hara S, Jones DM, Chen R, Taylor NG, Srinivasan P, et al. MicroRNAs regulate the immunometabolic response to viral infection in the liver. Nat Chem Biol 2015; 11:988-93.
10. Skalsky RL, Cullen BR. Viruses, microRNAs, and host interactions. Annu Rev Microbiol 2010; 64:123-41.
11. Cheung O, Puri P, Eicken C, Contos MJ, Mirshahi F, Maher JW, et al. Nonalcoholic steatohepatitis is associated with altered hepatic MicroRNA expression. Hepatology 2008; 48:1810-20.
12. Fichtlscherer S, Zeiher AM, Dimmeler S. Circulating microRNAs: biomarkers or mediators of cardiovascular diseases? Arterioscler Thromb Vasc Biol 2011; 31:2383-90.
13. Friel AM, Corcoran C, Crown J, O'Driscoll L. Relevance of circulating tumor cells, extracellular nucleic acids, and exosomes in breast cancer. Breast Cancer Res Treat 2010; 123:613-25.
14. Kosaka N, Iguchi H, Ochiya T. Circulating microRNA in body fluid: a new potential biomarker for cancer diagnosis and prognosis. Cancer Sci 2010; 101:2087-92.
15. Rabinowits G, Gercel-Taylor C, Day JM, Taylor DD, Kloecker GH. Exosomal microRNA: a diagnostic marker for lung cancer. Clin Lung Cancer 2009; 10:42-6.

16. Taylor DD, Gercel-Taylor C. MicroRNA signatures of tumor-derived exosomes as diagnostic biomarkers of ovarian cancer. Gynecol Oncol 2008; 110:13-21.
17. Kim J, Inoue K, Ishii J, Vanti WB, Voronov SV, Murchison E, et al. A MicroRNA feedback circuit in midbrain dopamine neurons. Science 2007; 317:1220-4.
18. Flinn RJ, Yan Y, Goswami S, Parker PJ, Backer JM. The Late Endosome is Essential for mTORC1 Signaling. Mol Biol Cell 2010; 21:833-41.
19. Tan YW, Ge GH, Pan TL, Wen DF, Chen L, Yu XJ, et al. A Serum MicroRNA Panel as Potential Biomarkers for Hepatocellular Carcinoma Related with Hepatitis B Virus. PLoS One 2014; 9.
20. Liu WH, Yeh SH, Chen PJ. Role of microRNAs in hepatitis B virus replication and pathogenesis. Biochim Biophys Acta 2011.
21. Guo H, Liu H, Mitchelson K, Rao H, Luo M, Xie L, et al. MicroRNAs-372/373 promote the expression of hepatitis B virus through the targeting of nuclear factor I/B. Hepatology 2011; 54:808-19.
22. Wang S, Qiu L, Yan X, Jin W, Wang Y, Chen L, et al. Loss of microRNA 122 expression in patients with hepatitis B enhances hepatitis B virus replication through cyclin G(1) -modulated P53 activity. Hepatology 2012; 55:730-41.
23. Zhang X, Zhang E, Ma Z, Pei R, Jiang M, Schlaak JF, et al. Modulation of hepatitis B virus replication and hepatocyte differentiation by MicroRNA-1. Hepatology 2011; 53:1476-85.
24. Potenza N, Papa U, Mosca N, Zerbini F, Nobile V, Russo A. Human microRNA hsa-miR-125a-5p interferes with expression of hepatitis B virus surface antigen. Nucleic Acids Res 2011; 39:5157-63.
25. Zhang X, Hou J, Lu M. Regulation of hepatitis B virus replication by epigenetic mechanisms and microRNAs. Front Genet 2013; 4:202.
26. Liu WH, Yeh SH, Chen PJ. Role of microRNAs in hepatitis B virus replication and pathogenesis. Biochim Biophys Acta 2011; 1809:678-85.
27. Huang JY, Chou SF, Lee JW, Chen HL, Chen CM, Tao MH, et al. MicroRNA-130a can inhibit hepatitis B virus replication via targeting PGC1alpha and PPARgamma. Rna 2015; 21:385-400.
28. Zhang X, Liu H, Xie Z, Deng W, Wu C, Qin B, et al. Epigenetically regulated miR-449a enhances hepatitis B virus replication by targeting cAMP-responsive element binding protein 5 and modulating hepatocytes phenotype. Sci Rep2016; 6:25389.
29. Guo HY, Liu HY, Mitchelson K, Rao HY, Luo MY, Xie L, et al. MicroRNAs-372/373

Promote the Expression of Hepatitis B Virus Through the Targeting of Nuclear Factor I/B. Hepatology 2011; 54:808-19.

30. Hu W, Wang X, Ding X, Li Y, Zhang X, Xie P, et al. MicroRNA-141 represses HBV replication by targeting PPARA. PLoS One 2012; 7:e34165.

31. Umbach JL, Kramer MF, Jurak I, Karnowski HW, Coen DM, Cullen BR. MicroRNAs expressed by herpes simplex virus 1 during latent infection regulate viral mRNAs. Nature 2008; 454:780-3.

32. Scaria V, Hariharan M, Pillai B, Maiti S, Brahmachari SK. Host-virus genome interactions: macro roles for microRNAs. Cell Microbiol 2007; 9:2784-94.

33. Winther TN, Bang-Berthelsen CH, Heiberg IL, Pociot F, Hogh B. Differential plasma microRNA profiles in HBeAg positive and HBeAg negative children with chronic hepatitis B. PloS one 2013; 8:e58236.

34. Akamatsu S, Hayes CN, Tsuge M, Miki D, Akiyama R, Abe H, et al. Differences in serum microRNA profiles in hepatitis B and C virus infection. J Infect 2015; 70:273-87.

35. Brunetto MR, Cavallone D, Oliveri F, Moriconi F, Colombatto P, Coco B, et al. A serum microRNA signature is associated with the immune control of chronic hepatitis B virus infection. PloS one 2014; 9:e110782.

36. Li F, Zhou P, Deng W, Wang J, Mao R, Zhang Y, et al. Serum microRNA-125b correlates with hepatitis B viral replication and liver necroinflammation. Clin Microbiol Infect 2016; 22: e1-384.e10.

37. Lei X, Bai Z, Ye F, Huang Y, Gao SJ. Regulation of herpesvirus lifecycle by viral microRNAs. Virulence 2010; 1:433-5.

38. Wang Y, Lu Y, Toh ST, Sung WK, Tan P, Chow P, et al. Lethal-7 is down-regulated by the hepatitis B virus x protein and targets signal transducer and activator of transcription 3. J Hepatol 2010; 53:57-66.

39. Sarnow P, Jopling CL, Norman KL, Schutz S, Wehner KA. MicroRNAs: expression, avoidance and subversion by vertebrate viruses. Nat Rev Microbiol 2006; 4:651-9.

40. Glebe D, Bremer CM. The molecular virology of hepatitis B virus. Semin Liver Dis 2013; 33:103-12.

41. Locarnini S. Molecular virology of hepatitis B virus. Semin Liver Dis 2004; 24 Suppl 1:3-10.

42. Howard CR. The biology of hepadnaviruses. J Gen Virol 1986; 67 (Pt 7):1215-35.

43. Tong S, Revill P. Overview of hepatitis B viral replication and genetic variability. J Hepatol 2016; 64:S4-16.

44. Yan H, Zhong G, Xu G, He W, Jing Z, Gao Z, et al. Sodium taurocholate cotransporting polypeptide is a functional receptor for human hepatitis B and D virus. eLife 2012; 3.
45. Ni Y, Lempp FA, Mehrle S, Nkongolo S, Kaufman C, Falth M, et al. Hepatitis B and D viruses exploit sodium taurocholate co-transporting polypeptide for species-specific entry into hepatocytes. Gastroenterology 2014; 146:1070-83.
46. Glebe D, Urban S, Knoop EV, Cag N, Krass P, Grun S, et al. Mapping of the hepatitis B virus attachment site by use of infection-inhibiting preS1 lipopeptides and tupaia hepatocytes. Gastroenterology 2005; 129:234-45.
47. McMahon BJ. The Natural History of Chronic Hepatitis B Virus Infection. Hepatology 2009; 49:S45-S55.
48. Urban S, Schulze A, Dandri M, Petersen J. The replication cycle of hepatitis B virus. J Hepatol 2010; 52:282-4.
49. Nassal M. HBV cccDNA: viral persistence reservoir and key obstacle for a cure of chronic hepatitis B. Gut 2015; 64:1972-84.
50. Decorsiere A, Mueller H, van Breugel PC, Abdul F, Gerossier L, Beran RK, et al. Hepatitis B virus X protein identifies the Smc5/6 complex as a host restriction factor. Nature 2016; 531:386-9.
51. Nassal M. Hepatitis B viruses: reverse transcription a different way. Virus Res 2008; 134:235-49.
52. Lucifora FZJ. The life cycle of hepatitis B virus and antiviral targets. Future Virol 2011; 6:599-614.
53. Beck J, Nassal M. Hepatitis B virus replication. World J Gastroenterol 2007; 13:48-64.
54. Bruss V. Hepatitis B virus morphogenesis. World J Gastroenterol 2007; 13:65-73.
55. Guidotti LG, Chisari FV. Immunobiology and pathogenesis of viral hepatitis. Annu Rev Pathol 2006; 1:23-61.
56. Schweitzer A, Horn J, Mikolajczyk RT, Krause G, Ott JJ. Estimations of worldwide prevalence of chronic hepatitis B virus infection: a systematic review of data published between 1965 and 2013. Lancet 2015; 386:1546-55.
57. Trepo C, Chan HL, Lok A. Hepatitis B virus infection. Lancet 2014; 384:2053-63.
58. Giordano S, Columbano A. MicroRNAs: new tools for diagnosis, prognosis, and therapy in hepatocellular carcinoma? Hepatology 2013; 57:840-7.
59. Tan YJ. Hepatitis B virus infection and the risk of hepatocellular carcinoma. World J Gastroenterol 2011; 17:4853-7.
60. Ganem D, Prince AM. Hepatitis B virus infection--natural history and clinical

consequences. N Engl J Med 2004; 350:1118-29.
61. Franceschi S, Montella M, Polesel J, La Vecchia C, Crispo A, Dal Maso L, et al. Hepatitis viruses, alcohol, and tobacco in the etiology of hepatocellular carcinoma in Italy. Cancer Epidemiol Biomarkers Prev 2006; 15:683-9.
62. Fattovich G, Stroffolini T, Zagni I, Donato F. Hepatocellular carcinoma in cirrhosis: incidence and risk factors. Gastroenterology 2004; 127:S35-50.
63. Kuo TC, Chao CC. Hepatitis B virus X protein prevents apoptosis of hepatocellular carcinoma cells by upregulating SATB1 and HURP expression. Biochem Pharmacol 2010; 80:1093-102.
64. Zhu YZ, Zhu R, Shi LG, Mao Y, Zheng GJ, Chen Q, et al. Hepatitis B virus X protein promotes hypermethylation of p16(INK4A) promoter through upregulation of DNA methyltransferases in hepatocarcinogenesis. Exp Mol Pathol 2010; 89:268-75.
65. Zhang XD, Zhang H, Ye LH. Effects of hepatitis B virus X protein on the development of liver cancer. J Lab Clin Med 2006; 147:58-66.
66. Nguyen DH, Ludgate L, Hu J. Hepatitis B virus-cell interactions and pathogenesis. J Cell Physiol 2008; 216:289-94.
67. Hino O, Kajino K. Hepatitis virus-related hepatocarcinogenesis. Intervirology 1994; 37:133-5.
68. Faria LC, Gigou M, Roque-Afonso AM, Sebagh M, Roche B, Fallot G, et al. Hepatocellular carcinoma is associated with an increased risk of hepatitis B virus recurrence after liver transplantation. Gastroenterology 2008; 134:1890-9.
69. Zoulim F, Durantel D. Antiviral therapies and prospects for a cure of chronic hepatitis B. Csh Perspect Med 2015; 5.
70. Lucifora J, Xia Y, Reisinger F, Zhang K, Stadler D, Cheng X, et al. Specific and nonhepatotoxic degradation of nuclear hepatitis B virus cccDNA. Science 2014; 343:1221-8.
71. Prange R. Host factors involved in hepatitis B virus maturation, assembly, and egress. Med Microbiol Immun 2012; 201:449-61.
72. Ma SW, Huang X, Li YY, Tang LB, Sun XF, Jiang XT, et al. High serum IL-21 levels after 12 weeks of antiviral therapy predict HBeAg seroconversion in chronic hepatitis B. J Hepatol 2012; 56:775-81.
73. Schoggins JW, Rice CM. Interferon-stimulated genes and their antiviral effector functions. Curr Opin Virol 2011; 1:519-25.
74. Wang SH, Yeh SH, Lin WH, Yeh KH, Yuan Q, Xia NS, et al. Estrogen receptor alpha represses transcription of HBV genes via interaction with hepatocyte nuclear factor 4alpha.

Gastroenterology 2012; 142:989-98 e4.
75. Levrero M, Pollicino T, Petersen J, Belloni L, Raimondo G, Dandri M. Control of cccDNA function in hepatitis B virus infection. J Hepatol 2009; 51:581-92.
76. Pollicino T, Belloni L, Raffa G, Pediconi N, Squadrito G, Raimondo G, et al. Hepatitis B virus replication is regulated by the acetylation status of hepatitis B virus cccDNA-bound H3 and H4 histones. Gastroenterology 2006; 130:823-37.
77. Deng W, Zhang X, Ma Z, Lin Y, Lu M. MicroRNA-125b-5p mediates post-transcriptional regulation of hepatitis B virus replication via the LIN28B/let-7 axis. RNA Biol 2017:0.
78. Zoulim F, Luangsay S, Durantel D. Targeting innate immunity: a new step in the development of combination therapy for chronic hepatitis B. Gastroenterology 2013; 144:1342-4.
79. Chang J, Block TM, Guo JT. The innate immune response to hepatitis B virus infection: implications for pathogenesis and therapy. Antiviral Res 2012; 96:405-13.
80. Guo HT, Zhou TL, Jiang D, Cuconati A, Xiao GH, Block TM, et al. Regulation of hepatitis B virus replication by the phosphatidylinositol 3-kinase-Akt signal transduction pathway. J Virol 2007; 81:10072-80.
81. Rawat S, Bouchard MJ. The hepatitis B virus (HBV) HBx protein activates AKT To simultaneously regulate HBV replication and hepatocyte survival. J Virol 2015; 89:999-1012.
82. Teng CF, Wu HC, Tsai HW, Shiah HS, Huang WY, Su IJ. Novel feedback inhibition of surface antigen synthesis by mammalian target of rapamycin (mTOR) signal and its implication for hepatitis B virus tumorigenesis and therapy. Hepatology 2011; 54:1199-207.
83. Li H, Zhu W, Zhang L, Lei H, Wu X, Guo L, et al. The metabolic responses to hepatitis B virus infection shed new light on pathogenesis and targets for treatment. Sci Rep 2015; 5:8421.
84. Su X, Yu Y, Zhong Y, Giannopoulou EG, Hu X, Liu H, et al. Interferon-gamma regulates cellular metabolism and mRNA translation to potentiate macrophage activation. Nat Immunol 2015; 16:838-49.
85. Sir D, Ann DK, Ou JH. Autophagy by hepatitis B virus and for hepatitis B virus. Autophagy 2010; 6:548-9.
86. Wang P, Guo QS, Wang ZW, Qian HX. HBx induces HepG-2 cells autophagy through PI3K/Akt-mTOR pathway. Mol Cell Biochem 2013; 372:161-8.
87. Sir D, Tian YJ, Chen WL, Ann DK, Yen TSB, Ou JHJ. The early autophagic pathway is activated by hepatitis B virus and required for viral DNA replication. P Natl Acad Sci USA

2010; 107:4383-8.

88. Tian Y, Sir D, Kuo CF, Ann DK, Ou JH. Autophagy required for hepatitis B virus replication in transgenic mice. J Virol 2011; 85:13453-6.

89. Li J, Liu Y, Wang Z, Liu K, Wang Y, Liu J, et al. Subversion of cellular autophagy machinery by hepatitis B virus for viral envelopment. J Virol 2011; 85:6319-33.

90. Mizushima N, Komatsu M. Autophagy: renovation of cells and tissues. Cell 2011; 147:728-41.

91. Yang Z, Klionsky DJ. Eaten alive: a history of macroautophagy. Nat Cell Biol 2010; 12:814-22.

92. Saftig P, Klumperman J. Lysosome biogenesis and lysosomal membrane proteins: trafficking meets function. Nat Rev Mol Cell Biol 2009; 10:623-35.

93. Jung CH, Jun CB, Ro SH, Kim YM, Otto NM, Cao J, et al. ULK-Atg13-FIP200 complexes mediate mTOR signaling to the autophagy machinery. Mol Biol Cell 2009; 20:1992-2003.

94. Alers S, Loffler AS, Wesselborg S, Stork B. Role of AMPK-mTOR-Ulk1/2 in the regulation of autophagy: cross talk, shortcuts, and feedbacks. Mol Cell Bio 2012; 32:2-11.

95. Blommaart EF, Luiken JJ, Blommaart PJ, van Woerkom GM, Meijer AJ. Phosphorylation of ribosomal protein S6 is inhibitory for autophagy in isolated rat hepatocytes. J Biol Chem 1995; 270:2320-6.

96. Brown EJ, Albers MW, Shin TB, Ichikawa K, Keith CT, Lane WS, et al. A mammalian protein targeted by G1-arresting rapamycin-receptor complex. Nature 1994; 369:756-8.

97. Kanazawa T, Taneike I, Akaishi R, Yoshizawa F, Furuya N, Fujimura S, et al. Amino acids and insulin control autophagic proteolysis through different signaling pathways in relation to mTOR in isolated rat hepatocytes. J Biol Chem 2004; 279:8452-9.

98. Neufeld TP. TOR-dependent control of autophagy: biting the hand that feeds. Curr opin Cell Biol 2010; 22:157-68.

99. Wei Y, Pattingre S, Sinha S, Bassik M, Levine B. JNK1-mediated phosphorylation of Bcl-2 regulates starvation-induced autophagy. Mol Cell 2008; 30:678-88.

100. Zalckvar E, Berissi H, Mizrachy L, Idelchuk Y, Koren I, Eisenstein M, et al. DAP-kinase-mediated phosphorylation on the BH3 domain of beclin 1 promotes dissociation of beclin 1 from Bcl-XL and induction of autophagy. EMBO Rep 2009; 10:285-92.

101. Saftig P, Klumperman J. Lysosome biogenesis and lysosomal membrane proteins: trafficking meets function. Nat Rev Mol Cell Bio 2009; 10:623-35.

102. Xie N, Yuan KF, Zhou L, Wang K, Chen HN, Lei YL, et al. PRKAA/AMPK restricts

HBV replication through promotion of autophagic degradation. Autophagy 2016; 12:1507-20.
103. Pareja ME, Colombo MI. Autophagic clearance of bacterial pathogens: molecular recognition of intracellular microorganisms. Front Cell Infect Microbiol 2013; 3:54.
104. Orvedahl A, MacPherson S, Sumpter R, Jr., Talloczy Z, Zou Z, Levine B. Autophagy protects against Sindbis virus infection of the central nervous system. Cell Host Microbe 2010; 7:115-27.
105. Dreux M, Gastaminza P, Wieland SF, Chisari FV. The autophagy machinery is required to initiate hepatitis C virus replication. P Natl Acad Sci USA 2009; 106:14046-51.
106. Fischl W, Bartenschlager R. Exploitation of cellular pathways by Dengue virus. Curr Opin Microbiol 2011; 14:470-5.
107. Kyei GB, Dinkins C, Davis AS, Roberts E, Singh SB, Dong C, et al. Autophagy pathway intersects with HIV-1 biosynthesis and regulates viral yields in macrophages. J Cell Biol 2009; 186:255-68.
108. Chen YC, Su YC, Li CY, Wu CP, Lee MS. A nationwide cohort study suggests chronic hepatitis B virus infection increases the risk of end-stage renal disease among patients in Taiwan. Kidney Int 2014; 87(5):1030-8.
109. Liu B, Fang M, Hu Y, Huang B, Li N, Chang C, et al. Hepatitis B virus X protein inhibits autophagic degradation by impairing lysosomal maturation. Autophagy 2014; 10:416-30.
110. Stenmark H. Rab GTPases as coordinators of vesicle traffic. Nat Rev Mol Cell Bio 2009; 10:513-25.
111. Hutagalung AH, Novick PJ. Role of Rab GTPases in membrane traffic and cell physiology. Physiol Rev 2011; 91:119-49.
112. Szatmari Z, Sass M. The autophagic roles of Rab small GTPases and their upstream regulators: a review. Autophagy 2014; 10:1154-66.
113. Numrich J, Ungermann C. Endocytic Rabs in membrane trafficking and signaling. Biol Chem 2014; 395:327-33.
114. Su WC, Chao TC, Huang YL, Weng SC, Jeng KS, Lai MM. Rab5 and class III phosphoinositide 3-kinase Vps34 are involved in hepatitis C virus NS4B-induced autophagy. J Virol 2011; 85:10561-71.
115. Stenmark H. Rab GTPases as coordinators of vesicle traffic. Nat Rev Mol Cell Bio 2009; 10:513-25.
116. Ravikumar B, Imarisio S, Sarkar S, O'Kane CJ, Rubinsztein DC. Rab5 modulates aggregation and toxicity of mutant huntingtin through macroautophagy in cell and fly models

of Huntington disease. J Cell Sci 2008; 121:1649-60.

117. Dou Z, Pan JA, Dbouk HA, Ballou LM, DeLeon JL, Fan Y, et al. Class IA PI3K p110beta subunit promotes autophagy through Rab5 small GTPase in response to growth factor limitation. Mol Cell 2013; 50:29-42.

118. Huotari J, Helenius A. Endosome maturation. Embo J 2011; 30:3481-500.

119. Wang T, Ming Z, Xiaochun W, Hong W. Rab7: role of its protein interaction cascades in endo-lysosomal traffic. Cell Signal 2011; 23:516-21.

120. Jager S, Bucci C, Tanida I, Ueno T, Kominami E, Saftig P, et al. Role for Rab7 in maturation of late autophagic vacuoles. J Cell Sci 2004; 117:4837-48.

121. Schroeder B, Schulze RJ, Weller SG, Sletten AC, Casey CA, McNiven MA. The small GTPase Rab7 as a central regulator of hepatocellular lipophagy. Hepatology 2015; 61:1896-907.

122. Su H, Li F, Ranek MJ, Wei N, Wang X. COP9 signalosome regulates autophagosome maturation. Circulation 2011; 124:2117-28.

123. Ganley IG, Wong PM, Gammoh N, Jiang X. Distinct autophagosomal-lysosomal fusion mechanism revealed by thapsigargin-induced autophagy arrest. Mole Cell 2011; 42:731-43.

124. Sun Q, Westphal W, Wong KN, Tan I, Zhong Q. Rubicon controls endosome maturation as a Rab7 effector. Proc Natl Acad Sci U S A 2010; 107:19338-43.

125. Lin WJ, Yang CY, Li LL, Yi YH, Chen KW, Lin YC, et al. Lysosomal targeting of phafin1 mediated by Rab7 induces autophagosome formation. Biochem Biophy Res Commun 2012; 417:35-42.

126. Itakura E, Kishi-Itakura C, Mizushima N. The hairpin-type tail-anchored SNARE syntaxin 17 targets to autophagosomes for fusion with endosomes/lysosomes. Cell 2012; 151:1256-69.

127. Yamaguchi H, Nakagawa I, Yamamoto A, Amano A, Noda T, Yoshimori T. An initial step of GAS-containing autophagosome-like vacuoles formation requires Rab7. PLoS Pathog 2009; 5:e1000670.

128. Zhang R, Chi X, Wang S, Qi B, Yu X, Chen JL. The regulation of autophagy by influenza A virus. Biomed Res Int 2014; 2014:498083.

129. Lee YR, Lei HY, Liu MT, Wang JR, Chen SH, Jiang-Shieh YF, et al. Autophagic machinery activated by dengue virus enhances virus replication. Virology 2008; 374:240-8.

130. Huang W, Zhao F, Huang Y, Li X, Zhu S, Hu Q, et al. Rapamycin enhances HBV production by inducing cellular autophagy. Hepat Mon 2014; 14:e20719.

131. Bridges D, Fisher K, Zolov SN, Xiong T, Inoki K, Weisman LS, et al. Rab5 proteins

regulate activation and localization of target of rapamycin complex 1. J Biol Chem 2012; 287:20913-21.

132. Vieira OV, Bucci C, Harrison RE, Trimble WS, Lanzetti L, Gruenberg J, et al. Modulation of Rab5 and Rab7 recruitment to phagosomes by phosphatidylinositol 3-kinase. Mol Cell Biol 2003; 23:2501-14.

133. Stone M, Jia S, Heo WD, Meyer T, Konan KV. Participation of rab5, an early endosome protein, in hepatitis C virus RNA replication machinery. J Virol 2007; 81:4551-63.

134. Stanssens P, Opsomer C, Mckeown YM, Kramer W, Zabeau M, Fritz HJ. Efficient oligonucleotide-directed construction of mutations in expression vectors by the gapped duplex DNA method using alternating selectable markers. Nucleic Acids Res 1989; 17:4441-54.

135. Di Leva G, Garofalo M, Croce CM. MicroRNAs in cancer. Annu Rev Pathol 2014; 9:287-314.

136. Cui L, Zhou H, Zhao H, Zhou Y, Xu R, Xu X, et al. MicroRNA-99a induces G1-phase cell cycle arrest and suppresses tumorigenicity in renal cell carcinoma. BMC cancer 2012; 12:546.

137. Li D, Liu X, Lin L, Hou J, Li N, Wang C, et al. MicroRNA-99a inhibits hepatocellular carcinoma growth and correlates with prognosis of patients with hepatocellular carcinoma. J Biol Chem 2011; 286:36677-85.

138. Qin C, Huang RY, Wang ZX. Potential role of miR-100 in cancer diagnosis, prognosis, and therapy. Tumor Biol 2015; 36:1403-9.

139. Wu FL, Jin WB, Li JH, Guo AG. Targets for human encoded microRNAs in HBV genes. Virus Genes 2011; 42:157-61.

140. Li XJ, Luo XQ, Han BW, Duan FT, Wei PP, Chen YQ. MicroRNA-100/99a, deregulated in acute lymphoblastic leukaemia, suppress proliferation and promote apoptosis by regulating the FKBP51 and IGF1R/mTOR signalling pathways. Brit J Cancer 2013; 109:2189-98.

141. Jin Y, Tymen SD, Chen D, Fang ZJ, Zhao Y, Dragas D, et al. MicroRNA-99 family targets AKT/mTOR signaling pathway in dermal wound healing. PLoS One 2013; 8:e20916.

142. Hu Y, Zhu Q, Tang LL. MiR-99a antitumor activity in human breast cancer cells through targeting of mTOR expression. PLoS One 2014; 9:e92099.

143. Ge YY, Shi Q, Zheng ZY, Gong J, Zeng C, Yang J, et al. MicroRNA-100 promotes the autophagy of hepatocellular carcinoma cells by inhibiting the expression of mTOR and IGF-1R. Oncotarget 2014; 5:6218-28.

144. Whittaker S, Marais R, Zhu AX. The role of signaling pathways in the development and

treatment of hepatocellular carcinoma. Oncogene 2010; 29:4989-5005.

145. Laplante M, Sabatini DM. mTOR signaling in growth control and disease. Cell 2012; 149:274-93.

146. Dazert E, Hall MN. mTOR signaling in disease. Curr Opin Cell Biol 2011; 23:744-55.

147. Jung CH, Seo M, Otto NM, Kim DH. ULK1 inhibits the kinase activity of mTORC1 and cell proliferation. Autophagy 2011; 7:1212-21.

148. Ro SH, Jung CH, Hahn WS, Xu X, Kim YM, Yun YS, et al. Distinct functions of Ulk1 and Ulk2 in the regulation of lipid metabolism in adipocytes. Autophagy 2013; 9:2103-14.

149. Hong L, Guo Y, BasuRay S, Agola JO, Romero E, Simpson DS, et al. A Pan-GTPase Inhibitor as a Molecular Probe. PLoS One 2015; 10:e0134317.

150. Tang H, Da L, Mao Y, Li Y, Li D, Xu Z, et al. Hepatitis B virus X protein sensitizes cells to starvation-induced autophagy via up-regulation of beclin 1 expression. Hepatology 2009; 49:60-71.

151. Lazar C, Uta M, Branza-Nichita N. Modulation of the unfolded protein response by the human hepatitis B virus. Fron Microbiol 2014; 5:433.

152. Lan SH, Wu SY, Zuchini R, Lin XZ, Su IJ, Tsai TF, et al. Autophagy suppresses tumorigenesis of hepatitis B virus-associated hepatocellular carcinoma through degradation of microRNA-224. Hepatology 2014; 59:505-17.

153. Kohno T, Tsuge M, Murakami E, Hiraga N, Abe H, Miki D, et al. Human microRNA hsa-miR-1231 suppresses hepatitis B virus replication by targeting core mRNA. J Viral Hepat 2014; 21:e89-97.

154. Wang YQ, Ren YF, Song YJ, Xue YF, Zhang XJ, Cao ST, et al. MicroRNA-581 promotes hepatitis B virus surface antigen expression by targeting Dicer and EDEM1. Carcinogenesis 2014; 35:2127-33.

155. Lerman G, Avivi C, Mardoukh C, Barzilai A, Tessone A, Gradus B, et al. MiRNA expression in psoriatic skin: reciprocal regulation of hsa-miR-99a and IGF-1R. PLoS One 2011; 6:e20916.

156. Chen Z, Jin Y, Yu D, Wang A, Mahjabeen I, Wang C, et al. Down-regulation of the microRNA-99 family members in head and neck squamous cell carcinoma. Oral Oncol 2012; 48:686-91.

157. Zhang J, Jin H, Liu H, Lv S, Wang B, Wang R, et al. MiRNA-99a directly regulates AGO2 through translational repression in hepatocellular carcinoma. Oncogenesis 2014; 3:e97.

158. Martinot-Peignoux M, Boyer N, Colombat M, Akremi R, Pham BN, Ollivier S, et al.

Serum hepatitis B virus DNA levels and liver histology in inactive HBsAg carriers. J Hepat 2002; 36:543-6.

159. Su TH, Hsu CS, Chen CL, Liu CH, Huang YW, Tseng TC, et al. Serum hepatitis B surface antigen concentration correlates with HBV DNA level in patients with chronic hepatitis B. Antivir Ther 2010; 15:1133-9.

160. Li Y, Hacker H, Kopp-Schneider A, Protzer U, Bannasch P. Woodchuck hepatitis virus replication and antigen expression gradually decrease in preneoplastic hepatocellular lineages. J Hepatol 2002; 37:478-85.

161. Jiang B, Himmelsbach K, Ren H, Boller K, Hildt E. Subviral Hepatitis B Virus Filaments, like Infectious Viral Particles, Are Released via Multivesicular Bodies. J Virol 2015; 90:3330-41.

162. Patient R, Hourioux C, Roingeard P. Morphogenesis of hepatitis B virus and its subviral envelope particles. Cell Microbiol 2009; 11:1561-70.

163. Lin Y, Deng W, Pang J, Kemper T, Hu J, Yin J, et al. The microRNA-99 family modulates hepatitis B virus replication by promoting IGF-1R/PI3K/Akt/mTOR/ULK1 signaling-induced autophagy. Cell Microbiol 2016; 23:546.

164. Bruss V. Envelopment of the hepatitis B virus nucleocapsid. Virus Res 2004; 106:199-209.

165. Huovila AP, Eder AM, Fuller SD. Hepatitis B surface antigen assembles in a post-ER, pre-Golgi compartment. J Cell Biol 1992; 118:1305-20.

166. Patzer EJ, Nakamura GR, Simonsen CC, Levinson AD, Brands R. Intracellular assembly and packaging of hepatitis B surface antigen particles occur in the endoplasmic reticulum. J Virol 1986; 58:884-92.

167. Inoue J, Krueger EW, Chen J, Cao H, Ninomiya M, McNiven MA. HBV secretion is regulated through the activation of endocytic and autophagic compartments mediated by Rab7 stimulation. J Cell Sci 2015; 128:1696-706.

168. Jordens I, Fernandez-Borja M, Marsman M, Dusseljee S, Janssen L, Calafat J, et al. The Rab7 effector protein RILP controls lysosomal transport by inducing the recruitment of dynein-dynactin motors. Curr Biol 2001; 11:1680-5.

169. Jiang P, Nishimura T, Sakamaki Y, Itakura E, Hatta T, Natsume T, et al. The HOPS complex mediates autophagosome-lysosome fusion through interaction with syntaxin 17. Mol Biol Cell 2014; 25:1327-37.

170. Ding B, Zhang G, Yang X, Zhang S, Chen L, Yan Q, et al. Phosphoprotein of human parainfluenza virus type 3 blocks autophagosome-lysosome fusion to increase virus

production. Cell Host Microbe 2014; 15:564-77.

9 Abbreviations

Abbreviations	Full name
3-MA	3-methyladenine
CQ	chloroquine
3'-UTR	3'-untranslated region
5'-UTR	5'-untranslated region
cccDNA	circular covalently closed DNA
CHB	chronic hepatitis B
CMIA	chemiluminescence immunoassay
GFP	green fluorescence protein
DMEM	Dulbecco’s Modified Eagles’s Medium
DMSO	dimethylsulfoxide
DNA	deoxyribonucleic acid
E.coli	Escherichia coli
EEs	early endosomes
EDTA	ethylenediaminetetraaceticacid
ER	endoplasmic reticulum
FBS	fetal bovine serum
g	gram
HBcAg	hepatitis B core antigen
HBsAg	hepatitis B surface antigen
HBV	hepatitis B virus
HBV RI	hepatitis B virus replicative intermediate
HBx	hepatitis B x antigen
HCC	hepatocellular carcinoma
HCV	hepatitis C virus
HIV	human immunodeficiency virus
IFN	interferon
IGF1R	insulin-like growth factor 1 receptor
kb	kilo base pair
l	liter
LAMP1	lysosomal-associated membrane protein 1
LEs	late endosomes
LC3	MAP1LC3, microtubule-associated protein 1 light chain 3 beta

LXRs	liver X receptors
m	milli
miRNA	microRNA
MEM	Dulbecco’s Modified Eagle Medium
min	minute
miRNAs	microRNAs
miR-C	control microRNA
mTOR	mammalian target of rapamycin
SQSTM1/p62	sequestosome 1
OSBPL1A/ORP1L	oxysterol-binding protein-like 1A
PBS	phosphate buffered saline
pCP	plasmid contains HBV core promoter region
PCR	polymerase chain reaction
PCR	polymerase chain reaction
pgRNA	pregenomic RNA
pHBV 1	plasmid contains HBV fragment 1
pHBV 2	plasmid contains HBV fragment 2
pHBV 3	plasmid contains HBV fragment 3
pHBV 3'UTR	plasmid contains HBV 3'-termnal region
pHBV FL	plasmid contains HBV full length genome
PHH	primary human hepatocyte
PI3K	phosphatidylinositol 3-kinase
RILP	Rab-interacting lysosomal protein
RT-PCR	reverse transcriptase polymerase chain reaction
SEM	standard error of the mean
siR-C	control small interfering RNA
siRNA	small interfering RNA

10 List of figures

11 Acknowledgements

I am deeply grateful to my first supervisor, Prof. Dr. rer. nat. Mengji Lu for providing me the opportunity to study and finish my PhD project in Institute of Virology, University Hospital Essen. I strongly appreciate his patient guidance and strict attitude in scientific work. With his help, I have not only gained a lot of knowledge and skills, but also learned to communicate and exchange with other people. Meanwhile, I would like to thank my second supervisor Prof. Dr. Mathias Günzer for his kindly support and guidance in my PhD project.

I also would like to thank Prof. Dr. Ulf Dittmer in our institute of Virology. He has provided me good welfare and much help in Germany in the pasted four years. Moreover, I want to appreciate their support and help from Ms. Ursula Schrammel, Ms. Katrin Palupsky, and Mrs. Elisabeth Zimmerman in my work and daily life during my stay in Germany.

Many thanks to our technician Mrs. Thekla Kemper and Mrs. Barbara Bleekmann in our group. Their technical assistance and help are very important for my PhD project. I also would like to appreciate my colleagues Dr. Jia Liu, Dr. Wanyu Deng, Dr. Jinke Pang, Dr. Weimin Wu, Dr. Jing Hu, Mr. Jianbo Xia, and all the other Chinese colleagues in University Hospital Essen. Their grateful help and care make my life much more joyous in Germany.

I am deeply grateful to my wife Chunyan Zhang for her understanding and supports. I also would like to thank my parents, sister, relatives and friends for their sustained encouragement and help.

I would like to appreciate the support and help from Prof. Dr. Astrid Westendorf, Prof. Dr. Jörg Timm, Prof. Dr. Mirko Trilling, and Ms. Daniela Catrini in Graduate Course RTG1949. I am deeply appreciated Ms. Meike Rückborn for helping me to modify my dissertation. Many thanks to my other classmates in RTG1949 for their accompany and help. I will deeply remember the good time and our friendship in the future. Finally, I want to convey my thanks to the financial support provided by Graduate Course RTG1949.

Curriculum vitae

The biography is not included in the online version for reasons of data protection

Erklärung

Hiermit erkläre ich, gem. § 6 Abs. 2, g der Promotionsordnung der Fakultät für Biologie zur Erlangung der Dr. rer. nat., dass ich das Arbeitsgebiet, dem das Thema „Hepatitis B virus production is modulated through microRNA-99 family induced-autophagy“ zuzuordnen ist, in Forschung und Lehre vertrete und den Antrag von (Yong Lin) befürworte.

Essen,den Prof. Dr. rer.nat. Mengji Lu _____

Name des wissenschaftl. Betreuers/Mitglieds der Universität Duisburg-Essen

Unterschrift d. wissenschaftl.Betreuers/ Mitglieds der Universität Duisburg-Essen

Erklärung:

Hiermit erkläre ich, gem. § 7 Abs. 2, d und f der Promotionsordnung der Fakultät für Biologie zur Erlangung des Dr. rer. nat., dass ich die vorliegende Dissertation selbständig verfasst und mich keiner anderen als der angegebenen Hilfsmittel bedient habe und alle wörtlich oder inhaltlich übernommenen Stellen als solche gekennzeichnet habe.

Essen, den _____ _____

Unterschrift des/r Doktoranden/in

Erklärung:

Hiermit erkläre ich, gem. § 7 Abs. 2, e und g der Promotionsordnung der Fakultät für Biologie zur Erlangung des Dr. rer. nat., dass ich keine anderen Promotionen bzw. Promotionsversuche in der Vergangenheit durchgeführt habe, dass diese Arbeit von keiner anderen Fakultät abgelehnt worden ist, und dass ich die Dissertation nur in diesem Verfahren einreiche.

Essen, den _____ _____

Unterschrift des/r Doktoranden/in